



Laporan Akhir Projek Penyelidikan Jangka Pendek

**Fundamental Properties and Evaluation of
Asphalt Mixes Incorporating Reclaimed
Asphalt Pavement (RAP)**

**by
Prof. Dr. Meor Othman Hamzah
Dr. Joewono Prasetejo**

2012



UNIVERSITI SAINS MALAYSIA

FUNDAMENTAL PROPERTIES AND EVALUATION OF ASPHALT MIXES INCORPORATING RECLAIMED ASPHALT PAVEMENT (RAP)

FINAL REPORT
RU Research Grant

December 2012

Prepared by:
Professor Dr. Meor Othman Hamzah
School of Civil Engineering
Engineering Campus
Universiti Sains Malaysia

SUBMITTED TO:
Fundamental Sciences Platform
Universiti Sains Malaysia
11800 MINDEN
PENANG

TABLE OF CONTENTS

TABLE OF CONTENTS

LIST OF FIGURES

LIST OF TABLES

LIST OF PLATES

LIST OF ABBREVIATIONS

CHAPTER 1: INTRODUCTION

- 1.1 General
- 1.2 Problem Statement
- 1.3 Objectives
- 1.4 Scope of Study
- 1.5 Significance of Study

CHAPTER 2: LITERATURE REVIEW

- 2.1 General
- 2.2 Reclaimed Asphalt Pavement (RAP)
- 2.3 Black Rock Study
- 2.4 Asphalt Chemistry
 - 2.4.1 Fourier Transform Infrared (FTIR)
 - 2.4.2 X-ray Diffraction (XRD)
 - 2.4.3 Differential Scanning Calorimetry (DSC)
- 2.5 Superpave Binder Grading and Binder Blending
- 2.6 Mixture Performance
- 2.7 Summary

CHAPTER 3: MATERIALS AND METHODS

- 3.1 Introduction
- 3.2 Aggregate
 - 3.2.1 Aggregate Type
 - 3.2.2 Aggregate Properties
 - 3.2.2.1 Specific Gravity and Water Absorption Tests
- 3.3 Asphalt Binder
 - 3.3.1 Binder Properties
 - 3.3.1.1 Penetration Test
 - 3.3.1.2 Ring and Ball Test
 - 3.3.1.3 Viscosity Test
 - 3.3.1.4 Dynamic Shear Rheometer
 - 3.3.1.5 Fourier Transform Infrared (FTIR) Spectroscopy
 - 3.3.1.6 X-Ray Diffraction

- 3.3.2 Aging Protocol
 - 3.3.2.1 Short-Term Aging
 - 3.3.2.2 Long-Term Aging
- 3.3.3 RAP Modified Binder Designation and Characterizing Flow Chart
- 3.4 Sample Preparation
 - 3.4.1 Marshall Specimen
 - 3.4.1.1 Determination of Specific Gravity and Air Voids
 - 3.4.1.2 Marshall Test
 - 3.4.2 RAP Materials
 - 3.4.2.1 RAP Binder Content Determination by Ignition Method
 - 3.4.2.2 RAP Aggregate Gradation
 - 3.4.2.3 Determining Weight of Dry RAP Material, RAP Aggregate and RAP Binder

CHAPTER 4: MIX DESIGN

- 4.1 Introduction
- 4.2 RAP Aggregate Gradation
 - 4.2.1 RAP Aggregate Gradation after Separating into Batching Sizes
- 4.3 RAP Binder
- 4.4 Optimum Asphalt Content
- 4.5 Summary

CHAPTER 5: PHYSICAL, RHEOLOGICAL AND CHEMICAL PROPERTIES OF RAP BINDER

- 5.1 Introduction
- 5.2 RAP Binder Content
- 5.3 RAP Aggregate Gradation
- 5.4 RAP Binder Physical Properties
- 5.5 RAP Binder Rheological Properties
- 5.6 Viscosity-Temperature Dependency of RAP Binder
- 5.7 Virgin Bitumen Incorporating Recovered Reclaimed Asphalt Pavement Binder
 - 5.7.1 Penetration
 - 5.7.2 Softening Point
 - 5.7.3 Viscosity
 - 5.7.4 Penetration Index
 - 5.7.5 Viscosity Aging Index
 - 5.7.6 Fourier Transform Infrared Spectroscopy
 - 5.7.7 X-ray Diffraction
 - 5.7.8 Carbonyl Groups of Modified RAP Binders
 - 5.7.9 Sulfoxide Groups of Modified RAP Binders
 - 5.7.10 Correlation between Penetration Index, Viscosity Aging Index and Area Ratio

- 5.7.11 Mixing and Compaction Temperatures
- 5.8 Characterization at High Temperatures
 - 5.8.1 Effects of RAP on Viscosity
 - 5.8.1.1 Effects of Sasobit[®] Content on Viscosity
 - 5.8.2 Effects of RAP Binder on Construction Temperatures
 - 5.8.3 Selection of RAP Source and RAP Content
 - 5.8.3.1 Scenario 1
 - 5.8.3.2 Scenario 2
 - 5.8.3.3 Scenario 3
- 5.9 Effects of Aged Binder Content on CO₂ Emission

CHAPTER 6: RAP MIXTURE PERFORMANCE

- 6.1 Introduction
- 6.2 Indirect Tensile Strength Test
- 6.3 Moisture Sensitivity Test
- 6.4 Resilient Modulus
 - 6.4.1 Resilient Modulus at Varying Binder Contents
 - 6.4.2 Effects of Short-term Ageing on Resilient Modulus of Porous Mixtures
 - 6.4.3 Effects of Long-term Ageing on Resilient Modulus of Porous Mixtures
- 6.5 Characterization at intermediate temperatures
 - 6.5.1 Rutting Parameter
 - 6.5.2 Effects of RAP Binder on Aging Factor
 - 6.5.3 Fatigue Parameter
 - 6.5.4 Analysis of Fuel Requirement and GHG Emissions
- 6.6 Dynamic Modulus
 - 6.6.1 Phase Angle
 - 6.6.2 Effect size of the main and interaction effects
- 6.7 Asphalt mixtures stiffness
- 6.8 Effects of RAP source and content on energy activations of asphalt binders
 - 6.8.1. AE based on viscosity
 - 6.8.2. AE based on $G^*/\sin \delta$
 - 6.8.2. AE based on $G^* \cdot \sin \delta$

CHAPTER 7: CONCLUSIONS

- 7.1 Conclusion

List of Figures

- Figure 2.1 : Schematic Life Cycle of Asphalt Pavements
- Figure 2.2 : Composite Layered System in RAP-Virgin Material Mixtures
- Figure 2.3 : Virgin Aggregate-RAP Mixtures (a) Before Dry Blending and (b) After Dry Blending
- Figure 2.4 : (a) Asphalt Content and (b) Percent of Asphalt Binder Loss of RAP Particles
- Figure 2.5 : Layers of Asphalt Coating RAP Aggregate
- Figure 2.6 : Functional Groups Present in Asphalt
- Figure 2.7 : Infrared Spectra of Fresh (RT-F) and Aged (RT-R after RTFO and RT-P after RTFO+PAV) Asphaltenes in the Carbonyl Region
- Figure 2.8 : The Peaks of an X-ray Diffractogram
- Figure 2.9 : DSC Curves of Straight Asphalt and Two Blown Asphalt; (a) Straight Run Asphalt; (b) Blown Asphalt (3 Hrs) and (c) Blown Asphalt (5 Hrs)
- Figure 2.10 : DSC Thermograms obtained at a Heating Rate of 5 °C/min for various Asphalts. The Glass Transition Temperature T_g at the Midpoint is marked on each Curve
- Figure 2.11 : Blending chart (RAP percentage known)
- Figure 2.12 : Blending chart (RAP percentage unknown)
- Figure 3.1 : Dynamic Shear Rheometer
- Figure 3.2 : A Flow Chart to Characterize the Physical, Rheological and Chemical Properties of RAP Modified Binder
- Figure 4.1 : Volumetric Properties of the Marshall Specimens in determining OBC for Virgin Mixture
- Figure 5.1 : Average Asphalt Content of Reclaimed Asphalt Pavement
- Figure 5.2 : Aggregate Gradations of PLUS and LDP RAP Samples (LLM-ACWC20)
- Figure 5.3 : Aggregate Gradations of JKR RAP Samples (JKR-ACWC14)
- Figure 5.4 : Stiffness of Recovered RAP Binders
- Figure 5.5 : DSR Test Results for Blended Unaged Binder with 15% Recovered RAP Binder
- Figure 5.6 : DSR Test Results for Blended Unaged Binder Incorporating 30%

Recovered RAP Binder

- Figure 5.7 : $G^*/\sin \delta$ for Unaged RAP Blends
- Figure 5.8 : Viscosity-Temperature Relationship of Unaged Virgin and Blended Binders
- Figure 5.9 : Viscosity-Temperature Relationship of Short-Term Aged Virgin and Blended Binders
- Figure 5.10 : Viscosity-Temperature Relationship of Short-Term Aged Virgin and Blended Binders
- Figure 5.11 : Penetration of RAP Modified Binder under different Aging Conditions
- Figure 5.12 : Softening Point of RAP Modified Binder under different Aging Conditions
- Figure 5.13 : Viscosity of RAP Modified Binder under different Aging Conditions at 135°C
- Figure 5.14 : FTIR Spectrum of Virgin Binder
- Figure 5.15 : FTIR Spectrum of Virgin Binder Blended with JKR RAP Binder
- Figure 5.16 : FTIR Spectrum of Virgin Binder Blended with LDP RAP Binder
- Figure 5.17 : FTIR Spectrum of Virgin Binder Blended with PLUS RAP Binder
- Figure 5.18 : Transform Infrared Spectroscopy Spectrum of RAP Modified Binders
- Figure 5.19 : The X-Ray Pattern of Virgin Binder Blended with JKR RAP Binder
- Figure 5.20 : Mixing and Compaction Temperatures
- Figure 5.21 : Viscosity-Temperature Dependency of Virgin and RAP Modified Binder
- Figure 5.22 : Viscosity–Sasobit[®] Content Dependency for (a) Unaged PG64, (b) Short Term Aged PG64, (c) Long Term Aged PG64, (d) Unaged PG70, (e) Short Term Aged PG70, (f) Long Term Aged PG70
- Figure 5.23 : Effects of Aged Binder Content on CO₂ Emission for Scenario 1
- Figure 5.24 : Effects of aged binder content on CO₂ emission for scenario 2
- Figure 6.1 : Indirect Tensile Strength of RAP Mixtures
- Figure 6.2 : Moisture Sensitivity Test Results
- Figure 6.3 : Resilient Modulus at 10°C versus Bitumen Content (Un-aged)
- Figure 6.4 : Resilient Modulus at 25°C versus Bitumen Content (Un-aged)

- Figure 6.5 : Resilient Modulus at 25°C versus Bitumen Content (Un-aged)
- Figure 6.6 : Relationship between $G^* \sin \delta$, Temperature, RAP Binder Source and Content
- Figure 6.7 : Dynamic Modulus at different RAP Content, Temperature and Frequency
- Figure 6.8 : Interaction Plot of Temperature and RAP against Dynamic Modulus at 10 Hz
- Figure 6.9 : Phase Angle at Different RAP Content, Temperature and Frequency
- Figure 6.10 : Interaction Plot of Temperature and RAP against Phase Angle at 10 Hz
- Figure 6.11 : Cole–Cole Curve of the Relationship between E' and E''
- Figure 6.12 : Master Curves at Different RAP Percentages
- Figure 6.13 : Relationship between Measured $|E^*|$ Laboratory and $|E^*|$ Predicted
- Figure 6.14 : Master Curve of Rutting Factor versus Frequency Sweep at Designated Temperatures
- Figure 6.15 : MasterCurve of Fatigue Factor versus Frequency Sweep at Designated Temperatures
- Figure 6.16 : Rutting Factor and Fatigue Parameter

List of Tables

- | | | |
|------------|---|--|
| Table 1.1 | : | Cost of Materials in a 1,000 kg Batch of HMA |
| Table 2.1 | : | Modes of Vibration and Peak Centre |
| Table 2.2 | : | Characteristics of the Asphalts |
| Table 3.1 | : | PWD Gradation Limits for Asphaltic Concrete ACW14 |
| Table 3.2 | : | Aggregate Specific Gravity and Water Absorption |
| Table 3.3 | : | Physical and Rheological Properties of Virgin and Recovered Binders |
| Table 3.4 | : | DSR Input parameter and test configuration |
| Table 3.5 | : | RAP Modified Binder Designation |
| Table 3.6 | : | Mixing and Compaction Temperatures |
| Table 4.1 | : | Average Gradation of RAP Aggregates |
| Table 4.2 | : | Average RAP Aggregate Separated into Batching Sizes |
| Table 4.3 | : | Average Gradation of PLUS RAP Aggregates Separated into Batching Sizes |
| Table 4.4 | : | Average Gradation of LDP RAP Aggregates Separated into Batching Sizes |
| Table 4.5 | : | Average Gradation of JKR RAP Aggregates Separated into Batching Sizes |
| Table 4.6 | : | Amount of Virgin Aggregates to Incorporate with PLUS RAP |
| Table 4.7 | : | Amount of Virgin Aggregates to Incorporate with LDP RAP |
| Table 4.8 | : | Amount of Virgin Aggregates to Incorporate with JKR RAP |
| Table 4.9 | : | Average Asphalt Content of RAP |
| Table 4.10 | : | Average Asphalt Content of RAP after Separating into Batching Sizes |
| Table 4.11 | : | Amount of Dry RAP and RAP Binder in Various Percentage of RAP |
| Table 4.12 | : | JKR ACW14 Specification Parameters |
| Table 4.13 | : | Optimum Asphalt Content of Recycled Mixtures |
| Table 4.14 | : | Percent virgin and RAP binder in recycled asphalt mixture |
| Table 5.1 | : | Percent Retained and Passing 5 mm Sieve of all RAP Aggregates |

Table 5.2	:	Penetration and Softening Point of Virgin and RAP Binders
Table 5.3	:	DSR Test Results of Recovered RAP Binders
Table 5.4	:	Results of DSR Testing of Unaged Blended Binders
Table 5.5	:	Rate of Increase in $G^*/\sin \delta$ for Unaged Blends
Table 5.6	:	Percent Increased in Viscosity of Unaged Blended Binders
Table 5.7	:	Percent Increased in Viscosity after Short-Term Aged Blended Binders
Table 5.8	:	Percent Increased in Viscosity after Long-Term Aged Blended Binders
Table 5.9	:	Percentage Change in Penetration and Softening Point of Modified RAP Binders
Table 5.10	:	Penetration Index and Viscosity Aging Index of RAP Modified Binders
Table 5.11	:	Percent Increased in Absorbance
Table 5.12	:	Area Ratio of RAP Modified Binders before and after Aging
Table 5.13	:	Coefficient of Correlation Analysis
Table 5.14	:	Results of Analysis of Variance (ANOVA) for Viscosity
Table 5.15	:	Construction Temperatures for Virgin and RAP Modified Binders
Table 6.1	:	Paired t-Test Comparisons of Strengths of Mixtures with different RAP Contents
Table 6.2	:	Resilient Modulus Test Results Subjected to STA
Table 6.3	:	Resilient Modulus Test Results Subjected to LTA
Table 6.4	:	$G^*/\sin \delta$ for Unaged and Short Term Aged Virgin and RAP Modified Binders
Table 6.5	:	Results of Analysis of Variance (ANOVA) for $G^*/\sin \delta$
Table 6.6	:	Upgrading of PG64 Binder due to Incorporating RAP Binder
Table 6.7	:	AF Values for Virgin and RAP Modified Binders
Table 6.8	:	Conversion Factors for Different Fuel Types (DTI, 2006)
Table 6.9	:	Conversion Factors for GHG (DEFRA, 2010)
Table 6.10	:	Fuel Requirements based on RAP Source and RAP Content
Table 6.11	:	GHG Emissions ^a based on RAP Source and RAP Content

- Table 6.12 : ANOVA Results on Main and Interaction Effects on Dynamic Modulus
- Table 6.13 : ANOVA Results on Main and Interaction Effects on Phase Angle
- Table 6.14 : Effect Size (ω^2) of the Main and Interaction Effects
- Table 6.15 : AE for the asphalt blends based on viscosity
- Table 6.16 : Difference AE values and change percentage due to short-term-aging based on viscosity
- Table 6.17 : AE for the asphalt blends based on $G^*/\sin \delta$
- Table 6.18 : Difference in AE values and change percentage due to short-term-aging based on $G^*/\sin \delta$
- Table 6.19 : AE for the asphalt blends based on $G^* \cdot \sin \delta$

List of Plates

Plate 3.1 : RAP Sample Before and After Ignition Oven Test

LIST OF ABBREVIATIONS

AAMAS	Asphalt Aggregate Mixture Analysis System
ACWC	Asphalt Cement Wearing Course
AE	Activation Energy
ANOVA	Analysis of Variance
BBR	Bending Beam Rheometer
DPE	DamansaraPuchong Expressway
DSC	Differential Scanning Calorimetry
DSR	Dynamic Shear Rheometer
FTIR	Fourier Transform Infrared
HMA	Hot Mix Asphalt
JKR	JabatanKerja Raya
LCA	Life Cycle Assessment
LDP	Lebuh Raya DamansaraPuchong
LEED	Leadership in Energy and Environmental Design
MEPDG	Mechanistic Empirical Pavement Design Guide
NSE	North South Expressway
OBC	Optimum Binder Content
PA	Porous Asphalt
PAV	Pressure Aging Vessel
PLUS	ProjekLebuh Raya Utara-Selatan
PWD	Public Work Department
RAP	Reclaimed Asphalt Pavement
RT-F	Infrared Spectra of Fresh
SCB	Semi-Circular Bending
TSR	Tensile Strength Ratio
XRD	X-ray Diffraction

LIST OF PUBLICATIONS
(Journals, proceedings, chapter in a book)

Che Wan C.N., Hamzah M.O. and Ramadhansyah P.J., (2010). Effects of Temperature and Binder Type on the Resilient Modulus Properties of Porous Asphalt Subjected to Ageing. Proceedings of the First Makassar International Conference on Civil Engineering (MICCE2010), Makassar, Indonesia March 9-10.

Hamzah M.O. and Shahadan Z., (2009). Rheological Properties of Recovered Binder from Aged Asphalt Pavements. International Conference on Building Science and Engineering (ICON-BSE), Universiti Tun Hussein Onn Malaysia.

Hamzah M.O. and Shahadan Z., (2011). Effects of Aging on the Physical, Rheological and Chemical Properties of Virgin Bitumen Incorporating Recovered Reclaimed Asphalt Pavement Binder. Australian Journal of Basic and Applied Science, ISSN 1991-8178, Vol. 5, No. 5, pp. 1323-1331.

Hamzah M.O., Jamshidi A. and Shahadan Z., (2010). Effects of Sasobit® on the Required Heat Energy Emission on Blended Asphalt Binder Incorporated Binder. European Journal of Scientific Research, ISSN 1450-216X, Vol. 42, No. 1, pp. 16-24.

Hamzah M.O., Jamshidi A., Kanitpong K. and Aman M. Y., (2012). Parameters to Characterise the Effects of Sasobit Content on the Rheological Properties of Unaged and Aged Asphalt Binders. Road Material and Pavement Design. DOI:10.1080/14680629.2012.668836.

Jamshidi A., Hamzah M.O. and Shahadan Z., (2012). Selection of Reclaimed Asphalt Pavement Sources and Contents for Asphalt Mix Production Based on Asphalt Binder Rheological Properties, Fuel Requirements and Greenhouse Gas Emissions. Journal of Cleaner Production, Vol. 23, pp. 20-27.

Hamzah M.O., Shahadan Z., Hasan M.R.M. and Jamshidi A., (2010). Sustainable Asphalt – The Way Forward for the Malaysian Asphalt Industry, 8th Malaysian Road Conference, Kuala Lumpur, 10-12 Oct.

Shahadan Z., Hamzah M.O., Yahya A.S. And Aman M.Y., (20xx). Evaluation Performance of Asphalt Mixture Incorporating Reclaimed Asphalt Pavement in Dynamic Modulus. Indian Journal of Engineering and Material Sciences (Under Review)

Ali Jamshidi, Meor Othman Hamzah, Zulkurnain Shahadan, (20xx), Rheological characterization of asphalt binders blended with different contents of recovered aged binders from various sources, Full paper completed and will be enhanced and formatted for submission to an ISI journal

Professorial talk booklet entitled: Sustainable Development in Asphalt Technology to Ensure the Survival of the Nation's Asphalt Industries, USM Publishers, 15 December 2010

CHAPTER ONE

INTRODUCTION

1.6 General

Reclaimed asphalt pavement (RAP) is a recycling hot mix asphalt (HMA) material results in a reusable mixture of aggregate and asphalt binder. Materials present in old Hot Mix Asphalt pavement still retain considerable value which can be incorporated into virgin asphalt mixture. In the light of increasing cost of asphalt due to escalating price of crude oil (asphalt is manufactured from crude oil), the scarcity of quality aggregates and the pressuring need to preserve the environment, recycling of asphalt pavement has been proven to be economical and environmentally sound in highway construction and rehabilitation (FHWA, 1997). In the USA, 80% of the total asphalt surface material removed during widening and resurfacing project is recycled and saving more than \$300 million annually (Holtz and Eighmy, 2000 and Sufian et al., 2007). While in Europe, engineering and environmental life-cycle cost and benefit are the basis for many of the recycling initiatives. Countries like Denmark and Netherland have used 100% RAP meanwhile Sweden and Germany recycled 95% and 55% of asphalt surface material respectively (Holtz and Eighmy, 2000). Table 1.1 shows cost of in-plant hot-mix incorporate with RAP in a 1,000 kg batch of HMA in Belgium. Pavement material costs are reduced approximately 26% if 40% RAP is used. After taking into account production costs, final cost of HMA ends up US\$18.40 per metric ton without RAP and US\$16.00 per metric ton with 40% RAP (Horvath, 2003).

Table 1.1: Cost of Materials in a 1,000kg Batch of HMA (Horvath, 2003)

Compound	Composition in the mixture, %	Unit Price (US\$/ton)	HMA without RAP (US\$/ton)	HMA with 40% RAP (US\$/ton)
Stones	58	10	5.8	3.5
Sand	30	8	2.4	1.5
Filler	7	20	1.4	0.84
Bitumen	5	100	5.0	3.0
RAP	0 – 40%	5		2.0
Total			14.6	10.8

The use of RAP also decreases the amount of waste produced and helps to resolve the disposal problems of highway construction material especially in large cities. In Malaysia, various recycling method techniques are adopted for rehabilitation work for asphalt pavement. There are approximately 1,190 km of highways and expressway, 13,592 km of paved federal roads and 36,263 km of paved state roads including municipal roads (Ahmad et. al., 2004). In every 3 to 5 years, the deteriorated wearing course is disposed of in large volumes in the form of waste and yet, no initiative taken by road builders to use RAP in construction or rehabilitation of highway and roads. Malaysia government should make it mandatory for the road builders rather than optional to use RAP in awarding contracts so that it will help in reducing abundance of reusable asphalt pavement material stockpiled in empty fields or by roadsides and subsequently, lower the cost of building new highway and roads. Many studies have shown that addition RAP in new HMA have no significant effect on pavement performance compare to virgin HMA at certain level percentage of RAP (Nassar and Nassar, 2006, Widyatmoko, 2008, Xiao et al., 2007). It is also been found that inclusion

of RAP in HMA increases the binder stiffness and hence the mixture stiffness which improved rutting performance of HMA and moisture resistance but at certain RAP contents its reduced fatigue life (Xiao et al., 2007, Aravind, 2007, Kennedy, 1998). It is hypothesized that RAP contents up to 20% incorporate in conventional HMA mixture, have no effect on binder and contribute equal or better performance than virgin HMA. This study will give better understanding of quality and performance of HMA mixture incorporate with RAP.

1.7 Problem Statement

Every year, millions of ton of severely deteriorated pavement and hot mix pavement that has reached service life are milled up and wasted even though it is still have substantial engineering value and economically it can save cost of construction or rehabilitation pavement surface if it is recycled. Currently, in this country, there is no attempt yet to incorporate recycling asphalt pavement in HMA produces in-plant maybe due to no guidelines and proper study on the mix design containing RAP and lack of information on performance of the RAP mixtures. Given the aforementioned benefits from the use of RAP in construction or rehabilitation pavement surface, a research should be conducted to determine how the use of RAP affects the mix design and performance of the mixtures that contain varying percentages of RAP materials.

1.8 Objectives

The study aimed to fulfill the following objectives:

- i. To investigate the RAP material characteristic and variability of three different RAP sources with respect of binder content, binder stiffness and aggregate gradation.
- ii. To evaluate the addition of various percentage of RAP binder from different RAP sources that affect the resulting physical, rheological and chemical properties of RAP modified binder.
- iii. To develop asphalt binder blending charts which can be used as guidelines for engineers to select RAP content so that the mix design specification requirement is fulfilled for a given project.
- iv. To evaluate the addition of various percentages of RAP in HMA mixtures that affect the performance of asphalt mixtures.

1.9 Scope of Study

To accomplish these objectives, a research plan was developed which involving extensive laboratory testing. RAP materials were obtained from milled up deteriorated asphalt cement wearing course (ACWC) from three different expressways in the country. The first test started with investigating the quality and gradation of virgin materials and RAP samples. It follows by exploring rheological properties of virgin, RAP binders and blended binders. After that developing blending binder charts. Then performing mixture designs for 100% virgin materials followed by mixture design for different RAP source and RAP content where for each mix, the optimum asphalt content and volumetric properties were determined. Finally, performance tests are carried out to evaluate the mixtures at different RAP sources and contents. A testing matrix was constructed for mixtures containing 5 different percentages of RAP and one virgin binder grades were used. The matrix was designed to determine the amount of RAP and virgin binder which may be added to the mixture in order to yield properties considered acceptable for a mixture composed entirely of virgin materials.

1.10 Significance of Study

- i. Use of RAP will change engineering properties of the resulting binder blend due to addition of old binder. The stiffness of the binder blend increases with RAP content.**
- ii. Increasing RAP content contributes to higher tensile strength, resistance to permanent deformation and fatigue performance.**
- iii. RAP contents up to 20% incorporate in conventional HMA mixture, have no effect on binder and give equal or better performance than virgin HMA.**
- iv. RAP content influences the tensile strength and fatigue life of the mixes. Increases RAP content will produce higher tensile strength but lower fatigue life.**
- v. Determination of maximum RAP content in HMA mix contribute to lower fatigue life than virgin HMA mix**
- vi. The government will save approximately RM90,000 for every kilometer if 20% RAP is incorporated in HMA for constructing/rehabilitating pavement surface (ACW) of a two-lane dual carriageway highway.**
- vii. The results of this research will be a guideline to engineers and quarry operators when designing and producing HMA incorporating with RAP.**

CHAPTER TWO

LITERATURE REVIEW

2.1 General

Waste materials from civil engineering construction and maintenance works have increasingly threatened the environment and public health. Environmental policy makers and project managers have tried to develop new technologies to recycle waste materials using energy efficient methods while simultaneously imposing minimum environmental loads. Therefore, factors related to sustainability and environmental impacts have equal if not greater importance for decision makers to consider in infrastructure construction. Currently, due to greater demands for natural resources conservation and sustainability, various construction and infrastructure development alternatives are assessed to select the most sustainable strategy using tools such as Life Cycle Assessment (LCA) and Leadership in Energy and Environmental Design (LEED) for all components and stages, including raw materials selection, method of construction, utility and recycling of a product, from cradle to the grave (Dovi et al., 2009; Millet et al., 2010; Huang et al., 2009; Optis and Wild, 2010; Bahr and Steen, 2004; Gabel et al., 2004 and Manfredi et al., 2011). For example, Khoo et al. (2010) found that the type of energy provided to the product's life cycle has a significant effect on the total environmental impacts. One alternative is the use of waste materials in infrastructure construction and rehabilitation.

2.2 Reclaimed Asphalt Pavement (RAP)

Pavements are one of the most important infrastructures that provide safe and efficient transportation for human communities while asphalt binder is the most prevalent material used in asphalt pavement construction. When an asphalt concrete pavement reaches the end of its design life, the road surfacing is milled, creating a milling waste material known as Reclaimed Asphalt Pavement as indicated by arrow A in Figure 2.1 (Al-Qadi et al., 2007). The RAP materials contain aggregates and asphalt binders which are transported to an asphalt plant for recycling (Arrow B in Figure 2.1). RAP is 100% recyclable and has become a popular waste material in pavement construction and rehabilitation as illustrated by Arrow C in Figure 2.1. RAP in old hot-mix asphalt pavement still retain considerable value which can be incorporated into the virgin asphalt mixture. In the light of increasing cost of asphalt due to escalating price of crude oil and availability in the past few years, the scarcity of quality aggregates and the pressuring need to preserve the environment, recycling of asphalt pavement has been proven to be economical and environmentally sound in highway construction and rehabilitation.

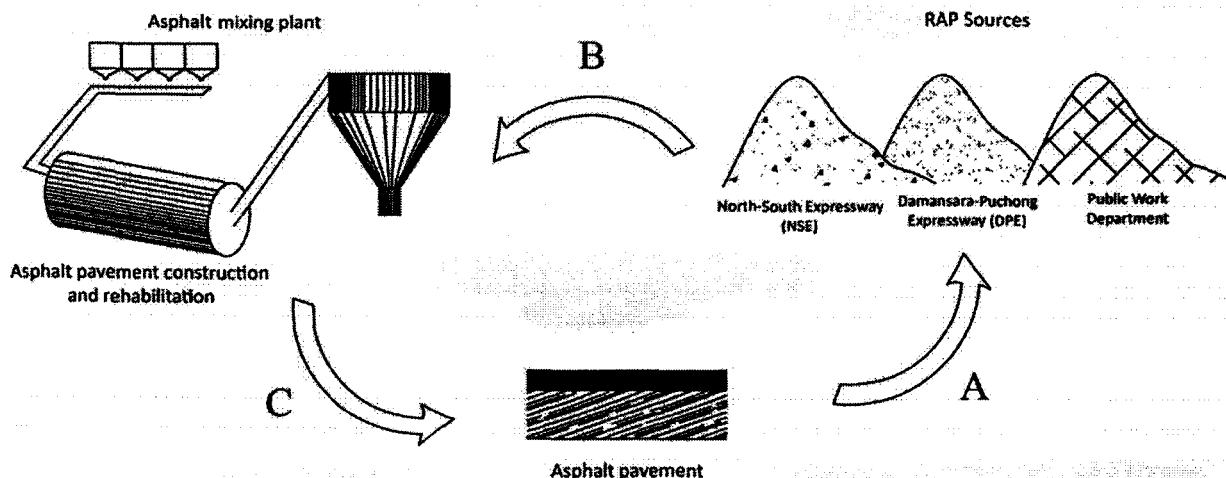


Figure 2.1: Schematic Life Cycle of Asphalt Pavements (Source: Al-Qadi et al., 2007)

RAP is one of the largest recycled materials produced by the asphalt industries. Nowadays the use of RAP as secondary material in the production of asphalt mixes has become a norm and a cost effective method of pavement construction and rehabilitation. For instance, in the United States, almost 100 million tons of RAP are produced annually, with about 60 million tons being reused in the construction of new asphalt pavements, while the remaining 40 million tons used in other pavement-related applications, such as aggregate road base (NAPA, 2009). Utilizing RAP or milling waste in asphalt mixes has offered many advantages which includes the preservation of existing road profile and the environment, conservation of asphalt binder and aggregate resources, conservation of energy and reduction in life-cycle cost (Kandhal and Mallick, 1997). Since aggregate materials are non-renewable natural resources, the primary benefit of using RAP is to reduce demand for extraction of new aggregate and helps to ease pressures on landfills (Chiu et al., 2008 and Huang et al., 2007). Lee et al. (2010) showed that the use of RAP in pavement base and sub-base layers could reduce global warming potentials (20%), energy consumption (16%), water consumption (11%), life cycle costs (21%) and, hazardous waste generation (11%). Consequently, the use of RAP is in harmony with efforts to develop sustainable pavements based on the green design concept since 40% of the global primary energy consumption and CO₂ emission is related to the production of materials (Hekkert et al., 2000).

Recycling of RAP has been practiced in the United States since 1915 and continues to increase appreciably in the 1970s with the Arab oil embargo causing inflation of construction cost due to limited oil supplies (Kandhal and Mallick, 1997). Today, the United States and several European countries have been using reclaimed asphalt pavement from 80% up to 100% in an effort to promote recycling in sustainable road construction (Holtz and Eighmy, 2009). In the USA, 80% of the total asphalt surface material removed during widening and resurfacing project is recycled and saving more than \$300 million annually (USDOT, 1997). While in Europe, engineering and environmental life-cycle cost and benefit are the basis for many of the recycling initiatives. Countries like Denmark and Netherland have used 100% RAP meanwhile Sweden and Germany recycled 95% and 55% of asphalt surface material respectively (Holtz and Eighmy, 2000). In terms of performance, studies have shown that addition of RAP in new HMA have no significant effects on pavement performance compared to virgin mix at certain percentage level of RAP (Aravind and Das, 2007). Many laboratory and field studies have shown that asphalt mixtures containing RAP performed

similar if not better than conventional asphalt materials in terms of indirect tensile strength, moisture susceptibility, permanent deformation and fatigue (Su et al., 2009 and Widyatmoko, 2008). It has also been found that the inclusion of RAP in HMA increases the mixture stiffness which improved rutting performance of HMA and moisture resistance (Xiao et al., 2007 and Widyatmoko, 2008). From fields test recycled asphalt pavement is able to withstand increasing number of vehicles and higher axle load imposed by different axle configurations and severe climatic conditions. Addition of reclaimed asphalt pavement in asphalt mixture has improved permanent deformation and fatigue distresses (Su et al., 2009; Aravind and Das, 2007 and Widyatmoko, 2008).

In Malaysia, recycling was started in 1993 with the arrival of first recycling machine and also the first Asian country to use cold in-place recycling (Lewis, 2004). However, the resulting recycled pavement exhibited poor durability. As technology developed, road concessionaires and JKR are adopting mill and pave technique as rehabilitation works on most of all surface distress pavements. In this method, the old asphalt pavement and distressed pavement are milled and replaced by new HMA. This is a good opportunity to reclaim and reuse the milled asphalt pavement rather than dump it elsewhere unused because it still has valuable properties and substantial strength to be incorporated in new mixes. Every year, hundreds of kilometres of asphaltic pavement is milled up in this country and wasted even though it still has substantial engineering value and economically it can save cost of construction or rehabilitation pavement surface if it is recycled. However, it is important to ensure that the RAP materials are compatible with the virgin materials and that the final blend meets all the mix and binder requirements. Currently, there appear to be a lack of an extensive study to incorporate recycling asphalt pavement in HMA produces via the quarry drum or batch plants maybe due to the absence guidelines on the mix design containing RAP and lack of information on performance of the local RAP mixed with virgin asphalt and aggregates.

2.3 Black Rock Study

The issue of whether RAP acts like a black rock or whether there is, in fact, some blending that occurs between the old, hardened RAP binder and the added binder has initiated many researches on binder blending and recycled mixture performance. If RAP were a black rock, the mixture properties would depend on the virgin binder with no effect of the RAP binder. A comprehensive study of RAP in HMA was reported in NCHRP 9-12 which concluded that at 40% RAP content, the black rock exhibited significant differences in laboratory performance compared with the actual practice and total blending mixture. There were no significant differences between the total blending and actual practice mixtures (McDaniel and Anderson, 2001). An investigation on the blending process between aged and virgin asphalt was carried out by Oliver (2001). It was found that aged and virgin binders might not fully blend in hot mix asphalt containing RAP materials. The formation of agglomerates of aggregate and filler made it harder for the fresh binder to penetrate. Even though the aged asphalt could not fully blend with the virgin asphalt, it forms a layer coating the RAP aggregate. After the long term aging, this layer is much stiffer than the virgin binder. Thus, a composite layered system exists in the RAP – virgin material mixture as shown in Figure 2.2. Such a composite structure would be favourable in reducing the stress concentration and potentially would enhance the performance of asphalt mixture (Huang et al, 2005).

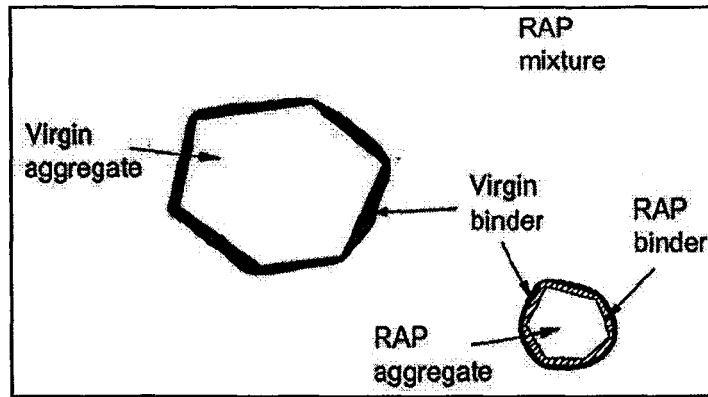


Figure 2.2: Composite Layered System in RAP-Virgin Material Mixtures
(Source: Huang et al., 2005)

Further investigation on the blending effect of the aged asphalt in RAP under normal mixing condition was carried out by Huang et al., (2005). In the test, RAP was blended with virgin aggregates only without any virgin asphalt binder being introduced. The virgin aggregates were all retained on No.4 sieve as coarse materials whereas the RAP particles were all screened by No.4 sieve, so they were easily separated after mixing. Three RAP proportions, 10%, 20% and 30% were considered and the blending was performed at 190 °C with 3 min mixing time. Figure 2.3 shows the materials before and after dry blending.

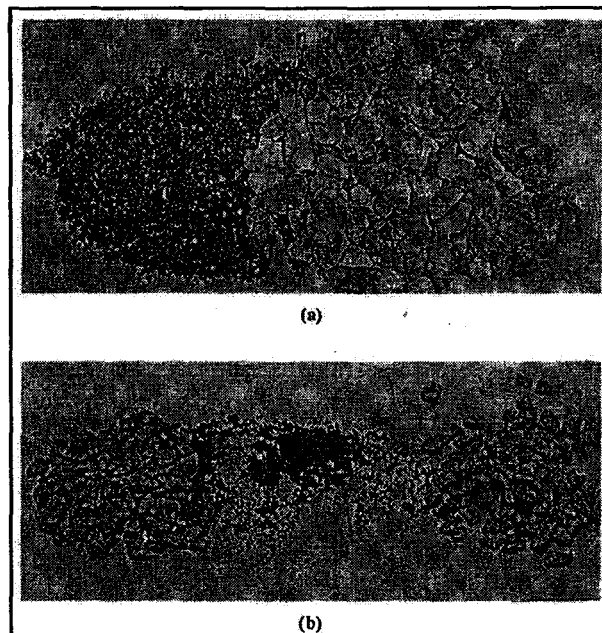


Figure 2.3: Virgin Aggregate-RAP Mixtures (a) Before Dry Blending and (b) After Dry Blending (Source: Huang et al., 2005)

Blending of virgin asphalt and aggregates with RAP materials was also carried out at the same mixing temperature and time. Virgin mixture consisted of coarse aggregates and RAP consisted of only fine particle after being separated. Staged extraction was used to obtain asphalt binders from different layers coating the RAP aggregates. Figure 2.4 shows the results of the asphalt contents and the percentage of asphalt binder loss for RAP particles due to pure mechanical dry blending. It appeared that regardless of RAP proportion, the asphalt

content of RAP was accounted for about 11% of binder loss due to pure mechanical blending. Only a small portion of the aged binder will be available to blend with virgin asphalt. Figure 2.5 presents the thicknesses of corresponding layers from the staged extraction. The thickness of corresponding layers around RAP particles from first to fourth layer were 2.0, 1.1, 1.8, and 1.6 micron assuming that the asphalt film thicknesses for different aggregate sizes were the same. The study also shows that asphalt viscosity increased aging from the outside layer to the inside where the asphalt in layer 3 and 4 was much stiffer than asphalt in layer 1 and 2. These results provide compelling evidence that RAP does not act like a black rock. Moreover, total blending of the RAP binder and virgin binder ever occurs but partial blending apparently occurs to some extent.

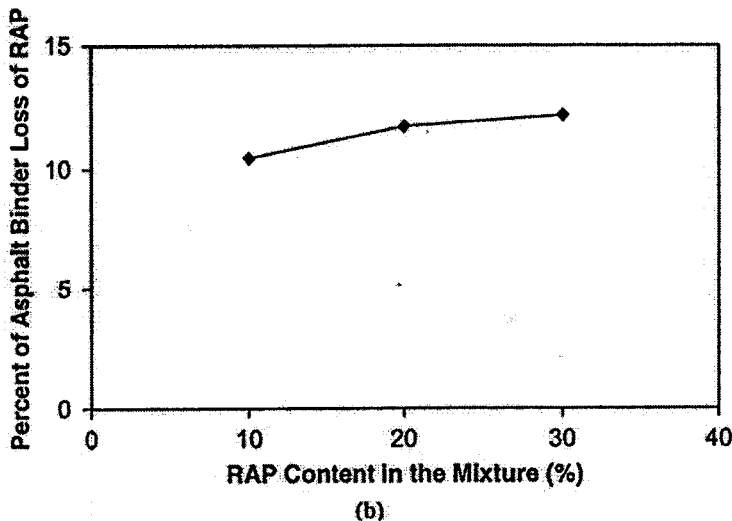
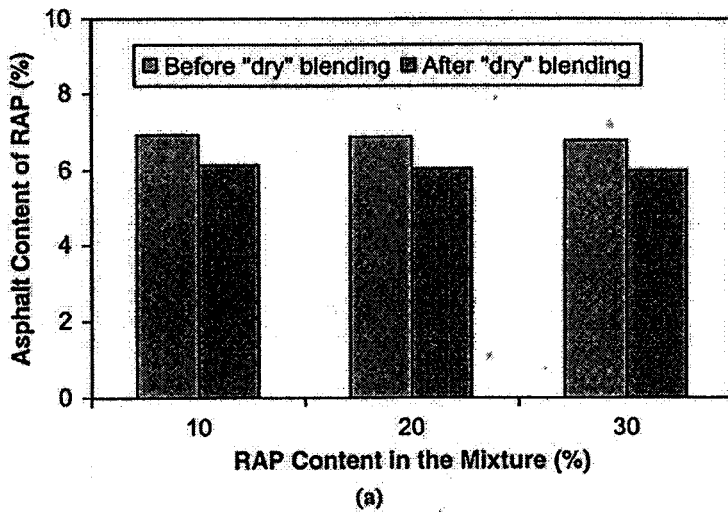


Figure 2.4: (a) Asphalt Content and (b) Percent of Asphalt Binder Loss of RAP Particles
(Source: Huang et al., 2005)

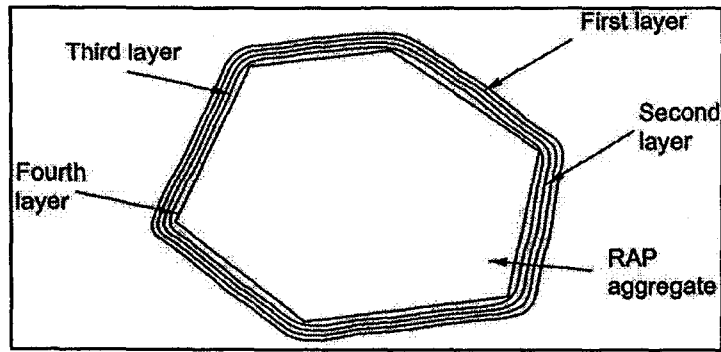


Figure 2.5: Layers of Asphalt Coating RAP Aggregate
(Source: Huang et al., 2005)

2.4 Asphalt Chemistry

During mixing, RAP materials are heated and blended at high temperature with hot virgin bitumen and fresh aggregates. It is expected that the highly oxidized RAP binder will melt off from RAP aggregate and intimately blended with the virgin bitumen and fresh aggregates. During this blending process, the virgin bitumen is supposed to rejuvenate the RAP binder such that the resultant binder meets the target viscosity. However, the chemical change that takes place in the RAP binder and virgin binder blends after mixing in-plant and during pavement service life is very much unknown. This is particularly of great concern since the RAP binder is known to be readily oxidized and the mixing process further aged the RAP binder. Under extreme aging conditions, even conventional binder is prone to lose its binding capacity. Subsequently it becomes less adhesive but more cohesive, and make it increasingly brittle (Valcke et al., 2009). Asphalt compound consists of asphaltenes, saturates, aromatics and resin fractions. Asphalt density at room temperature lies typically between 1.01 and 1.04 g/cm³ depending on the crude source and grade (Read and Whiteoak, 2003). Asphalt exhibits a glass transition around -20 °C, although it varies in a wide range from +5 °C down to -40 °C depending on the crude oil origin. The transition range normally spans from 30 to 45 °C and -20 °C which correspond to the midpoint value. Therefore, in thermodynamic standpoint, asphalt is very viscous at room temperature. The complexity of asphalt chemistry lies on many different chemicals that are present. Carbon and hydrogen are dominant constituents in asphalt chemical structures. This follows by sulphur in the form of sulphide, thiols and sulfoxide. Oxygen is typically present in the form of ketone, phenols and carboxylic acid. Nitrogen exists in pyrrolic and pyridinic structures, and in the form of amphoteric species, such as 2-quinolones. Figure 2.6 shows the functional groups that present in asphalt. The oxidation of binder further contributes to change in the structural and functional grouping that is responsible for chemical and physical aging (Lamontagne et al., 2001). The chemical change in asphalt structure after oxidation is easily detected because of the new chemistry elements that are formed. Chemically, aging leads to a decrease in aromatic content and subsequently increase in resin content together with higher asphaltenes content (Lesueur, 2009). A study by Zhang et al., (2011) found that after the short-term aging, the proportion of bitumen compounds such as asphaltene and resins were increased. Further aging the bitumen by subjecting to Pressure Aging Vessel (PAV) caused the asphaltenes and resins content to continually increase while the saturate contents remained constant. Apparently, severe oxidation on bitumen produces more asphaltenes which are present in the micelle form in a colloidal structure of bitumen, directly influencing physical, rheological and chemical properties of the bitumen (Lu and Isacsson, 2002; Lesueur D., 2009; Le Guern et al., 2010). There are three methods that can be used to examine asphalt

chemical properties. The methods are Fourier transform infrared, x-ray diffraction and differential scanning calorimetry.

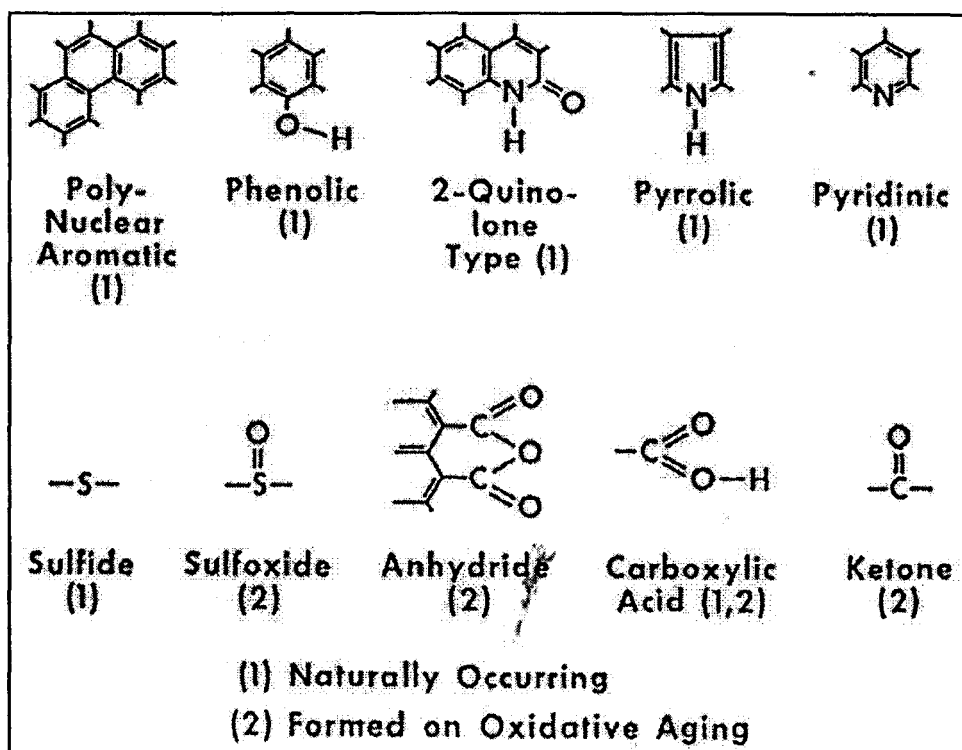


Figure 2.6: Functional Groups Present in Asphalt
(Source: Lesueur, 2009)

2.4.1 Fourier Transform Infrared (FTIR)

Fourier Transform Infrared Spectroscopy (FTIR) is used to study the distribution of functional group types that present in asphalts. FTIR is an excellent and popular tool to identify chemical evolution in bitumen and able to indicate the severity of oxidation experienced by the bitumen after aging. It has been a major analytical technique to study aging mechanism in asphalt through the characterisation of oxygen-containing functional and hydrocarbon groups. The FTIR can also yield quick qualitative and quantitative results that are highly reproducible. This technique can easily differentiate stretching vibration of carbonyl mode which is largely dominated by asphaltene compound after the aging process (Toteva et al., 2009). FTIR spectroscopy proved to be a very useful technique in analyzing structural changes in the fractions following RTFO and PAV tests of asphalts (Siddiqui and Ali, 1999; Lu and Isacson, 2002). Table 2.1 shows various modes of vibration and their peaks centre for asphalt (Siddiqui and Ali, 1999).

Table 2.1 Modes of Vibration and Peak Centre (Source: Siddiqui and Ali, 1999)

Modes of Vibration	Peak Centre (cm ⁻¹)	Area of Peak Between (cm ⁻¹)
C-H asymmetric stretch in CH ₃	2954	2972-2952
C-H in-phase stretch in CH ₂	2926	2936-2916
C-H out-of-phase stretch in CH ₂	2854	2863-2843
C-H symmetric deform in CH ₃	1376	1385-1365
C-H asymmetric deform in CH ₂ and CH ₃	1456	1490-1430
C=C stretch in aromatics	1605	1642-1547
C=O stretch in carbonyl/carboxylic	1698,1704	1752-1653
S=O stretch in sulfoxide types	1032	1065-1007

The carbonyl and/or carboxylic groups are indicated by the C=O stretch absorption at 1698 and 1704 cm⁻¹ in IR spectra. The area of the carbonyl absorption is calculated between 1752-1653 cm⁻¹, this covered the region containing the absorption peaks for carboxylic acid ketones and anhydrides. Ketones and anhydrides form on oxidative aging and carboxylic acids that occur naturally in asphalt but increased with oxidative aging. These three functional groups are the most significant chemical functionalities which are an integral part of large molecules and can be related to oxidative aging. Figure 2.7 shows infrared spectra of fresh and aged RT asphaltenes showing changes in the carbonyl region (Siddiqui and Ali, 1999).

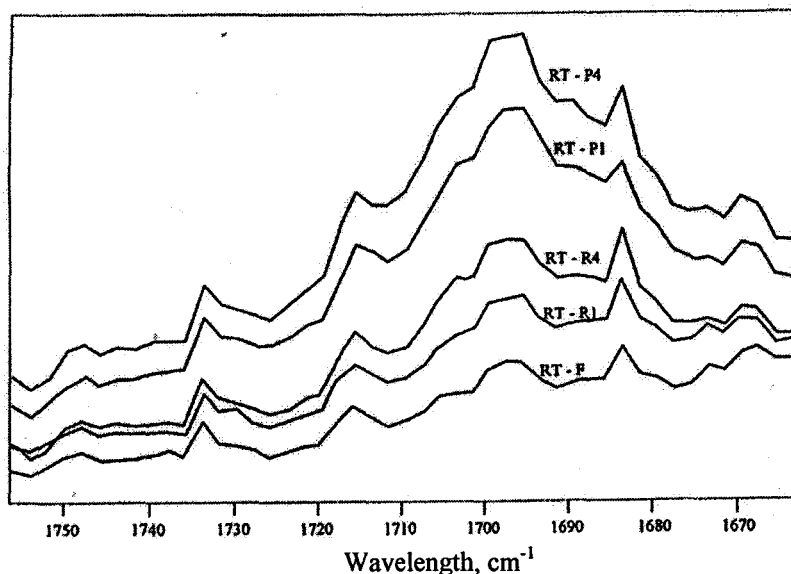


Figure 2.7: Infrared Spectra of Fresh (RT-F) and Aged (RT-R after RTFO and RT-P after RTFO+PAV) Asphaltenes in the Carbonyl Region (Source: Siddiqui and Ali, 1999)

2.4.2 X-ray Diffraction (XRD)

X-ray diffraction is the most commonly used technique for examining a structure or crystallization of asphalt compound by monitoring the position, shape, and intensity of the basal reflections of XRD pattern of the asphalt material (Jahromi and Khodaii, 2009). Figure 2.8 presents the peaks of an X-ray diffractogram. There are four peaks in the XRD pattern of asphaltenes and resin. The γ peak is thought to be the packing distance of saturated distance of structure which arises from X-ray scattered by aliphatic chains or condensed saturated

rings. The graphene peak or (002) peak comes from diffraction of X-rays of the stacks of aromatic molecules. The (10) and (11) peak reflections in the X-ray pattern are from the in-plane structure of the aromatics. They correspond to the first and second nearest neighbours in the rings compounds. The broader the peak in the XRD patterns, the more short-range order and less long-range order exists in the structure type. In general, sharp narrow XRD pattern peaks are from highly crystalline samples with high degree of long-range order (Siddiqui et al., 2002; Yufeng et al., 2009).

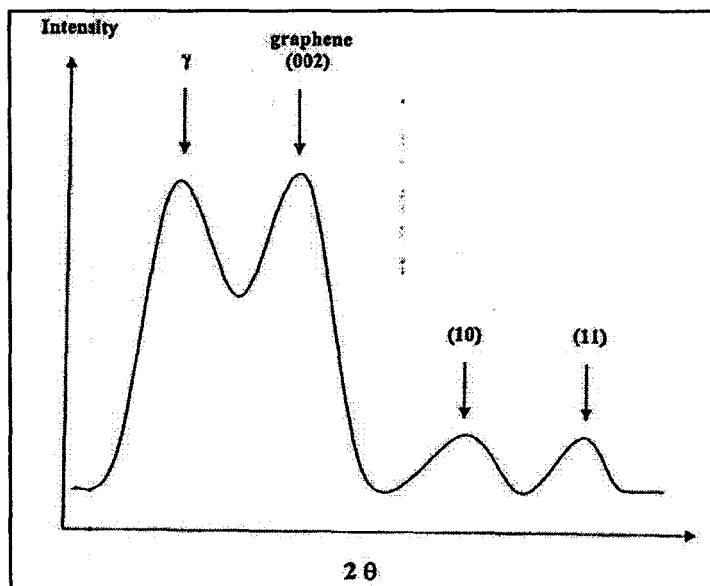


Figure 2.8: The Peaks of an X-ray Diffractogram
(Source: Siddiqui et al., 2002)

2.4.3 Differential Scanning Calorimetry (DSC)

Giavarini and Pochetti (1972) studied DSC analysis on a straight run asphalt and two blown asphalts which had been blowing for three hours and five hours respectively. Their findings indicate that glass transition temperature (T_g) for blown asphalts occur at high temperatures compared to straight run asphalt. Moreover, the longer the blowing time, the higher the glass transition temperature. The increase in T_g is due to the oxidation during the blowing process which has changed the chemical compound in the asphalt. The DSC curves for the asphalts are exhibited in Figure 2.9. The characteristic of the asphalt is summarized in Table 2.2. The researchers also believed that there is a connection between T_g and brittle point of a given asphalt.

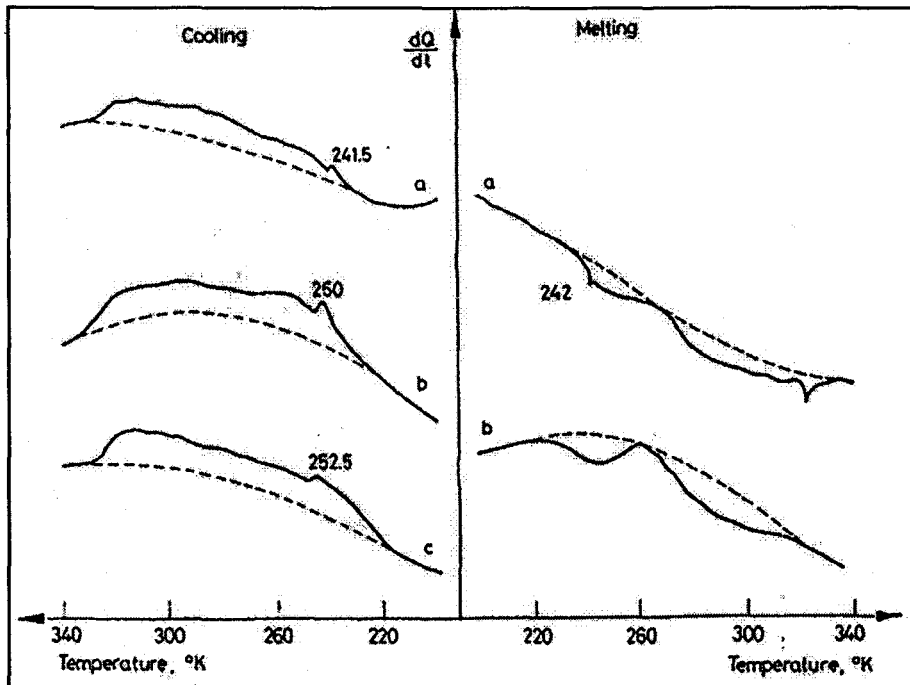


Figure 2.9: DSC Curves of Straight Asphalt and Two Blown Asphalt; (a) Straight Run Asphalt; (b) Blown Asphalt (3 Hrs) and (c) Blown Asphalt (5 Hrs) (Source: Giavarini and Pochetti, 1972)

Table 2.2: Characteristics of the Asphalts (Source: Giavarini and Pochetti, 1972)

Asphalt	Blowing time hrs	Penetration at 25°C d, mm	Asphaltenes (n-pentane) %	T _g , °K
Straight run (a)	0	186	22	241.5
Blown (b)	3	24	41	250.0
Blown (c)	5	15	45	252.5

Memon and Chollar (1997) investigated the glass transition temperature of different asphalts (virgin, chemically modified, and crumb rubber modified asphalt) with the creep stiffness, the rate of change of creep stiffness, and the low specification temperature of the PG grading of those asphalt. The results showed that there is correlation of rheological properties (m and S) for virgin and modified asphalt with T_g at low temperature (at heating rate 3 °C min⁻¹). They had also concluded that this thermal procedure is a fast and easy way to characterize the low temperature properties of asphalt.

Lesueur (2009) highlighted that waxes normally crystallize in asphalt at temperature starting from 90 °C down to the glass transition temperature. Since this crystallization is an exothermic process, Differential Scanning Calorimetry (DSC) is the preferred technique for quantifying the amount of paraffin-like crystalline materials within asphalt. The DSC thermograms as in Figure 2.10, shows that one or more endothermic peaks upon heating of asphalt specimen.

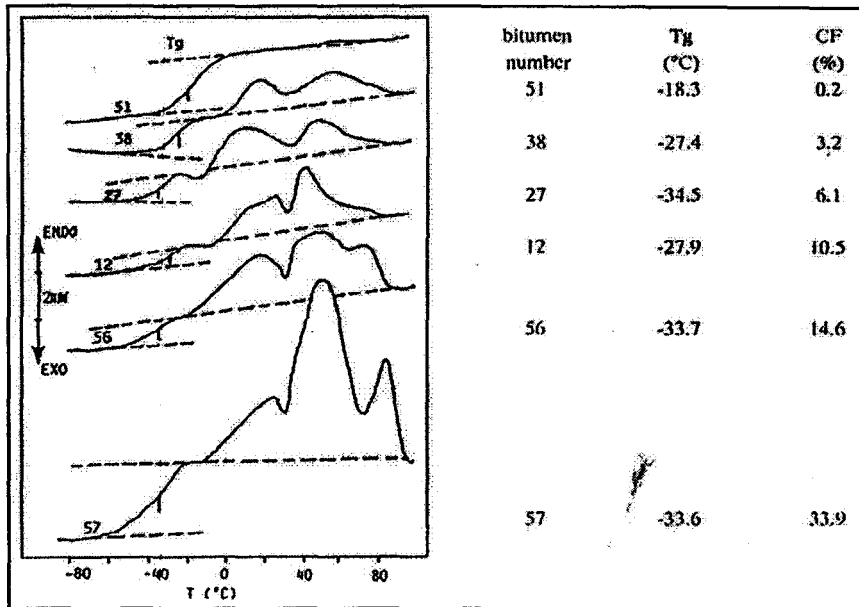


Figure 2.10: DSC Thermograms obtained at a Heating Rate of 5 °C/min for various Asphalts. The Glass Transition Temperature T_g at the Midpoint is marked on each Curve (Source: Lesueur, 2009)

2.8 Superpave Binder Grading and Binder Blending

The Superpave Mixture Expert Task Group guidelines described by Bukowski (1997), suggest that Superpave mixture containing RAP should follow the same mix design requirements as conventional mixtures. The aggregates and asphalt binder in the RAP should be considered as part of aggregate and asphalt binder of the total mix. The process of binder selection is categorized into three tiers depending on the RAP content.

1. Less than 15% RAP

The asphalt binder grade should remain the same as what would be chosen for a mix design using only virgin materials

2. 15% to 25%

Guidelines suggest using a binder one grade lower for both the high and low temperature required for virgin binder. It also suggest that the low temperature grade may not need to be adjusted for temperate climates, and that binder grade be selected using a blending chart if the designer compensates for the stiffness of the RAP binder

3. More than 25%

A blending chart for high and low temperatures should be used to select the grade for new asphalt binder

For higher level RAP content ($\geq 25\%$), it is necessary to extract, recover and test RAP binder to construct a blending chart. A comprehensive recommendations and methods for extraction and recovery of the RAP binder are well documented in NCHRP Report 452 (McDaniel and Anderson, 2001). To construct a blending chart, the following item are need:

- The desired final binder grade
- The physical properties and critical temperatures of the recovered RAP binder

- Either the physical properties and critical temperatures of the virgin binder or the percentage of RAP in the mixture

NCHRP has employed Dynamic Shear Rheometer (DSR) and Bending Beam Rheometer (BBR) tests in determining physical properties and critical temperatures of the recovered binder. The DSR is used to measure the complex shear modulus G^* and the phase angle δ for the asphalt binder at high and intermediate temperature. The BBR is used to measure the low temperature creep stiffness(S) and the log creep rate (slope, m) of the asphalt binder. The BBR test is performed to evaluate the resistance characteristics of asphalt binder against thermal cracking at low temperature (USDOT, 1994). The following are the formulas that can be used to determine critical temperature of the recovered binder.

- DSR test at high temperature without aging and DSR test at high temperature after RTFO test at which $G^*/\sin \delta = 1$ kPa;

$$T_c(\text{High}) = \left(\frac{\log(1.00) - \log(G_1)}{a} \right) + T_1 \quad \text{Equation (2.1)}$$

Where,

$G_1 = G^*/\sin \delta$ at temperature T_1

$a =$ slope of the stiffness-temperature curve at $\Delta \log (G^*/\sin \delta) / \Delta T$

- DSR test at high and intermediate temperatures after RTFO and PAV tests at which $G^*/\sin \delta = 2.2$ kPa and $G^* \sin \delta = 5000$ kPa respectively;

$$T_c(\text{High}) = \left(\frac{\log(2.20) - \log(G_1)}{a} \right) + T_1 \quad \text{Equation (2.2)}$$

Where,

$G_1 = G^*/\sin \delta$ at temperature T_1

$a =$ slope of the stiffness-temperature curve at $\Delta \log (G^*/\sin \delta) / \Delta T$

$$T_c(\text{Int}) = \left(\frac{\log(5000) - \log(G_1)}{a} \right) + T_1 \quad \text{Equation (2.3)}$$

Where,

$G_1 = G^* \sin \delta$ at temperature T_1

$a =$ slope of the stiffness-temperature curve at $\Delta \log (G^* \sin \delta) / \Delta T$

- BBR test at low temperature after RTFO at which the stiffness and m-value are 300 MPa and 0.30 respectively;

$$T_c(S) = \left(\frac{\log(300) - \log(S_1)}{a} \right) + T_1 \quad \text{Equation (2.4)}$$

Where,

$S_1 =$ the S-value at at temperature T_1

a = slope of the stiffness-temperature curve at $\Delta \log(S) / \Delta T$

$$T_c(m) = \left(\frac{0.3 - m_1}{a} \right) + T_1 \quad \text{Equation (2.5)}$$

Where,

m_1 = the m-value at temperature T_1

a = slope of the stiffness-temperature curve at $\Delta m / \Delta T$

There are two blending methods that can be used in deciding grade of virgin asphalt binder or maximum percentage of RAP material in recycled asphalt mixture.

Method A: The percentage of RAP is known and the grade of virgin asphalt binder unknown

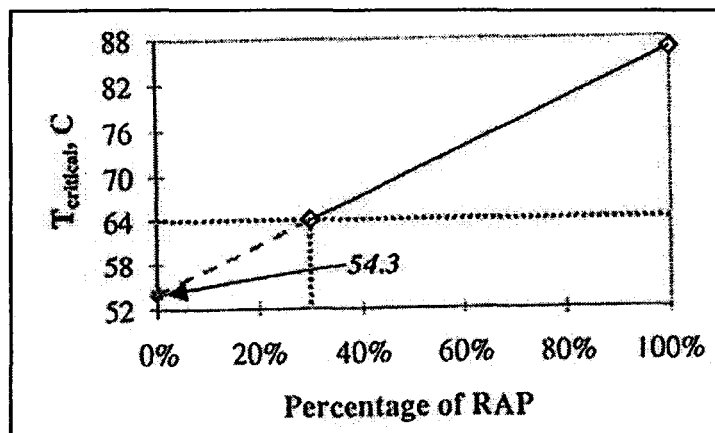
The following equation relates the critical temperature of the blended asphalt binder to its two components to determine virgin asphalt temperature;

$$T_{\text{virgin}} = \frac{T_{\text{Blend}} - (\% \text{RAP} \times T_{\text{RAP}})}{(1 - \% \text{RAP})} \quad \text{Equation (2.6)}$$

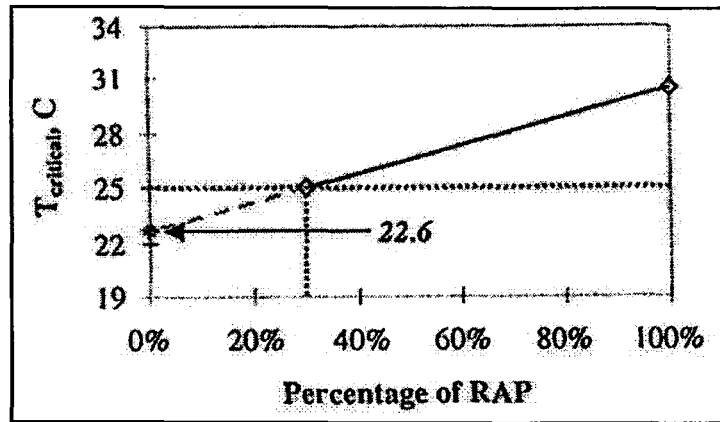
Where,

- T_{virgin} = critical temperature of the virgin asphalt binder
- T_{Blend} = critical temperature of the blended asphalt binder
- $\% \text{RAP}$ = percentage of RAP expressed in decimal
- T_{RAP} = critical temperature of recovered RAP binder

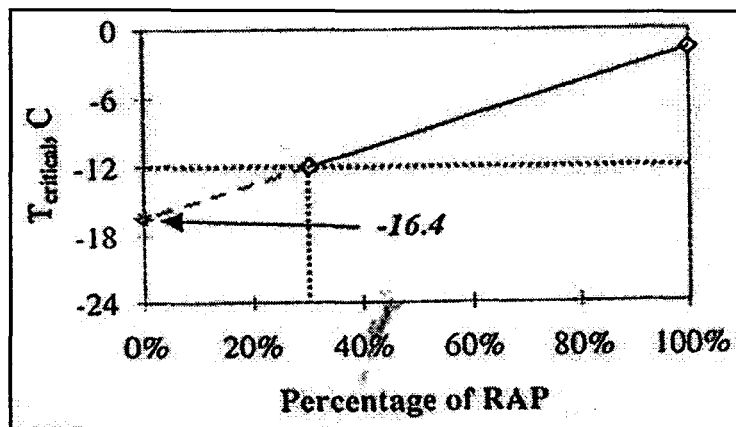
Figure 2.11 shows an example of determining the virgin asphalt binder grade based on high, intermediate and low temperatures for 30% RAP and the desired blended binder grade is PG64-22.



(a) High Temperature



(b) Intermediate Temperature



(c) Low Temperature

Figure 2.11: Blending chart (RAP percentage known) (Source: McDaniel and Anderson, 2001)

Method B: The grade of the virgin asphalt binder is known and the maximum percentage of the RAP is unknown.

When the virgin asphalt binder grade has been decided, the percentage of RAP can be determined by rearranging equation 6 as follow,

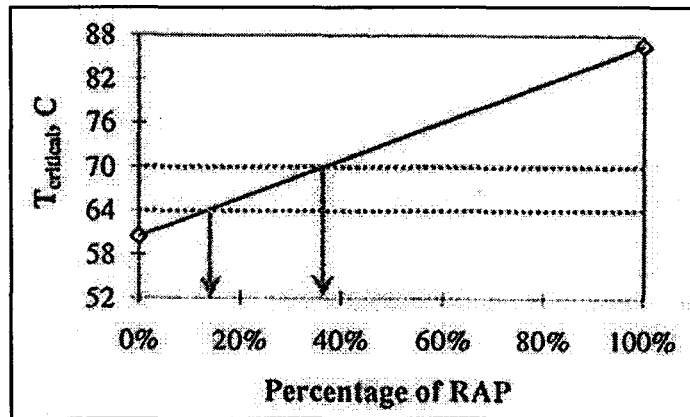
$$\%RAP = \frac{T_{Blend} - T_{Virgin}}{T_{RAP} - T_{Virgin}} \quad \text{Equation}$$

(2.7)

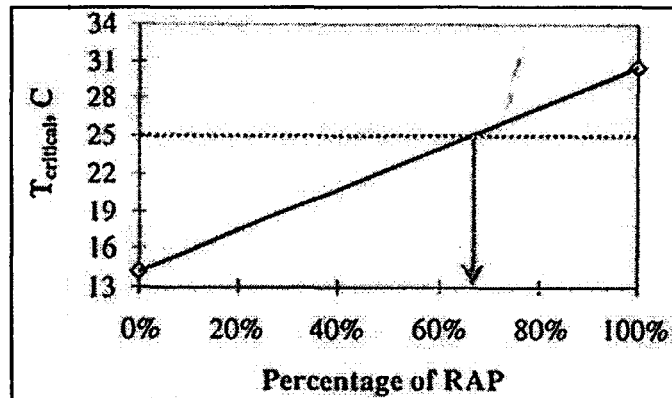
Where,

- T_{Virgin} = critical temperature of the virgin asphalt binder
- T_{Blend} = critical temperature of the blended asphalt binder
- $\%RAP$ = percentage of RAP expressed in decimal
- T_{RAP} = critical temperature of recovered RAP binder

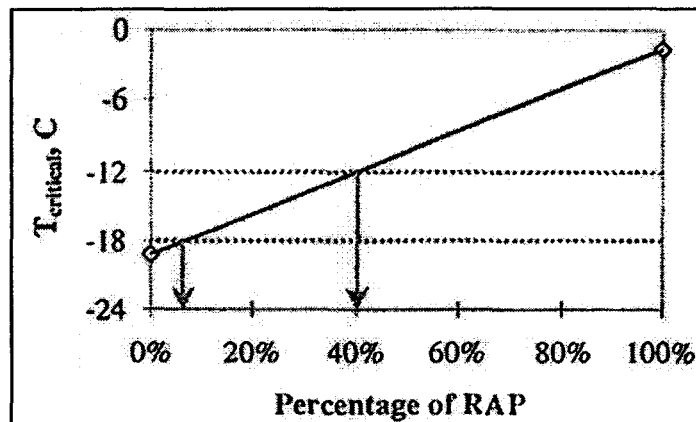
Figure 2.12 shows example of determining percentage of RAP based on high, intermediate and low temperatures when the desired blended binder grade is PG64-22.



(a) High Temperature



(b) Intermediate Temperature



(c) Low Temperature

Figure 2.12: Blending chart (RAP percentage unknown)

(Source: McDaniel and Anderson, 2001)

Kennedy et al. (1998) studied the effect of reclaimed asphalt pavement on binder properties based on Superpave specification. In this study, six asphalts that are part of the core asphalts used in the SHRP were chosen. Two of these six asphalts were aged for 85

minutes at 163 °C to simulate RAP binder with short-term aging and aged for 20 hours at 100 °C and pressure of 2.1 MPa using the pressure aging vessel (PAV) to simulate the field aging in the first 5 to 10 years of pavement service. The DSR and BBR tests were performed on the virgin-RAP blends. The findings of the study are:

1. The stiffness ($G^*/\sin \delta$, $G^*\sin \delta$, creep stiffness) of the binder is higher at higher percentage of RAP binder
2. The rate of change of stiffness is either constant from 0 – 100% or increases with lower temperatures
3. The rate of change of stiffness is either constant from 0 – 100% or increases at higher percentages of RAP binder in the blend

Another study on the rheological and mechanical properties of blended asphalts containing recycled asphalt pavement binder was conducted by Lee et al. (1999). Two binder types PG58-28 and PG64-22 were blended with different amounts of RAP binders in proportions of 0, 10, 20, 30, 40, 50, 75 and 100% by weight. The DSR test was carried out at high temperature (52, 58, 64, 70 and 76 °C) an intermediate temperature (19, 22, 25, 28 and 31 °C). A plot of log-log between rheological and amount of RAP binder shows a good linear relationship. Subsequently, BBR test was performed at -6, -12, -18 and -24 °C. The result shows that the creep stiffness increased and m-value decreased for all temperatures as the amount of RAP content increased. In other words, the addition of RAP content reduces binder resistance to low temperature cracking.

2.9 Mixture Performance

Many studies on RAP materials incorporated in asphalt mixtures have shown that the recycled asphalt pavement performs as well as a pavement that is made up from totally virgin materials. Kandhal et al. (1995) investigated the performance of recycled hot mix asphalt mixture where five projects that consist of a recycled section in each project were subjected to detailed evaluation. In-situ properties (air voids, resilient modulus and indirect tensile strength), recovered asphalt binder properties (penetration, viscosity, complex modulus, phase angle) and laboratory recompacted mix properties (gyratory stability index, confined dynamic creep modulus) were measured. A paired t-test shows that no significant difference between virgin and recycled asphalt pavement properties which have been in service for 1.5 to 2.25 years.

Puttagunta et al. (1997) studied the performance of 25% and 50% RAP modified mixtures based on the Asphalt Aggregate Mixture Analysis System (AAMAS) design procedure. The modified mixtures were tested for indirect tensile, resilient modulus and fatigue tests. The results from indirect tensile test at 5, 22 and 40 °C indicate that the rate of decrease in tensile strength with temperature for recycled mixtures is slower compared to the virgin mixtures. Similarly, resilient modulus test at 5 and 22 °C show that the rate of decrease for recycled mixtures is slower than the virgin mixtures but almost equal between 22 and 40 °C. Fatigue test show that all mixtures have good resistance to fatigue cracking even though the 50% recycled mixtures just satisfied the requirements. Moreover, the resistance to moisture damage is higher with increasing of percentage of RAP material in the mixtures. Inclusion of RAP in an asphalt mixture has somewhat changed the properties of the hot mix asphalt. The change in the recycled asphalt mixture properties is primarily due to the introduction of aged binder as part of the RAP in the asphalt mixture. Consequently, the

addition of RAP increased the binder stiffness and decreased its shear strain (McDaniel and Anderson, 2001).

Su et al. (2009) studied the possibility of using recycled asphalt concrete as surface course in airport pavement. The laboratory tests were performed to evaluate the performance of recycled asphalt concrete containing 0%, 40% and 70% RAP. An experimental pavement consisting of three sections corresponding to the three levels of RAP percentage were constructed to verify laboratory results. The mixtures were subjected to ravelling, rutting, moisture susceptibility and three point bending tests. The findings show that recycled asphalt concrete containing 40% RAP can be used as surface course in airport pavement as it has exhibited similar performance as the control mixture from laboratory and experimental pavement. However, recycled asphalt concrete containing 70% RAP show poor fatigue property where its stiffness has increased 60% in the three Point Bending test at 20 °C.

Li et al. (2008) conducted laboratory study on ten asphalt mixtures, including two different RAP sources, three RAP percentages (0%, 20%, 40%) and two different asphalt binders (PG58-28 and PG58-34). The dynamic modulus, a newly developed mechanistic-empirical design guide was performed on all mixtures at different temperatures and frequencies. Semi-Circular Bending (SCB) fracture testing was performed for all mixtures at three low temperatures. The findings show that asphalt mixtures containing RAP have higher dynamic modulus values than the control mixtures containing no RAP. Furthermore, asphalt mixtures containing 40% RAP were found to have higher or similar dynamic modulus with mixtures containing 20% RAP at high temperature. However, most mixtures containing 20% RAP were observed to have highest dynamic modulus at lower temperature or high frequencies. Fracture testing results show that control mixtures have highest fracture energy and 20% RAP mixtures have similar fracture resistance abilities to the controls mixtures.

Widyatmoko (2008) carried out a study on asphalt mixtures containing RAP for wearing course and base course that were evaluated using a mechanistic-empirical approach. Three level percentages of RAP (10%, 20% and 50%) were incorporated in the asphalt concrete mixtures and 80/100 pen virgin bitumen was used as a base in producing the recycled mixtures. The finding shows that rutting and fatigue resistance of the recycled mixtures have performed equally or better than the control mixture. Moreover, the recycled mixtures were also not sensitive to moisture induce damage when their retain stiffness were all greater than 0.8.

Studies by Xiao et al. (2007) and Gui-Ping and Wing-Gun (2008) incorporating RAP materials in rubberized asphalt concrete pavements and foamed asphalt mix, respectively, generally have shown that the mechanical and durability properties are better than asphalt mixture without RAP especially in permanent deformation and moisture damage. Currently, dynamic modulus (E^*) is the preferred asphalt mix structural contribution parameter and is one of the most important parameters required in flexible pavement design based on the Mechanistic Empirical Pavement Design Guide (MEPDG) (NCHRP, 2004). The dynamic modulus is a crucial parameter used in evaluating rutting and fatigue cracking distresses prediction in the MEPDG (Witczak et al., 2002). The dynamic modulus represents asphalt mixtures stiffness in response to application of haversine compressive load on a cylindrical sample over several temperatures and loading frequencies. Stiffness is reflected by the load spreading ability of an asphalt mix. A master curve is developed to represent stiffness relationship of asphalt mixture in relation to temperatures and loading frequencies

2.10 Summary

Blended asphalt binder properties are directly influenced by the chemical composition of saturates, aromatics, resin and asphaltenes upon aging. It is very important to ensure that the properties of blended asphalt binder are achieved and met specification requirements when high percentage of RAP material is used in mixture. Improper use of virgin asphalt grade could result early structural failure of pavement due to stiffness contributed by aged binder from the RAP material in the hot asphalt mix especially in fatigue. Generally, recycled mixture with certain percentage of RAP has significantly improved the strength and durability of mixture in tensile strength, resilient modulus, rutting, fatigue, moisture damage and dynamic modulus compared to virgin mixtures.

CHAPTER FOUR

MIX DESIGN

4.1 Introduction

The nature of RAP aggregate gradation is entirely depending on RAP material taken from respective site. The output of the design is based on the RAP aggregate gradation and RAP binder content consist in the dry RAP material. The amount of binder and aggregate sizes from RAP will be taken into account in fabrication of sample as it significantly contributes to the strength of a specimen. The role of RAP in a mixture is assumed to give a similar effect as new materials.

4.2 RAP Aggregate Gradation

Table 4.1 shows average gradation of RAP aggregate from 3 RAP types. It can be noticed that PLUS and LDP RAP aggregates are nearly 100% passing at sieve size 20 mm due to disintegration and degrading of RAP aggregates during milling process which created more fines compared to its virgin mixes. Large fraction of coarse RAP aggregates can be expected to decrease and subsequently contribute to increasing percentage of retained finer RAP aggregates.

Table 4.1: Average Gradation of RAP Aggregates

Sieve Sizes (mm)	PLUS		LDP		JKR	
	%	Std. Dev.	%	Std. Dev.	%	Std. Dev.
	Passing		Passing		Passing	
20	99.5	0.38	99	0.78	100	0
14	93	1.08	93.8	1.46	99.6	0.26
10	84.3	1.46	87.4	2.13	98	0.78
5	63.7	3.51	73.2	3.7	75.3	3.36
3.35	54.1	3.74	63.5	4.26	64.5	4.35
1.18	34	3.22	38.2	4.21	40	3.84
0.425	21.3	21.3	21.7	2.77	24.6	2.22
0.150	11.2	0.85	10.9	0.98	13.5	0.96
0.075	6.3	0.41	6.3	0.95	8.1	0.63

4.2.1 RAP Aggregate Gradation after Separating into Batching Sizes

The need to separate RAP into batching sizes has the same reason as virgin aggregate is separated into individual size fraction which is for accurate control of mixture gradation. Furthermore, due to nature of RAP with lots of variability and limited flexibility would very much effect the mixture gradation if it was not properly controlled. Table 4.2 presents average RAP aggregate retain and passing 5 mm sieve. It can be seen that LDP and JKR RAPs have high standard deviation compared to PLUS RAP due to RAP material variability. Table 4.3 – 4.5 show average gradation of 3 types of RAP after separated into 2 sizes particle which are retained 5 mm sieve and passing 5 mm sieve. From these results it can be seen that the RAP aggregate retained on the 5 mm sieve is containing aggregate that smaller than 5mm.

These results were expected as knowing that the asphalt binder in the RAP would cause aggregate agglomerations of various sizes. The mild heating and sieving process used to separate the RAP material into two sizes batch groups unable to completely break down these agglomerations. Heating the RAP material higher than that would further aged the RAP material and hence, most probably change the mixture properties and should be avoided. The gradation of the RAP aggregate is based on JKR ACWC 14 gradation specification.

Table 4.2: Average RAP Aggregate Separated into Batching Sizes

Material	RAP					
	PLUS		LDP		JKR	
	retain 5mm	passing 5mm	retain 5mm	passing 5mm	retain 5mm	passing 5mm
Aggregates, %	51	49	48	52	50	50
Std. Dev.	2.04	2.04	7.71	7.71	7.21	7.21

Table 4.3: Average Gradation of PLUS RAP Aggregates Separated into Batching Sizes

Sieve Size (mm)	Retain 5 mm		Passing 5mm	
	% Passing	Std. Dev.	% Passing	Std. Dev.
20	100.0	0.00	0.0	0.00
14	88.0	3.12	0.0	0.00
10	72.2	3.76	0.0	0.00
5	30.0	1.17	0.0	0.00
3.35	22.4	0.71	88.2	2.28
1.18	16.2	0.45	51.4	4.06
0.425	11.5	0.29	30.7	2.42
0.150	6.7	0.11	15.0	0.60
0.075	3.8	0.15	7.9	0.30

Table 4.4: Average Gradation of LDP RAP Aggregates Separated into Batching Sizes

Sieve Size (mm)	Retain 5 mm		Passing 5mm	
	% Passing	Std. Dev.	% Passing	Std. Dev.
20	100.0	0.00	0.0	0.00
14	88.0	3.31	0.0	0.00
10	76.4	3.31	0.0	0.00
5	47.2	1.23	0.0	0.00
3.35	37.4	0.86	90.0	1.67
1.18	24.8	0.71	52.7	4.94
0.425	15.2	0.57	29.4	3.32
0.150	8.2	0.31	15.1	1.19
0.075	5.0	0.21	8.9	0.58

Table 4.5: Average Gradation of JKR RAP Aggregates Separated into Batching Sizes

Sieve Size (mm)	Retain 5 mm sieve		Passing 5mm sieve	
	% Passing	Std. Dev.	% Passing	Std. Dev.
20	100.0	0.00	0.0	0.00
14	98.4	0.68	0.0	0.00
10	95.2	1.57	0.0	0.00
5	51.9	1.24	0.0	0.00
3.35	39.5	1.67	90.6	1.93
1.18	26.8	0.89	54.5	4.60
0.425	17.9	0.49	32.7	3.21
0.150	10.2	0.23	16.9	1.08
0.075	6.0	0.17	9.1	0.56

Tables 4.6 to 4.8 show calculated amount of virgin aggregate requires after taking into account various percentages of RAP material incorporated in the mixture. It can be seen that a substantial decrease in amount of virgin aggregate used with increasing percentage of RAP added into the mixture.

Table 4.6: Amount of Virgin Aggregates to Incorporate with PLUS RAP

Sieve Size (mm)	RAP Aggregate		Virgin Aggregate required with			
	% Retain		10%	20%	30%	40%
	Retain	Passing	RAP (g)	RAP (g)	RAP (g)	RAP (g)
	5 mm sieve	5 mm Sieve				
20	0	0	0	0	0	0
14	12.0	0.0	52.7	45.3	38.0	30.6
10	15.8	0.0	158.3	148.7	139.0	129.3
5	42.2	0.0	274.2	248.3	222.5	196.7
3.35	7.6	11.8	96.4	84.8	73.2	61.6
1.18	6.2	36.8	226.6	201.1	175.7	150.3
0.425	4.7	20.7	81.0	65.9	50.9	35.8
0.15	4.8	15.7	83.8	71.7	59.5	47.3
0.075	2.9	7.1	42.1	36.1	30.2	24.2
Filler	3.8	7.9	65.0	58.1	51.1	44.1

Table 4.7: Amount of Virgin Aggregates to Incorporate with LDP RAP

Sieve Size (mm)	RAP Aggregate		Virgin Aggregate required with			
	% Retain		10%	20%	30%	40%
	Retain	Passing	RAP (g)	RAP (g)	RAP (g)	RAP (g)
	5 mm sieve	5 mm Sieve				
20	0	0	0	0	0	0
14	12.0	0.0	53.1	46.2	39.3	32.4
10	11.6	0.0	161.3	154.6	148.0	141.3
5	29.2	0.0	283.2	266.4	249.5	232.7
3.35	9.8	10.0	96.1	84.2	72.3	60.5
1.18	12.6	37.3	221.5	190.9	160.4	129.9
0.425	9.6	23.3	75.9	55.9	35.8	15.7
0.15	7.0	14.3	83.0	70.1	57.1	44.2
0.075	3.2	6.2	42.3	36.6	30.9	25.2
Filler	5.0	8.9	63.6	55.1	46.7	38.3

Table 4.8: Amount of Virgin Aggregates to Incorporate with JKR RAP

Sieve Size (mm)	RAP Aggregate		Virgin Aggregate required with			
	% Retain		10%	20%	30%	40%
	Retain	Passing	RAP (g)	RAP (g)	RAP (g)	RAP (g)
	5 mm sieve	5 mm Sieve				
20	0	0	0	0	0	0
14	1.6	0.0	59.0	58.1	57.1	56.2
10	3.2	0.0	166.1	164.2	162.2	160.3
5	43.3	0	274.0	248.0	222.1	196.1
3.35	12.4	9.4	94.9	81.8	68.8	55.7
1.18	12.7	36.1	222.7	193.4	164.2	134.9
0.425	8.9	21.8	77.6	59.2	40.7	22.3
0.15	7.7	15.8	81.9	67.8	53.7	39.6
0.075	4.2	7.8	40.8	33.6	26.4	19.2
Filler	6.0	9.1	62.9	53.9	44.8	35.8

4.3 RAP binder

The average RAP binder content for three RAP types are exhibited in Table 4.9. After separating the RAP material into two batching sizes, it can be noticed that in Table 3.10, the average asphalt content of RAP passing 5 mm sieve is higher than retain 5 mm sieve all RAP types. This is happened due to fine aggregate particles have a higher surface area by volume compared to coarse aggregate which have higher relative percentage of binder by mass. The separation of RAP into two batching sizes has added one advantage in controlling of a mixture gradation inclusion of RAP material since a given percentage of RAP aggregates will set together with amount of asphalt content contributed by the RAP in a mixture.

Table 4.9: Average Asphalt Content of RAP

Material	RAP		
	PLUS	LDP	JKR
Asphalt Content, %	4.37	4.57	4.44
Std. Dev.	0.18	0.22	0.15

Table 4.10: Average Asphalt Content of RAP after Separating into Batching Sizes

Material	RAP					
	PLUS		LDP		JKR	
	retain 5mm	passing 5mm	retain 5mm	passing 5mm	retain 5mm	passing 5mm
Asphalt Content, %	2.75	5.78	3.39	5.48	3.53	5.17
Std. Dev.	0.12	0.21	0.09	0.33	0.10	0.23

From the analysis of RAP gradation and RAP binder, the amount of dry RAP and RAP binder to be added at various percentages of RAP in the recycled asphalt concrete mixture is presented in Table 4.11.

Table 4.11: Amount of Dry RAP and RAP Binder in Various Percentage of RAP

RAP TYPE	Material	10% RAP		20% RAP		30% RAP		40% RAP	
		Retain	Passing	Retain	Passing	Retain	Passing	Retain	Passing
		5 mm sieve							
		(g)							
PLUS	Dry RAP	62.9	62.4	125.9	124.8	188.8	187.2	251.7	249.6
	RAP Binder	5.3		10.7		16.0		21.3	
LDP	Dry RAP	59.6	66.0	119.2	132.0	178.9	198.1	238.5	264.1
	RAP Binder	5.6		11.3		16.9		22.6	
JKR	Dry RAP	62.2	63.3	124.4	126.5	186.6	189.8	248.8	253.1
	RAP Binder	5.5		10.9		16.4		21.9	

4.4 Optimum Asphalt Content

The optimum asphalt content is determined based on JKR (2008) parameters on asphalt concrete wearing course mix design as shown in Table 4.12.

Table 4.12: JKR ACW14 Specification Parameters

Design Bitumen Contents	4.0 – 6.0 %
Stability	> 8000 N
Flow	2.0 – 4 mm
Stiffness (S/F)	> 2000 kN/mm
Air void in mix	3.0% – 5.0%
Void in aggregate filled with bitumen	70% – 80%

All the data from the Marshall test were plotted to show the relationship between the volumetric properties and asphalt contents for the virgin mixture as presented in Figure 4.1. The optimum binder content was determined by averaging asphalt binder content from 5

parameters on JKR specification. The optimum asphalt content for virgin mix design is 4.6%. Table 4.13 presents optimum binder contents for recycled mixtures for three types of RAP at 10, 20, 30 and 40% RAP which were determined same manner as virgin mixture.

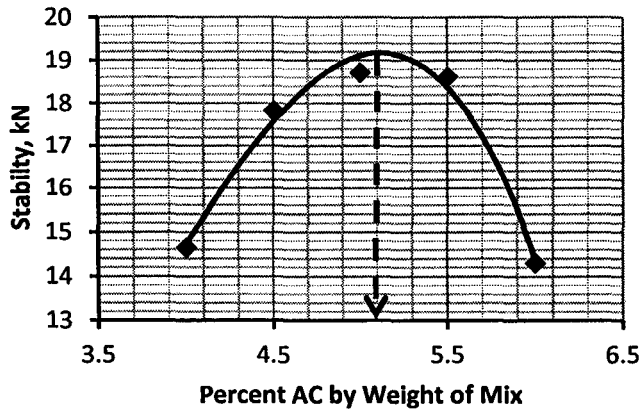
Table 4.13: Optimum Asphalt Content of Recycled Mixtures

RAP Type	Optimum asphalt content, %			
	10% RAP	20% RAP	30% RAP	40% RAP
PLUS	4.8	4.9	5.1	5.3
LDP	4.9	5.2	5.3	5.4
JKR	4.8	4.9	5.1	5.3

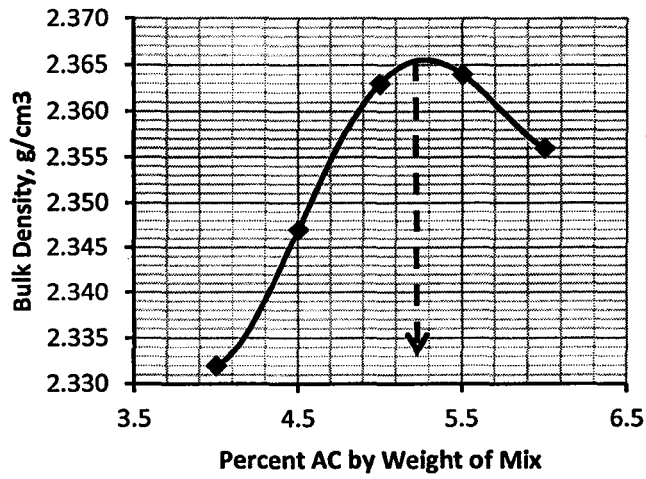
The impact of addition of RAP can be seen in Table 4.14, where, as the percentage of RAP increases, the ratio of RAP-virgin asphalt content increases as well. LDP RAP has the highest asphalt content ratio which is consistent with higher amount of RAP binder present in the LDP dry RAP.

Table 4.14: Percent virgin and RAP binder in recycled asphalt mixture

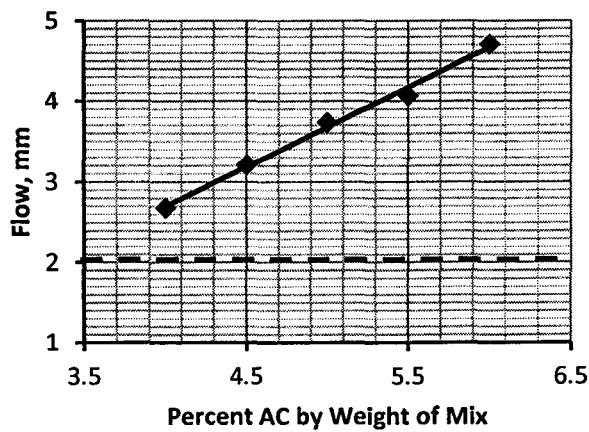
MIX TYPE	% RAP	Virgin AC %	RAP AC %	Ratio RAP AC/ Virgin AC
Virgin	0	4.6	0.0	0.00
PLUS	10	4.4	0.4	0.09
	20	4.1	0.9	0.22
	30	3.9	1.3	0.33
	40	3.7	1.7	0.46
LDP	10	4.5	0.5	0.11
	20	4.3	0.9	0.21
	30	4.0	1.4	0.35
	40	3.7	1.9	0.51
JKR	10	4.4	0.5	0.11
	20	4.1	0.9	0.22
	30	3.9	1.4	0.36
	40	3.6	1.8	0.50



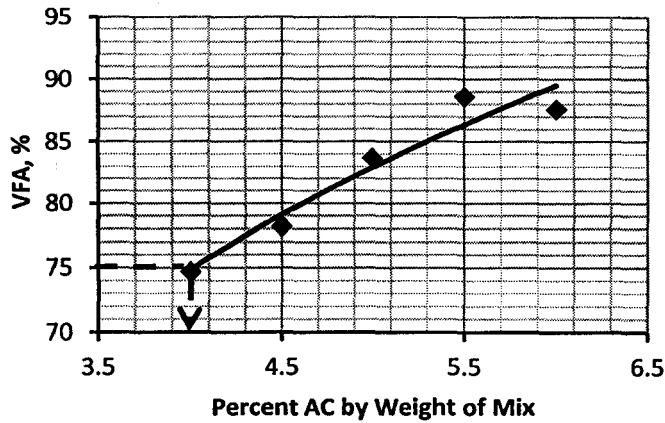
(a) Stability versus asphalt content



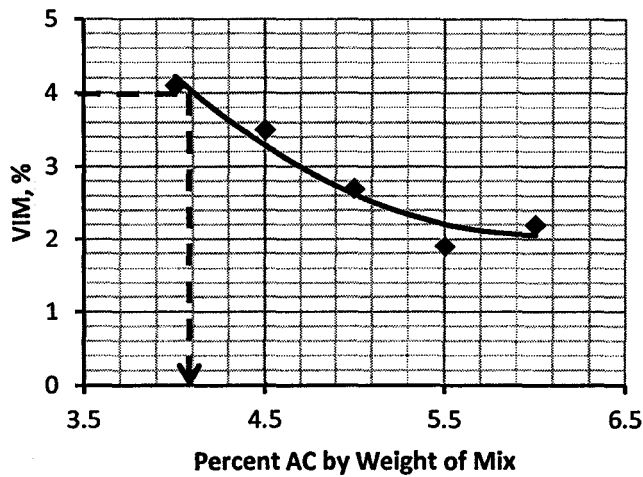
(b) Bulk density versus asphalt content



(c) Flow vs. asphalt content



(d) VFA versus asphalt content



(e) VIM versus asphalt content

Figure 4.1: Volumetric Properties of the Marshall Specimens in determining OBC for Virgin Mixture

4.5 Summary

Evaluation of the RAP aggregate gradation has been described. The selected gradations and their OPC were used for the mix preparation stage and performance test. It can be concluded that the original coarse aggregate fraction of RAP aggregates has become finer than virgin aggregate primarily due to disintegration during the milling process and also previous handling and placement of the materials. The amount of RAP binder content in RAP particles passing 5 mm sieve is higher compared to those retained on 5 mm sieve since finer particles have larger surface area by volume. The amount of virgin asphalt requires in the recycled asphalt mixture decreases as percentage of RAP increases. An average saving of 38% in virgin binder when 40% dry RAP is incorporated in the recycled asphalt mixture.

CHAPTER FIVE

PHYSICAL, RHEOLOGICAL AND CHEMICAL PROPERTIES OF RAP BINDER

5.1 Introduction

RAP were removed by cold-milling from Lebu Raya Damansara Puchong (LDP), Projek Lebu Raya Utara-Selatan (PLUS) and JKR (Federal Road) roads which were experiencing crack distressed pavements after 4-5 years in service. Approximately 500 kilograms of RAP materials were obtained from each site and kept in the barrels. The RAP samples consist of both ACW20 and ACW14 which were normally used by the Lembaga Lebu Raya Malaysia and Jabatan Kerja Raya respectively. Virgin binder grade 80/100 (PG64) was used as a base binder in this study.

5.2 RAP Binder Content

Figure 5.1 shows the average asphalt content obtained via the ignition oven method. It can be seen that RAP from LDP samples exhibit the highest average asphalt content at 4.57% while PLUS RAP has the lowest average asphalt content at 4.37%. RAP binder from JKR is within the optimum asphalt binder content ranging from 4 to 6% for asphalt wearing course.

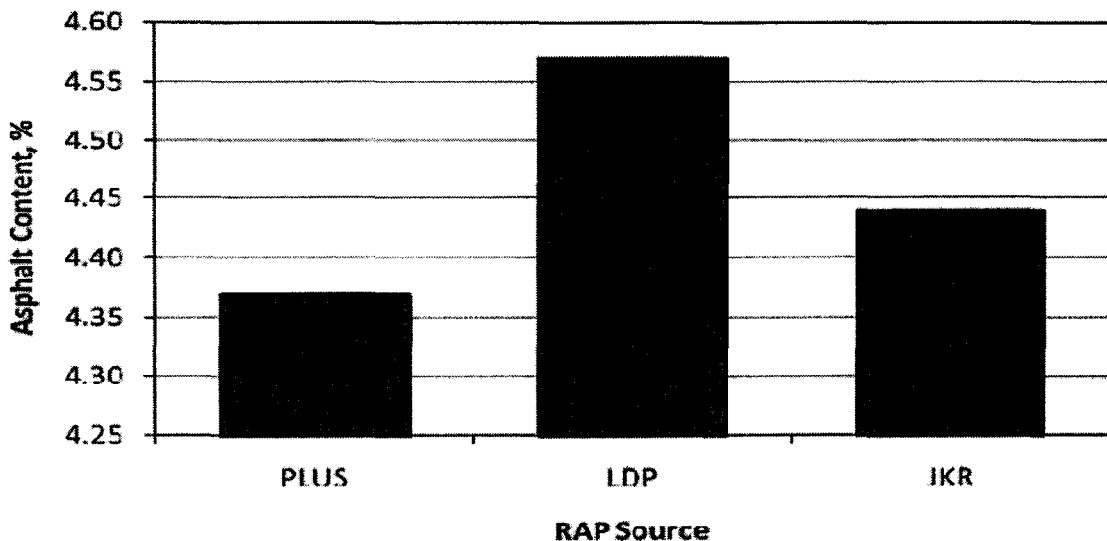


Figure 5.1: Average Asphalt Content of Reclaimed Asphalt Pavement

5.3 RAP Aggregate Gradation

The by-product of the ignition test was then used to determine aggregate gradation by sieving the RAP aggregates through selected sieve sizes. Figures 5.2 and 5.3 present gradation curves of RAP aggregates plotted based on Lembaga Lebu Raya and Jabatan Kerja Raya specification limits respectively. It can be seen that some portions of the aggregate gradations from the three RAP sources are either on the borderline or outside the accepted specification limits. This happened mainly due to disintegration and degrading of RAP aggregates during milling process which created more fines compared to virgin mixes. Large

fraction of coarse RAP aggregates can be expected to decrease and subsequently contribute to increasing percentage of retained finer RAP aggregates. Based on 5 mm sieve analysis as summarized in Table 5.1, it is found that the average percent retained on 5 mm sieve for PLUS and LDP are about 36% and 27% respectively which is about 23% to 43% lower than percentage retained of the virgin aggregates. However, the percentage retained of JKR RAP aggregate at 5 mm sieve is reduced by 34% to approximately 25% retained after the milling process.

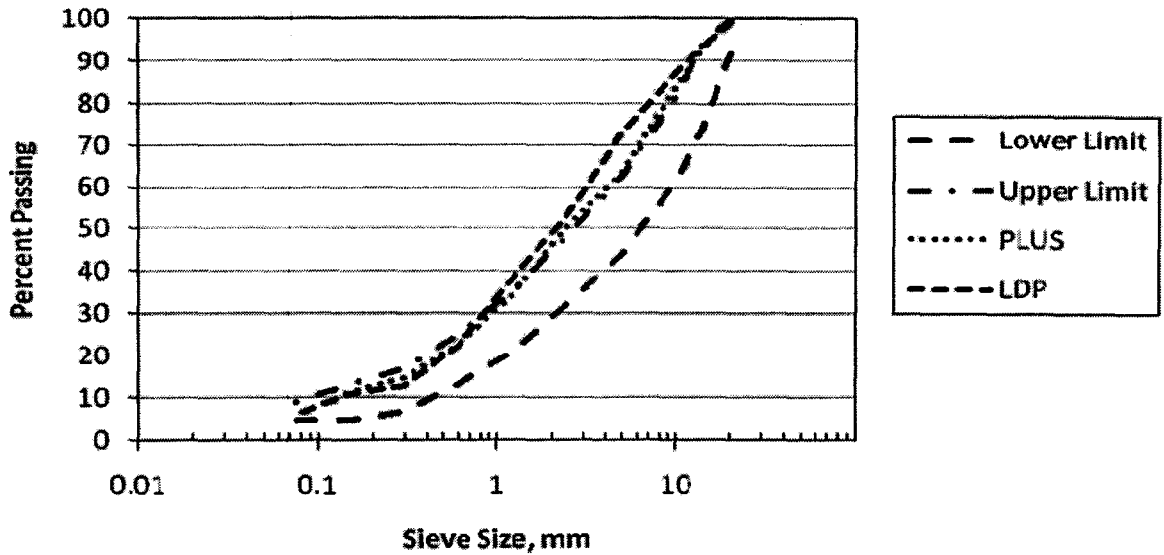


Figure 5.2: Aggregate Gradations of PLUS and LDP RAP Samples (LLM-ACWC20)

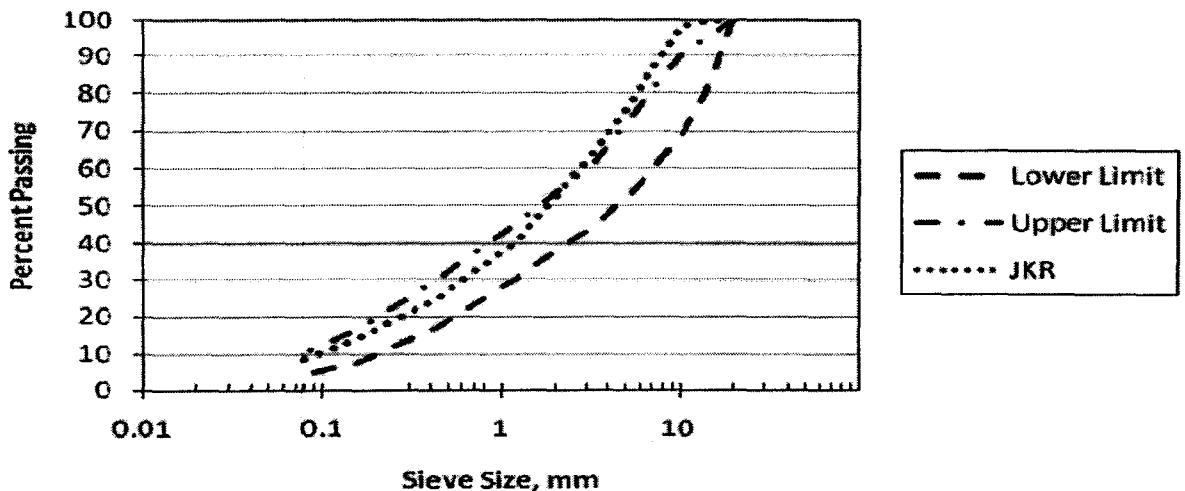


Figure 5.3: Aggregate Gradations of JKR RAP Samples (JKR-ACWC14)

Table 5.1: Percent Retained and Passing 5 mm Sieve of all RAP Aggregates

RAP Source	% retain 5 mm sieve	% passing 5 mm sieve
------------	---------------------	----------------------

PLUS	36	64
LDP	27	73
JKR	25	65

5.4 RAP Binder Physical Properties

Recovered RAP binders and unaged original 80/100 binder were tested for penetration and softening point. Table 5.2 shows the result of penetration test of recovered RAP binders which is about 85% lower compared to virgin binder. The low penetration values are expected since aged binder hardens over time due to oxidation while pavements are in service. All three RAP binders exhibit almost similar penetration depth because the RAPs were milled from pavements that had been in service for about 4 to 5 years. The softening point of recovered JKR RAP binder is the highest which complement with its lowest penetration value among the recovered RAP binders. Recovered RAP binder from PLUS and LDP have similar softening point.

Table 5.2: Penetration and Softening Point of Virgin and RAP Binders

Test	Virgin Binder	RAP Binder		
		PLUS	LDP	JKR
Penetration, dmm	88	14	13	11
Softening Point, °C	46	67.5	67.5	72

5.5 RAP Binder Rheological Properties

The recovered RAP binders were further tested for rheological property for unblended and blended of unaged recovered RAP binders. Table 5.3 shows the average value of $G^*/\sin \delta$ for unblended RAP binders at high temperature test. It can be seen that $G^*/\sin \delta$ value is decreased as the temperature is increased. From Figure 5.4, the binder extracted from JKR RAP has the highest stiffness at all temperatures. This is in parallel with this RAP binder having the lowest penetration and highest softening values. Both recovered binder from PLUS and LDP RAP exhibit similar stiffness. From this result, the high temperature performance grade can be estimated at a PG88 for all recovered RAP binders.

Table 5.3: DSR Test Results of Recovered RAP Binders

Temperature °C	Average $G^*/\sin \delta$, kPa		
	PLUS	LDP	JKR
52	254.0	171.1	253.6
58	98.0	78.0	109.8
64	38.0	36.1	47.8
70	16.1	16.4	20.7
76	6.88	7.39	8.99
82	3.13	3.43	4.13
88	1.56	1.68	2.00

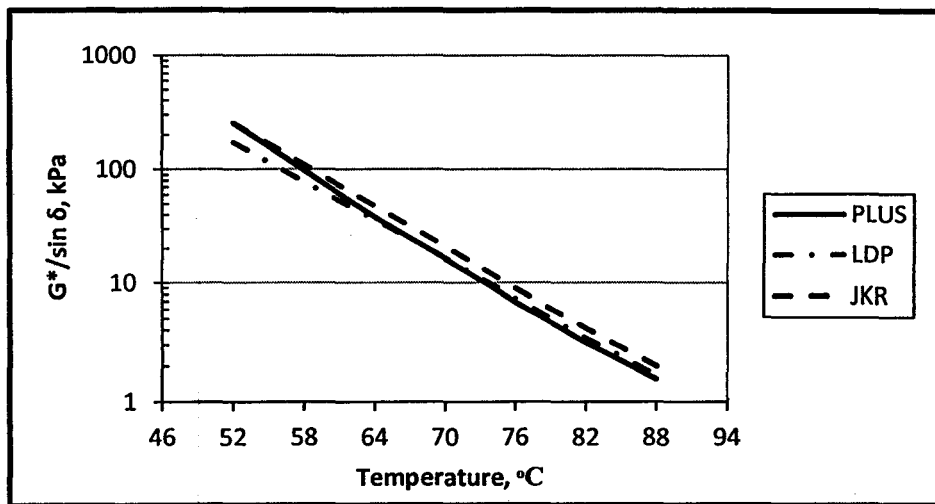


Figure 5.4: Stiffness of Recovered RAP Binders

Table 5.4 summarizes the results of DSR testing on the unaged blended binders. These results show that doubling the RAP binder concentration from 15% to 30% resulted in increasing the stiffness from 46 to 91 percent. PLUS RAP blend has the highest stiffness effect after doubling the concentration. The temperature – stiffness curves in Figure 5.5 shows LDP and JKR blends are identical while in Figure 5.6, LDP and PLUS blends curves almost overlap with each other which suggests that both RAP blends exhibit similar stiffness property. The stiffness – temperature relationships of the blended binders can be used to grade the unaged binder high temperature performance of each blend by determining the maximum temperature that satisfy the $G^*/\sin \delta \geq 1.0$ kPa requirement. For all RAP binder types, the addition of 15% of RAP binder increases the stiffness of the binder blend one grade higher to PG70 than that of the base virgin binder (PG64). As the RAP binder concentration doubles to 30%, the stiffness of the blend increase by two grades to become PG76 compared to base virgin binder.

Table 5.4: Results of DSR Testing of Unaged Blended Binders

Temp., °C	G*/sin δ, kPa								
	PLUS			LDP			JKR		
	% RAP Binder		% increased	% RAP Binder		% increased	% RAP Binder		% increased
	15	30		15	30		15	30	
52	14.3	22.1	54	12.1	23.1	91	12.0	19.0	59
58	5.46	8.47	55	4.55	8.69	91	4.58	7.44	63
64	2.28	3.53	55	1.96	3.81	95	1.96	3.12	59
70	1.09	1.59	46	0.93	1.71	83	0.94	1.43	52
76	0.52	0.78	50	0.45	0.84	88	0.45	0.67	50
82	0.26	0.39	51	0.22	0.41	83	0.23	0.34	49

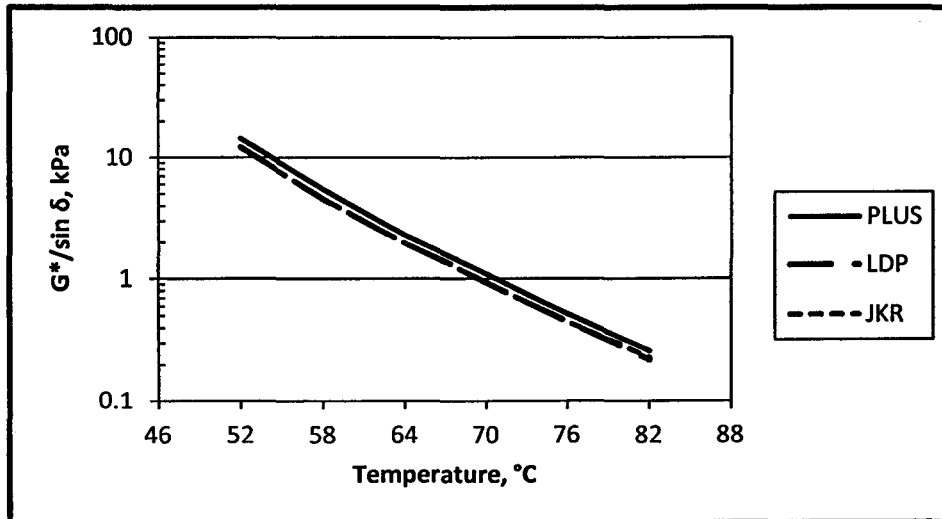


Figure 5.5: DSR Test Results for Blended Unaged Binder with 15% Recovered RAP Binder

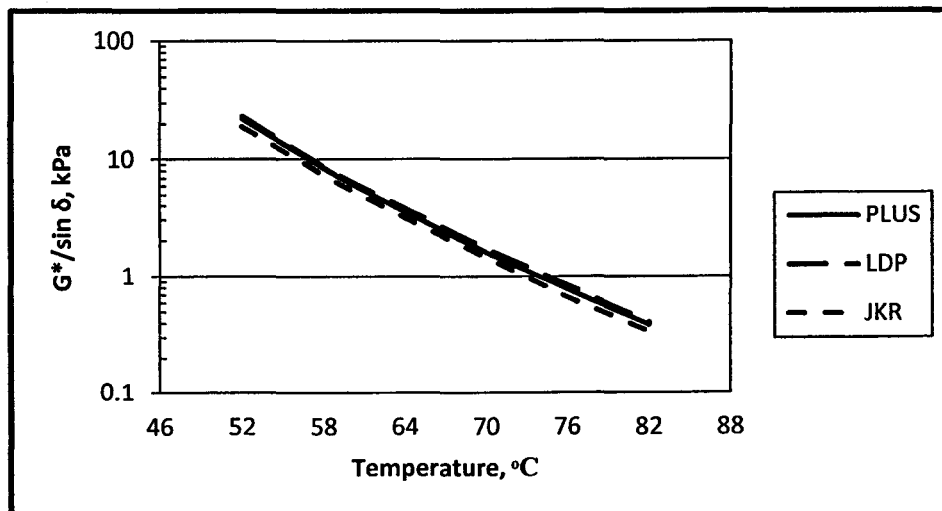
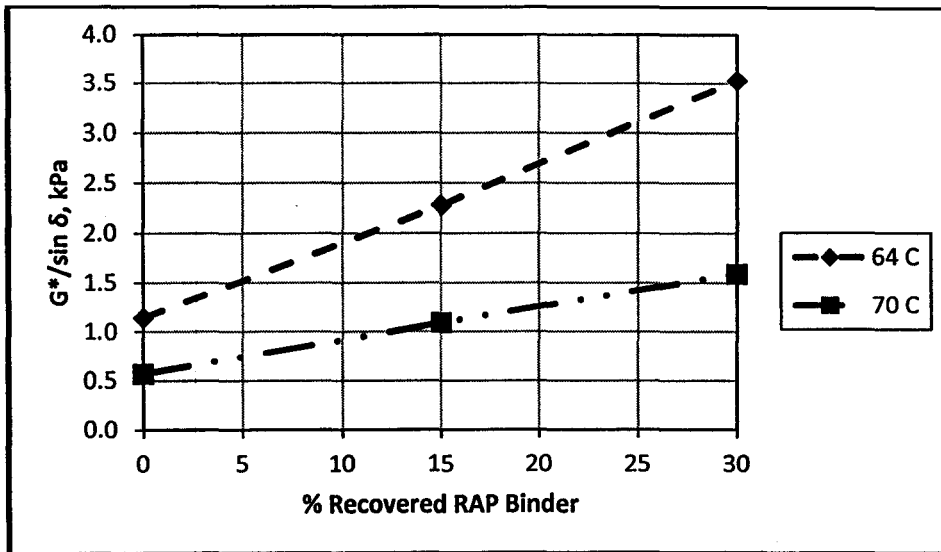
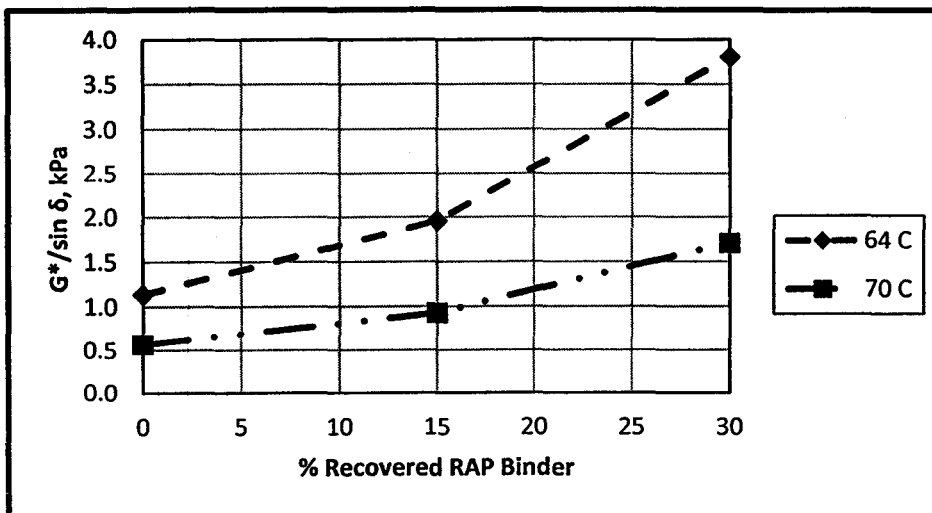


Figure 5.6: DSR Test Results for Blended Unaged Binder Incorporating 30% Recovered RAP Binder

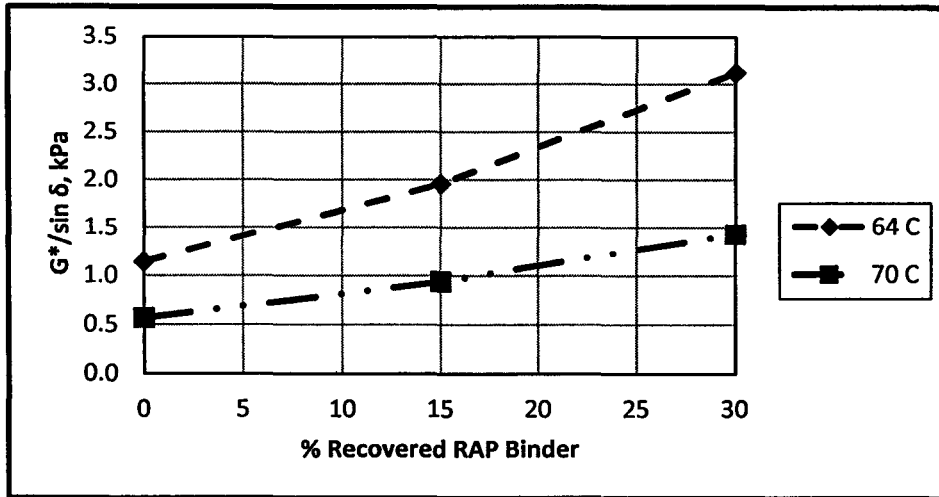
Figure 5.7 shows the relationship between $G^*/\sin \delta$ versus percent recovered RAP binder for unaged RAP blend. Clearly, $G^*/\sin \delta$ is higher at lower temperature and increases with the addition of RAP binder. The RAP binder produces stiffer blends. The rate of increase is high at lower temperatures and at higher percent of RAP as shown in Table 5.5. There is a noticeable increase in $G^*/\sin \delta$ at 64°C and 70°C, immediately after RAP binders were added to the virgin binder. At 64 °C, the PLUS RAP and LDP RAP blends exhibit the highest rate of increase in stiffness at 15% and 30% of RAP binder respectively.



(a) PLUS RAP Binder



(b) LDP RAP Binder



(c) JKR RAP binder

Figure 5.7: $G^*/\sin \delta$ for Unaged RAP Blends

Table 5.5: Rate of Increase in $G^*/\sin \delta$ for Unaged Blends

RAP Source	% RAP	Rate of Increase in $G^*/\sin \delta$ (kPa/%RAP)	
		64 °C	70 °C
PLUS	15	0.076	0.035
	30	0.080	0.034
LDP	15	0.055	0.036
	30	0.089	0.038
JKR	15	0.055	0.025
	30	0.066	0.029

5.6 Viscosity-Temperature Dependency of RAP Binder

Figures 5.8 to 5.10 show the viscosity-temperature dependency of asphalt binders with different percentages of virgin asphalt binder and RAP binders after being unaged, short-term aged (RTFO) and long-term aged (RTFO+PAV). The blended binders were consisted 15% and 30% of RAP binder from each RAP type. The graphs were purposely plotted on the linear scale so that the reflective effect of temperatures on viscosity was clearly distinguished. The typical relationship between viscosity and temperature on a semi-log scale would appear linear and difficult to see the exact trend after the effect of temperatures on viscosity (Gudimettla et al., 2003). Generally, from the figures as the temperature increased from 125 °C to 165 °C, the viscosity of all binders decreased at the all aging conditions. However the rate of decrease was not constant. Initially, there was a large reduction in viscosity. After reaching a temperature of about 155 °C the rate of decrease in viscosity was much lower. It can be noticed that the trend of the curves was all similar even though the magnitude of the viscosity was different at a particular temperature and aging condition for all these binders. Furthermore, addition of RAP binder to virgin binder has resulted in a modification of viscosity at the same temperature in different aging condition for all RAP types. This modification has changed the blended binders become more viscous and it has very much effect the workability of a recycled mixture.

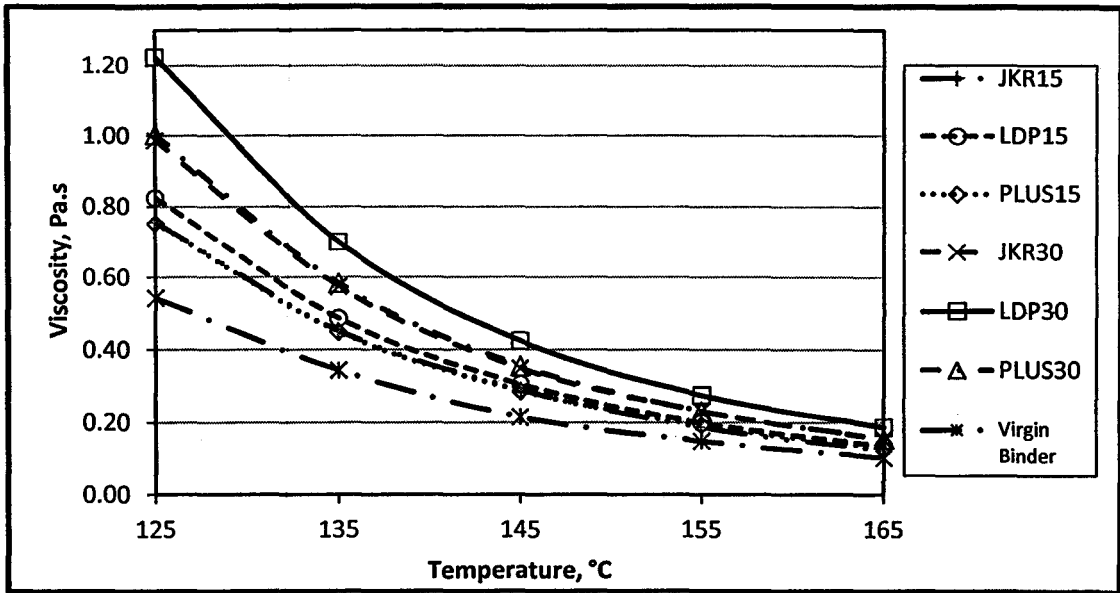


Figure 5.8: Viscosity-Temperature Relationship of Unaged Virgin and Blended Binders

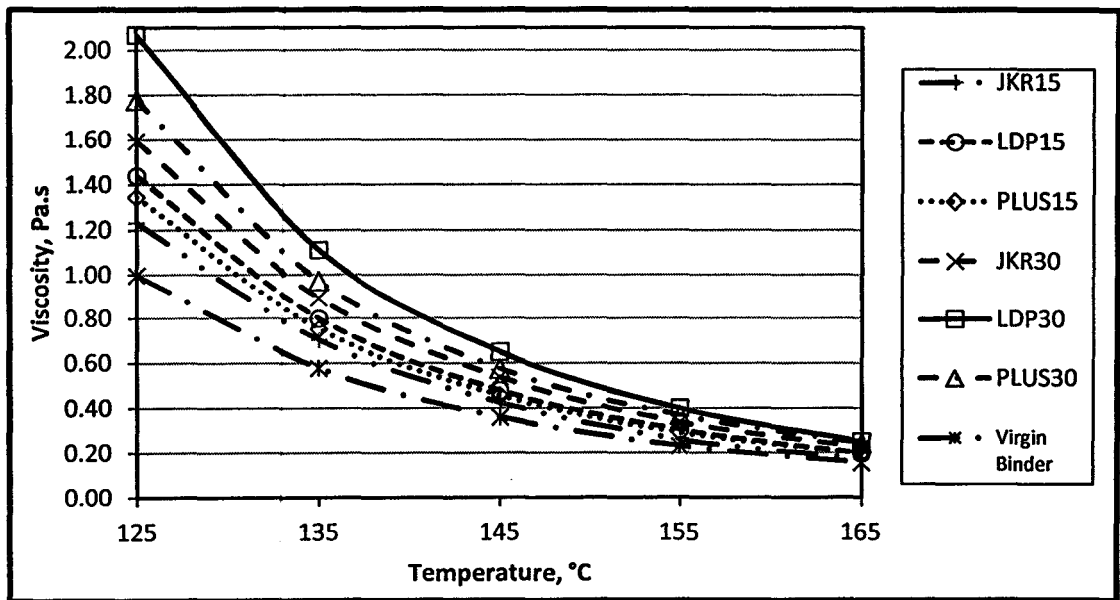


Figure 5.9: Viscosity-Temperature Relationship of Short-Term Aged Virgin and Blended Binders

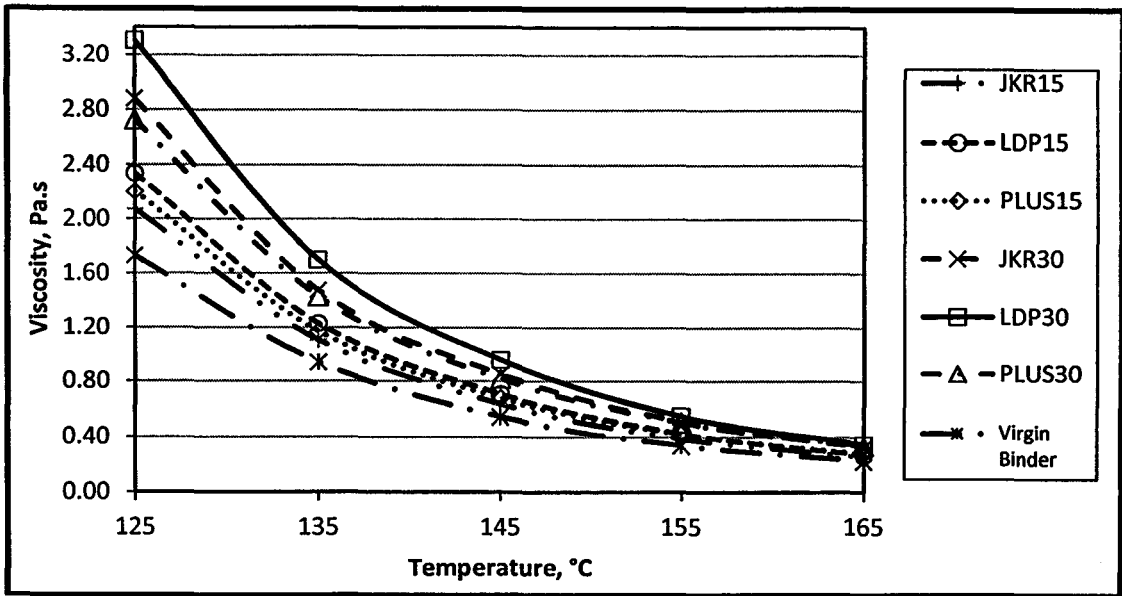


Figure 5.10: Viscosity-Temperature Relationship of Short-Term Aged Virgin and Blended Binders

Tables 5.6 to 5.8 present percent increased in viscosity in 3 aging conditions. For all aging conditions and RAP type the viscosity increased with increasing addition of RAP binders. It can be noted that LDP RAP has the highest percent increased in viscosity and it follows by PLUS RAP and JKR RAP for all aging conditions. However, at temperature 155°C and 165°C, blended binder with 30% JKR RAP binder has greater percent increased in viscosity compared to 30% PLUS RAP binder at unaged and short-term aging conditions. Subsequently, at long-term aging condition, blended binder with 30% PLUS RAP binder has lower increased in viscosity compare to JKR RAP binder at all temperatures. Percent of increased in viscosity is dropping as blended binders undergoes aging process from unaged to short-term and long-term aged.

Table 5.6: Percent Increased in Viscosity of Unaged Blended Binders

Temp., °C	% increased in viscosity					
	JKR RAP		LDP RAP		PLUS RAP	
	15%	30%	15%	30%	15%	30%
125	39	31	52	48	39	33
135	32	27	42	44	31	30
145	35	20	42	39	33	24
155	25	23	33	38	29	19
165	21	25	33	36	27	19

Table 5.7: Percent Increased in Viscosity after Short-Term Aged Blended Binders

Temp., °C	% increased in viscosity					
	JKR RAP		LDP RAP		PLUS RAP	
	15%	30%	15%	30%	15%	30%
125	24	29	45	44	35	32

135	22	27	38	39	30	29
145	18	26	33	36	27	26
155	12	30	31	32	26	27
165	12	29	26	27	26	24

Table 5.8 Percent Increased in Viscosity after Long-Term Aged Blended Binders

Temp., °C	% increased in viscosity					
	JKR RAP		LDP RAP		PLUS RAP	
	15%	30%	15%	30%	15%	30%
125	20	39	35	41	27	24
135	18	34	31	38	25	22
145	17	34	30	36	25	21
155	15	31	26	29	25	19
165	13	28	19	29	24	20

5.7 Virgin Bitumen Incorporating Recovered Reclaimed Asphalt Pavement Binder

5.7.1 Penetration

Figure 5.11 shows the penetration values of RAP modified binder after subjected to short term and long term aging. The penetration of RAP modified binder decreases as the RAP modified binders were further aged. The hardening trend of RAP modified binders is consistent with all RAP binder sources and proportions. For the respective RAP binder proportions, the penetration values of D15 and D30 RAP modified binders after the long term aging are 28 dmm and 24 dmm respectively, and are the lowest.

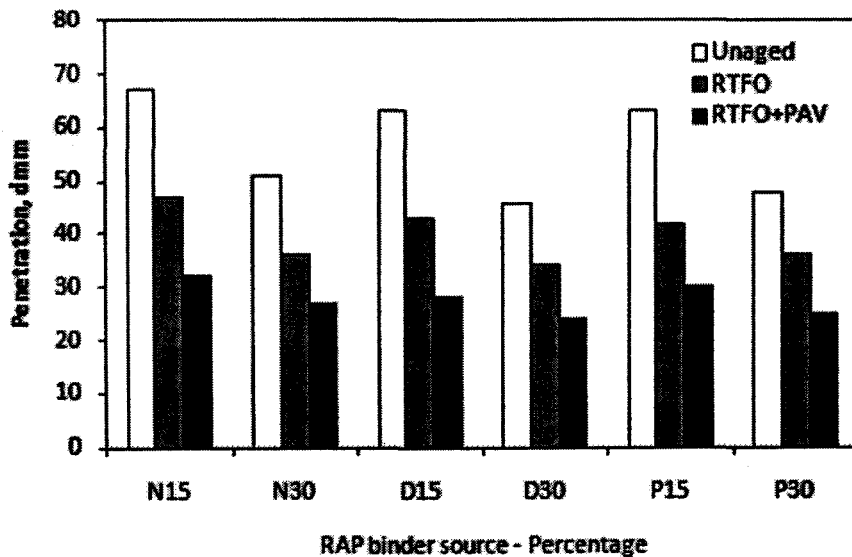


Figure 5.11: Penetration of RAP Modified Binder under different Aging Conditions

5.7.2 Softening Point

The softening point of all RAP binder sources and proportions increase as they undergo aging as shown in Figure 5.12. For the respective RAP binder proportions, the D15 and D30 RAP modified binders exhibit the highest softening point at 64°C and 67°C, respectively after subjected to long term aging.

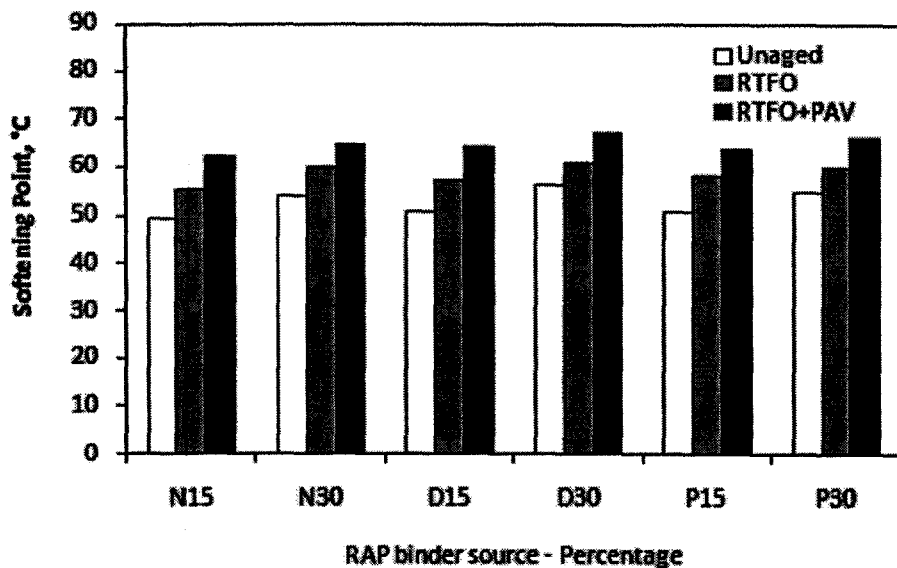


Figure 5.12: Softening Point of RAP Modified Binder under different Aging Conditions

Table 5.9 shows the percentage decrease and increase of penetration and softening point values, respectively of RAP modified binders after the short term and long term aging. It can be seen that the percentage decrease of penetration from unaged to short term and long term is nearly doubled for all RAP modified binders. Similar trend is also observed for percentage increase of softening point for all RAP binders. It is interesting to note that for RAP modified binder N15P, P15P, D30R, P30R, N30P, D30P and P30P have similar magnitude of percentage decrease within their RAP binder proportion groups and aging conditions. This relates well with similar magnitude of percentage increase in softening point in the groups. The effect of doubling the RAP binder content is to slightly reduce the percentage decrease and increase in penetration and softening point, respectively.

Table 5.9: Percentage Change in Penetration and Softening Point of Modified RAP Binders

RAP Modified Binder	Percentage Decrease in Penetration	Percentage Increase in Softening Point
N15R	29.9	10.8
N15P	52.2	20.2
N30R	29.4	10
N30P	47.1	16.3
D15R	31.7	11.4
D15P	55.6	21.1
D30R	26.1	8.2
D30P	47.8	16.4
P15R	33.3	12.9
P15P	52.4	20.5
P30R	25	8.3
P30P	47.9	16.7

Viscosity is a measure of a fluid’s resistance to flow. Figure 5.13 shows consistent increase in RAP modified binder viscosity with percentage of RAP binder as well as level of oxidation increase regardless of RAP binder sources. The N15U and P15U, and N30U and P30U RAP modified binders exhibit similar viscosity values of 0.45 Pa.s and 0.58 Pa.s, respectively. The viscosities of the D15P and D30P samples are the highest which corresponds to the most viscous binders among the RAP modified binders tested. The N15P and P30P RAP modified binders exhibit 61.5% and 60.8% increase respectively and are the highest in their groups. However, P15R and P30R have the lowest viscosity increments at 35.7% and 34.8%, respectively.

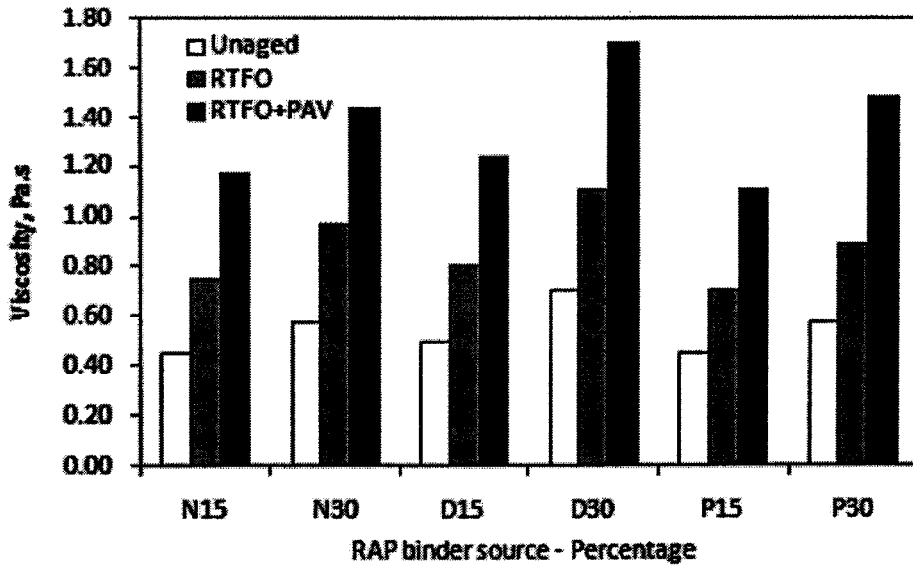


Figure 5.13: Viscosity of RAP Modified Binder under different Aging Conditions at 135°C

5.7.4 Penetration Index

The penetration index (PI) is a measure bitumen susceptibility to temperature and is calculated using Equation 1 (Read and Whiteoak, 2003). The PI for all modified RAP binder lies between +1 and -1 as depicted in Table 4, which is within the PI range for conventional bitumen (Roberts et al., 1991).

$$PI = \frac{1952 - 500 \log \text{pen} - 20SP}{50 \log \text{pen} - SP - 120} \quad (1)$$

Where,

Pen = penetration at 25°C

SP = softening point

Table 5.10 also indicates that as RAP modified binders are further aged, the penetration index is also increased. This means that the RAP modified binders are less temperature susceptible. It can be seen that for the respective RAP binder proportions, P15P and D30P RAP modified binders exhibit higher penetration index at 0.52 and 0.66 respectively, after long term aging.

5.7.5 Viscosity Aging Index

The viscosity aging index is defined by Equation (2). Table 5.10 also shows the viscosity aging index of the RAP modified binders from the three sources after short term and long term aging.

$$VAI = \frac{\text{Viscosity of aged RAP modified binder}}{\text{Viscosity of unaged RAP modified binder}} \quad (2)$$

It can be seen that for the respective RAP binder proportions, N15P and P30P RAP modified binders exhibit higher viscosity aging index at 2.60 and 2.55 respectively, after subjected to long term aging. This high rate of hardening is contributed to the increasing asphaltene compounds in the modified RAP binder due to severe oxidative process.

Table 5.10: Penetration Index and Viscosity Aging Index of RAP Modified Binders

Modified RAP Binder	Penetration Index	Viscosity Aging Index
N15R	-0.06	1.67
N15P	0.38	2.6
N30R	0.26	1.67
N30P	0.48	2.46
D15R	0.05	1.63
D15P	0.47	2.51
D30R	0.33	1.59
D30P	0.66	2.43
P15R	0.21	1.55
P15P	0.52	2.47
P30R	0.26	1.53
P30P	0.58	2.55

5.7.6 Fourier Transform Infrared Spectroscopy

The Infrared spectroscopy is used to study the distribution of functional group types present in the asphaltenes of asphalt binders. It has proved to be very useful technique in analyzing structural changes in the fractions following RTFO and PAV test of asphalt binders. In this study, the most distinguished IR vibrations of particular interest were for C=O and S=O. At wavelength 1704 cm⁻¹, IR spectra displayed a distinct C=O absorption due to carbonyl and/or carboxyl groups. While an intense peak at 1030 cm⁻¹ was assigned to the stretching vibration of sulfoxide, S=O (Siddiqui and Ali, 1999; Wu et al., 2009). Chemically,

aging has led to a decrease in aromatic content and subsequent increase in resin content and generate high asphaltenes content (Lesueur D, 2009). The oxidation of asphaltenes by short-term and long-term aging of the asphalt is distinctly large as compared with most of the hydrocarbon absorption peaks. The stronger absorption of oxygen band make the difference among them more easy to measured and characterized than any other hydrocarbon structures present in the asphalt binder (Siddiqui and Ali, 1999).

Figure 5.14 shows FTIR spectra plot for a virgin binder with different aging condition. It can be seen that the trend of the plot is the same for all blended binders as presented in Figures 5.15 to 5.17. The peaks at the respective wavelength indicate the growth of carbonyl compounds and sulfoxides which were formed during the process of RTFO and PAV. Virgin binder and blended binders IR spectra plots clearly exhibit the changes in the chemical structural composition of the binder after each aging stage.

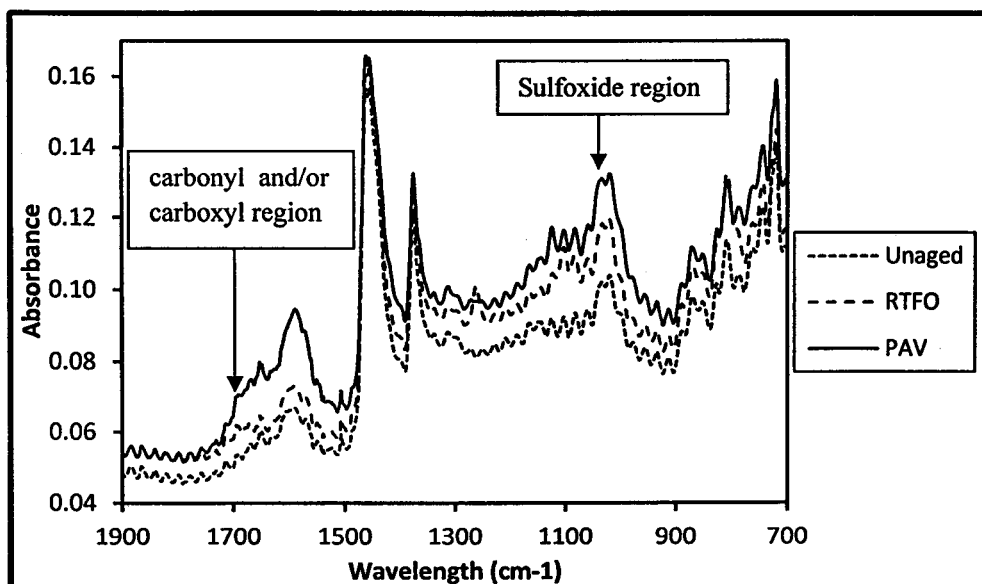
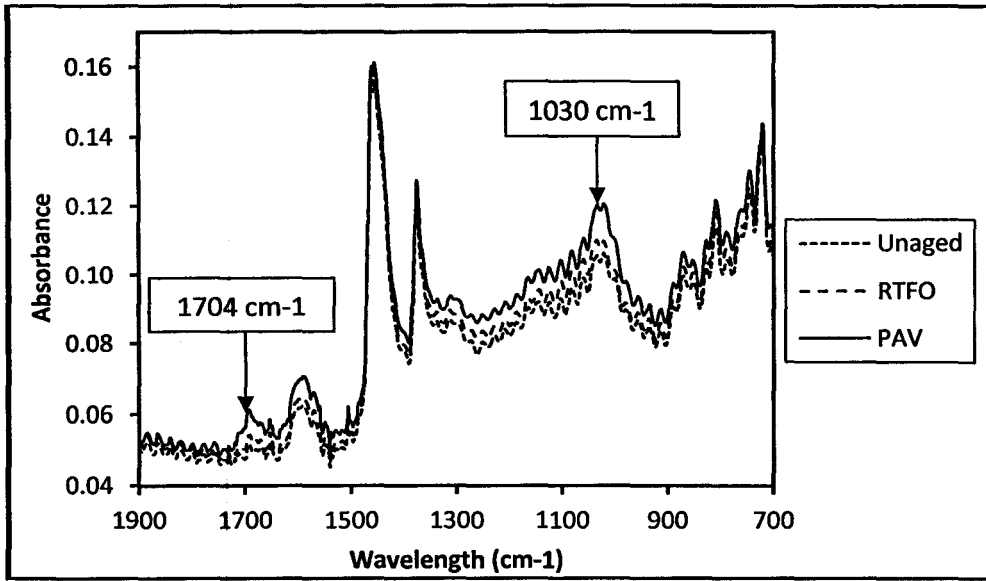
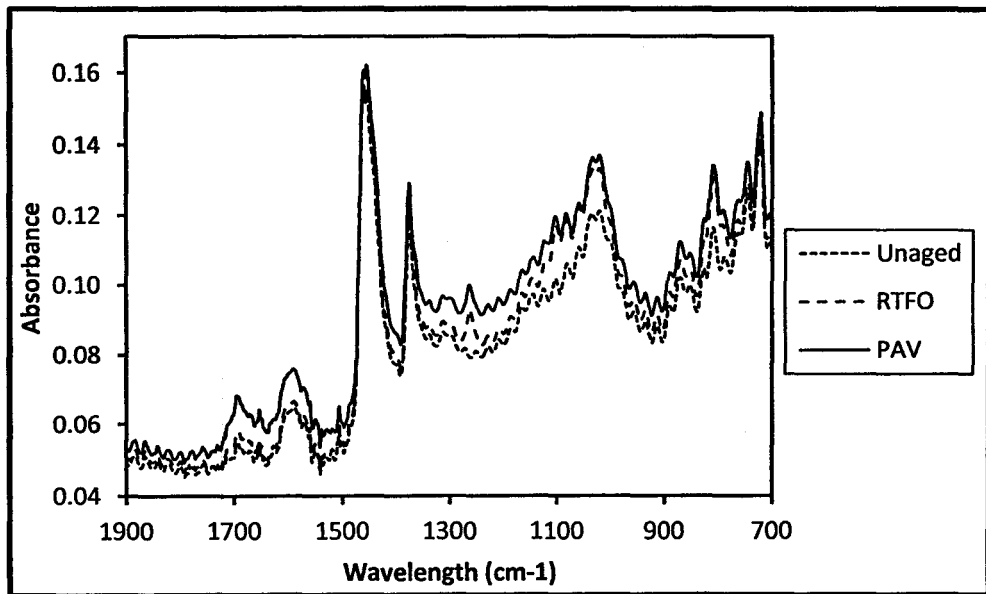


Figure 5.14: FTIR Spectrum of Virgin Binder

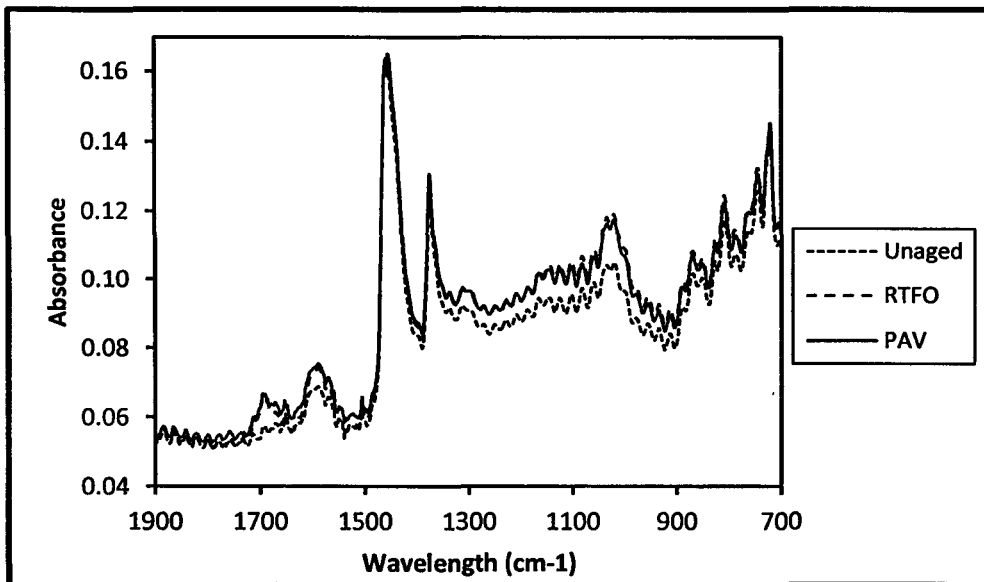


a) 15% JKR RAP Binder

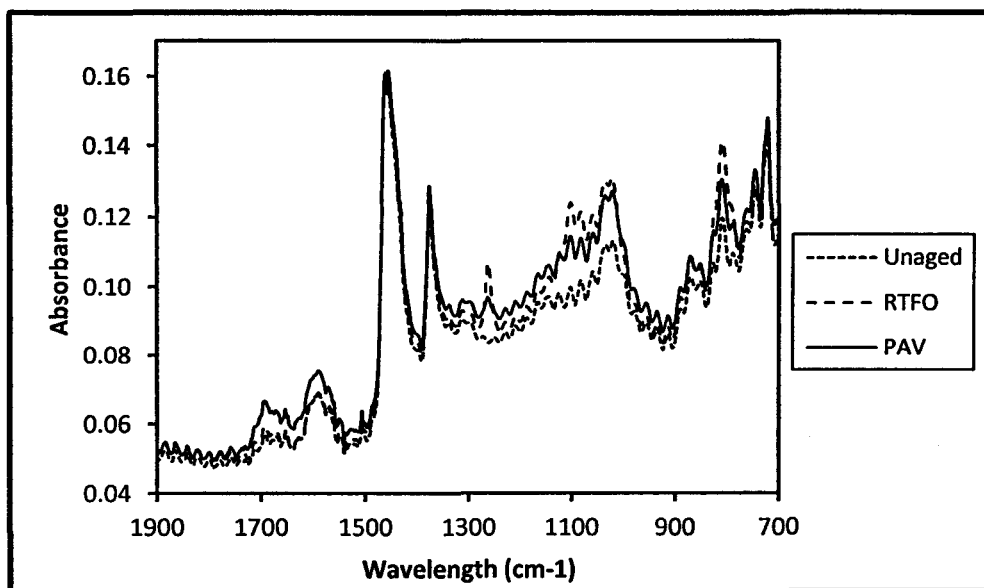


b) 30% JKR RAP Binderfl

Figure 5.15: FTIR Spectrum of Virgin Binder Blended with JKR RAP Binder

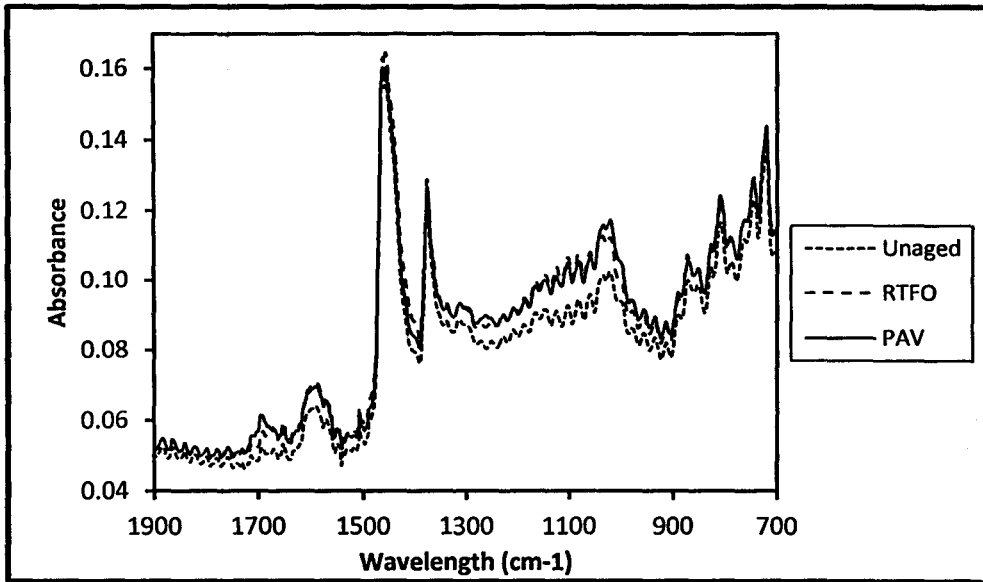


a) 15% LDP RAP Binder

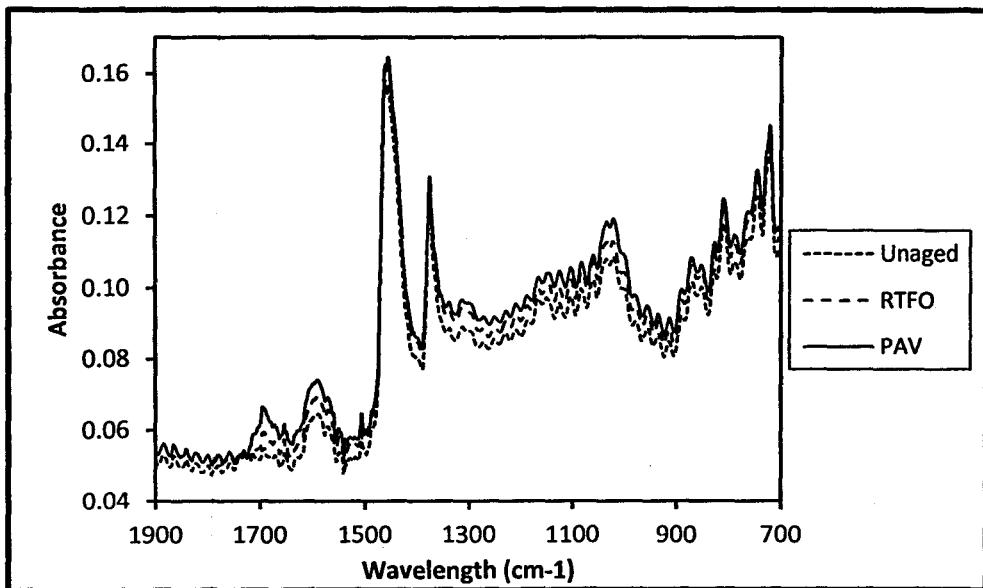


b) 30% LDP RAP Binder

Figure 5.16: FTIR Spectrum of Virgin Binder Blended with LDP RAP Binder



a) 15% PLUS RAP Binder



b) 30% PLUS RAP Binder

Figure 5.17: FTIR Spectrum of Virgin Binder Blended with PLUS RAP Binder

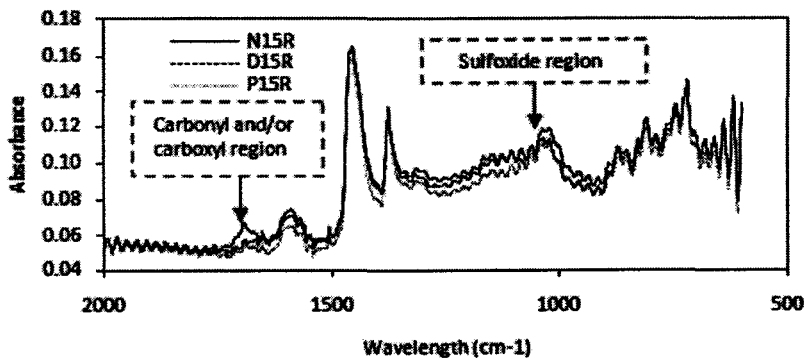
In Table 5.11, generally at wavelength 1705 cm^{-1} , the percent increased in absorbance is higher for the PAV samples compared to RTFO samples. Conversely, at wavelength 1030 cm^{-1} , the percent increased in absorbance is lower for the PAV samples compared to RTFO samples. It can be observed that when the percent increased is high in the RTFO so we can expect low percent increased in PAV and vice versa. Blended binders from JKR and PLUS RAPs have nearly similar absorbance rate compared to LDP RAP which can be interpreted that they have almost the same level of aged.

Table 5.11: Percent Increased in Absorbance

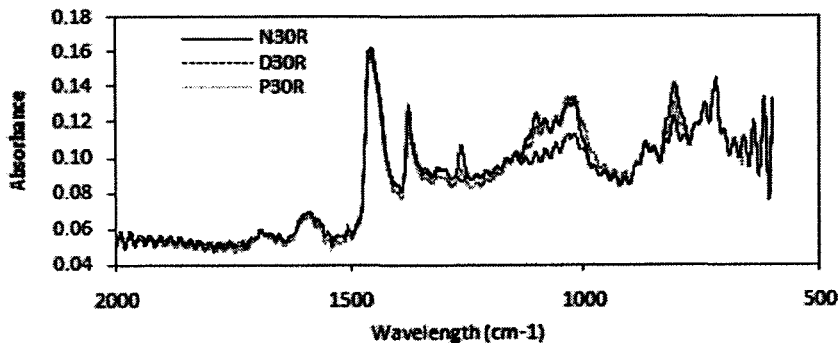
Binder	% increased in Absorbance
--------	---------------------------

Type	1705 cm-1		1030 cm-1	
	RTFO	PAV	RTFO	PAV
Virgin	15.7	9.7	16.0	10.5
15% JKR RAP	4.8	10.8	4.0	9.8
30% JKR RAP	5.1	16.6	10.7	2.6
15% LDP RAP	12.6	1.5	13.7	-1.5
30% LDP RAP	4.2	10.7	16.4	-3.2
15% PLUS RAP	8.1	7.5	10.7	3.5
30% PLUS RAP	6.0	9.8	4.3	5.3

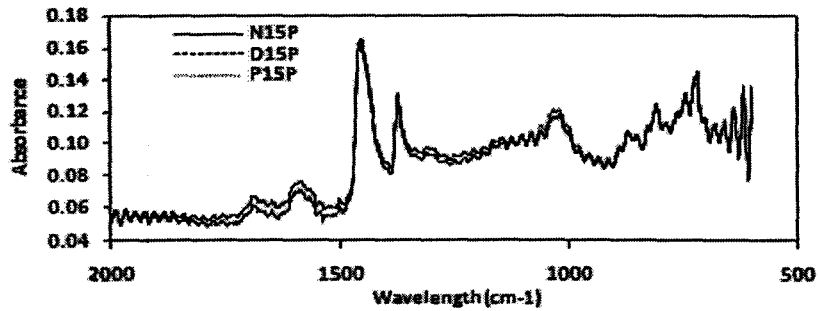
During the artificial aging processes, the modified RAP binders were severely oxidized in which aromatization, dehydrogenation and intermolecular and intramolecular hydrogen bonding of polar groups were substantially increased. The chemical functional and structural changes are precisely analyzed through infrared at vibration modes of C=O and S=O. Figure 5.18 illustrates the infrared spectra of the RAP modified binders for the three RAP sources. The figures clearly show the increasing trend of spectra at carbonyl and sulfoxide groups with increased RAP binder content and aging period as well as aging condition. It can be observed that the absorbance value increases at every level of oxidation at carbonyl and sulfoxide regions.



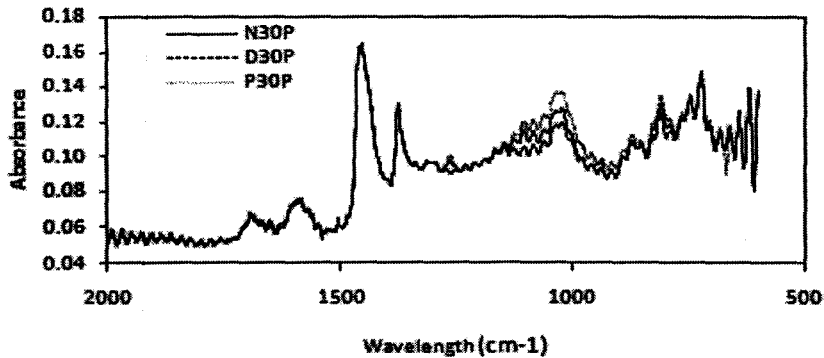
(a) Short Term Aging (15% RAP binder)



(b) Short Term Aging (30% RAP binder)



(c) Long Term Aging (15% RAP binder)

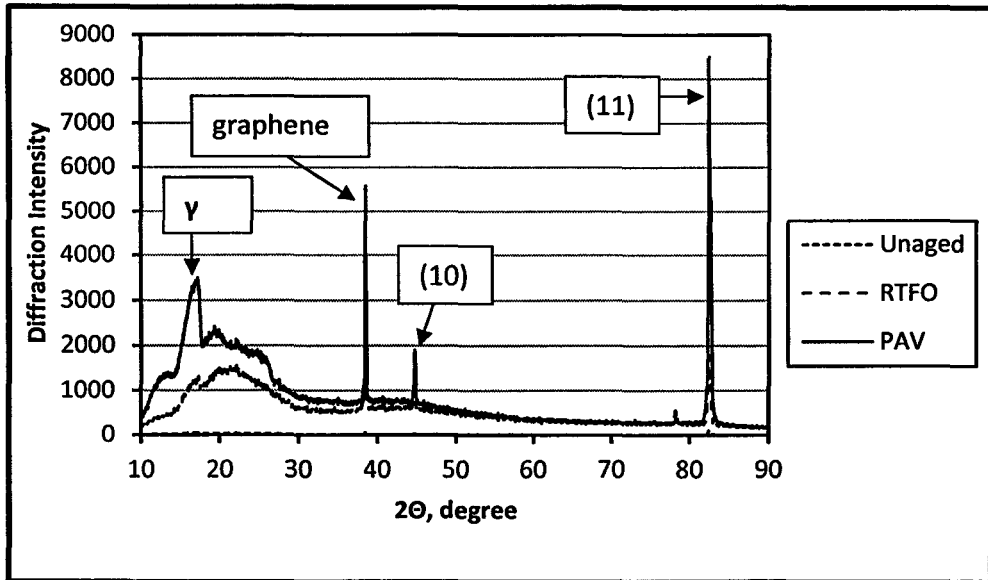


(d) Long Term Aging (30% RAP binder)

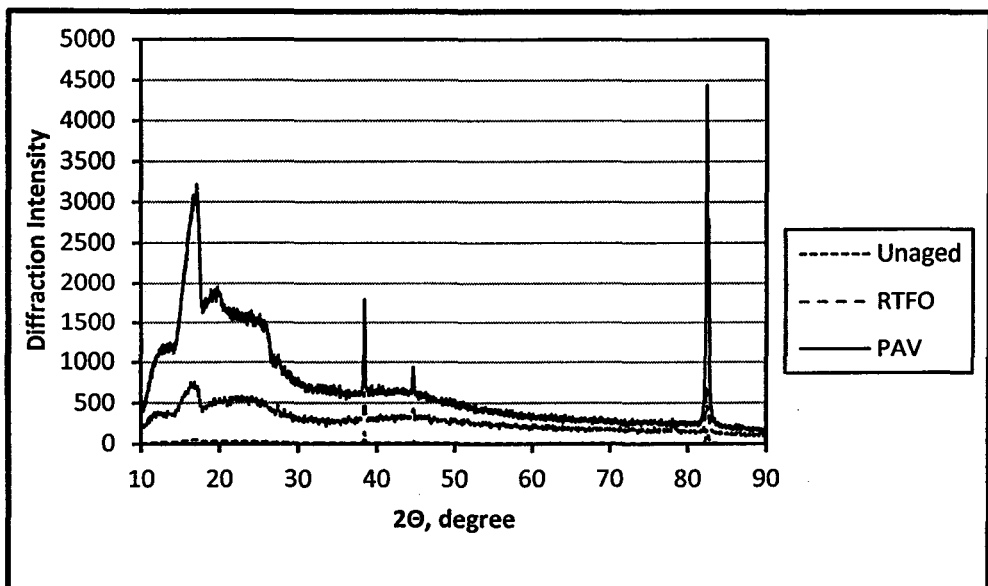
Figure 5.18: Fourier Transform Infrared Spectroscopy Spectrum of RAP Modified Binders

5.7.7 X-ray Diffraction

Figure 5.19 presents X-ray patterns of virgin binder blended with 15% and 30% JKR RAP binder at different aging condition. Generally, the plot contains four peaks of asphaltenes and resin pattern in which each peak represents γ peak, graphene layer stacking peak, the (10) peak and the (11) peak. The sharp narrow pattern peaks indicate highly crystalline with high degree of long range order due to forming of asphaltenes and resin during the aging process. It can be seen that in the both figures the curves have similar trend and order. The diffraction intensity increases as blended RAP binder was aged from unaged to short-term and long-term aged. The aging process has resulted in reducing aromatic component and increasing the asphaltene compound of the blended RAP binder. The results also show that the graphene and (11) peaks which comes from the x-ray diffraction of aromatic planar structure of asphaltenes and resin have reduced 88% and 47% in diffraction intensity respectively as percentage of JKR RAP binder increases from 15% to 30%. This is attributed to lower composition of aromatic compound in the 30% RAP binder blend.



a) 15% JKR RAP Binder



b) 30% JKR RAP Binder

Figure 5.19: The X-Ray Pattern of Virgin Binder Blended with JKR RAP Binder

5.7.8 Carbonyl Groups of Modified RAP Binders

Carbonyl and/or carboxyl groups were detected by IR spectra with the presence of distinct C=O absorption at 1700 cm^{-1} wavelength. The area of the carbonyl absorption was measured from valley to valley of the peak between 1726 and 1675 cm^{-1} by using Spectrum version 5.0.1 software, which corresponds to the region containing the absorption peaks for carboxylic acid, ketones and anhydrides. Carboxylic acids occur naturally in bitumen while ketones and anhydrides form on oxidative aging. The oxidative aging is well related to the existence of these three functional groups which are an integral part of large asphalt

Table 5.12 shows the area ratio of unaged and aged RAP modified binders. It can be seen that the area ratio of all carbonyl groups increased consistently in both short term aging and long term aging for the three RAP sources. The D15P and P30P RAP modified binders exhibit the highest ratio at 0.124 and 0.175 after long term aging, respectively. The unaged RAP modified binder, N15U and P15U have the lowest C=O area ratio value. On the contrary, the area ratio of N15U and P15U increased by 63.1% and 58.2%, respectively after long term aging, representing the higher percent increase in area ratio among the RAP modified binders tested. This indicates that the evolution of RAP modified binder structures has taken place after extreme aging conditions. During that period, the amount of asphaltene compound has increased due to oxygenation of resin. During the aging process oxygen was being taken up by asphaltene molecular structure. This is similar to the findings of Siddiqui and Ali, (1999) where there was an increase in the percent weight of oxygen in asphaltene molecules which indicate insertion of substantial amount of oxygen in the asphaltene after each level of oxidation. Furthermore, the long term aging is attributed to a large quantity of oxygen incorporated in the newly formed oxygen-containing groups such as hydroxyl, carbonyl, and carboxylic groups. The consistent increase in area ratio correlates well to the increase in the level of oxidation which caused a pronounced increase C=O in the carbonyl region.

Table 5.12: Area Ratio of RAP Modified Binders before and after Aging

RAP Modified binder	Carbonyl	Sulfoxide
	C=O (1700 cm ⁻¹)	S=O (1030 cm ⁻¹)
N15U	0.041	0.51
N15R	0.046	0.54
N15P	0.111	0.55
N30U	0.109	0.54
N30R	0.127	0.543
N30P	0.14	0.56
D15U	0.1	0.514
D15R	0.11	0.551
D15P	0.124	0.553
D30U	0.125	0.564
D30R	0.132	0.582
D30P	0.149	0.603
P15U	0.041	0.535
P15R	0.047	0.539
P15P	0.098	0.599
P30U	0.108	0.597
P30R	0.12	0.616
P30P	0.175	0.664

5.7.9 Sulfoxide Groups of Modified RAP Binders

Vibration of sulfoxide (S=O), a functional group most easily formed in bitumen upon oxidation of sulphide compound was captured at intense peak 1030 cm⁻¹ from the IR spectra. The wavenumber of sulfoxide vibration covered the wavelength between 1051 and 1027 cm⁻¹.

Table 5 relates similar trend for sulfoxide groups in which the area ratio of all sulfoxide groups increased consistently in both short term aging and long term aging for the three RAP sources. The increase aging time subsequently increase the area ratio in S=O where during the oxidation process, oxygen was absorbed by the sulphide compound of asphaltene molecular structures. This chemical reaction is contributed to further hardening of the RAP modified binder. The P15P and P30P RAP modified binders exhibit the highest S=O ratio at 0.599 and 0.664 at long term aging respectively.

5.7.10 Correlation between Penetration Index, Viscosity Aging Index and Area Ratio

Table 5.13 shows a high significance and Pearson correlation values between penetration index and viscosity aging index, and between penetration index and area ratio of the RAP modified binders. This is evident by high penetration index well corresponds to high viscosity aging index and area ratio of the RAP modified binders. Even though as viscosity aging index increase, the area ratio of carbonyl groups also increases, however in general there is no significant correlation between the parameters.

Table 5.13: Coefficient of Correlation Analysis

Correlation between	Pearson correlation	p-value (2-tailed)	Significant
PI*VAI	0.784	0.003	Yes
PI*AR	0.712	0.009	Yes
VAI*AR	0.501	0.097	No

Notes: PI –Penetration Index, VAI –Viscosity Aging Index, A –Area Ratio

5.7.11 Mixing and Compaction Temperatures

Figure 5.20 presents mixing and compaction temperatures for virgin and recycled mixtures corresponding with binder viscosity values of 0.17 ± 0.02 Pa.s and 0.28 ± 0.03 Pa.s, respectively (The Asphalt Institute, 2001). The trend of the lines in the graph indicates that as the percentage of RAP binder increases the mixing and compaction temperatures increases as well.

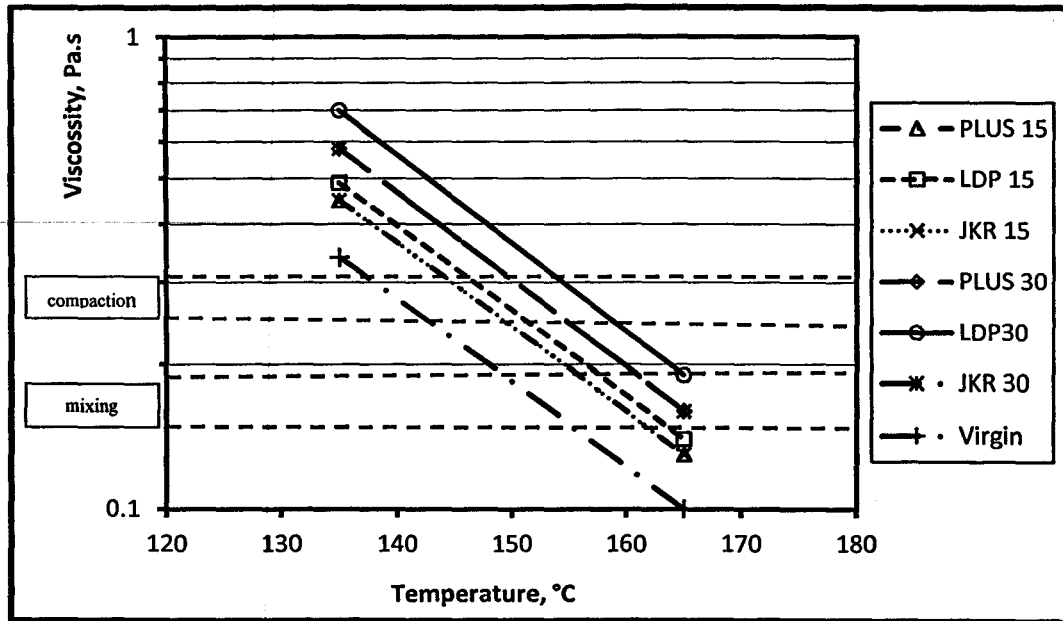


Figure 5.20: Mixing and Compaction Temperatures

Recycled mixtures incorporated with JKR RAP and PLUS RAP for all percentages have similar ranges of mixing and compaction temperatures as the lines are superimposed each other. Recycled mixture containing LDP RAP has the highest mixing and compaction temperatures. The average mixing and compaction temperatures for all recycled mixtures containing RAP are at 160°C and 150°C respectively. While mixing and compaction temperatures for virgin mixture is at 155 °C and 145 °C, respectively. The higher temperature limit is used for determining average mixing and compaction temperatures because at higher temperature the viscosity of binder is decreased and the mix workability would be better. Furthermore, the virgin material will mix better with RAP material at higher temperature.

5.8 Characterization at High Temperatures

5.8.1 Effects of RAP on Viscosity

Viscosity behavior differs according to binder types and aging conditions. The relationships between viscosity and temperature of unaged, short term aged, and long term aged asphalt binder at the sweep temperatures are illustrated in Figure 5.21.

Figure 5.21 shows that the viscosity-temperature dependency exhibits a polynomial trend with R^2 greater than 0.9 at the sweep temperatures irrespective of RAP binder sources and sample aging conditions. It also shows that D30 sample exhibits the highest viscosity regardless of aging state. The results of analysis of variance (ANOVA) in Table 5.14 also show that RAP source and RAP content have significant effects on the viscosity.

Table 5.14: Results of Analysis of Variance (ANOVA) for Viscosity

Source	Sum of squares	df	Mean square	F	p-Value	Significant
Intercept	149596262.296	1	149596262.296	464411.032	<0.001	Yes
Source	605067.480	2	302533.740	939.195	<0.001	Yes
Temperature	76570477.604	4	19142619.401	59426.910	<0.001	Yes
Aging	19979584.643	2	9989792.322	31012.605	<0.001	Yes
Content	2915891.280	1	2915891.280	9052.179	<0.001	Yes
Source*temperature	464449.089	8	58056.136	180.231	<0.001	Yes
Source*aging	73245.227	4	18311.307	56.846	<0.001	Yes
Temperature*aging	13803084.301	8	1725385.538	5356.338	<0.001	Yes
Source*temperature*aging	85382.941	16	5336.434	16.567	<0.001	Yes
Source*content	127102.117	2	63551.059	197.290	<0.001	Yes
Temperature*content	1881280.599	4	470320.150	1460.076	<0.001	Yes
Source*temperature*content	98846.584	8	12355.823	38.358	<0.001	Yes
Aging*content	365173.278	2	182586.639	566.827	<0.001	Yes
Source*aging*content	40527.460	4	10131.865	31.454	<0.001	Yes
Temperature*aging*content	293594.643	8	36699.330	113.930	<0.001	Yes
Source*temperature*aging*content	41225.701	16	2576.606	7.999	<0.001	Yes
Error	57981.670	180	322.120			
Total	266999176.915	270				
Corrected total	117402914.619	269				

*: Interaction; source: RAP source; content: RAP content.

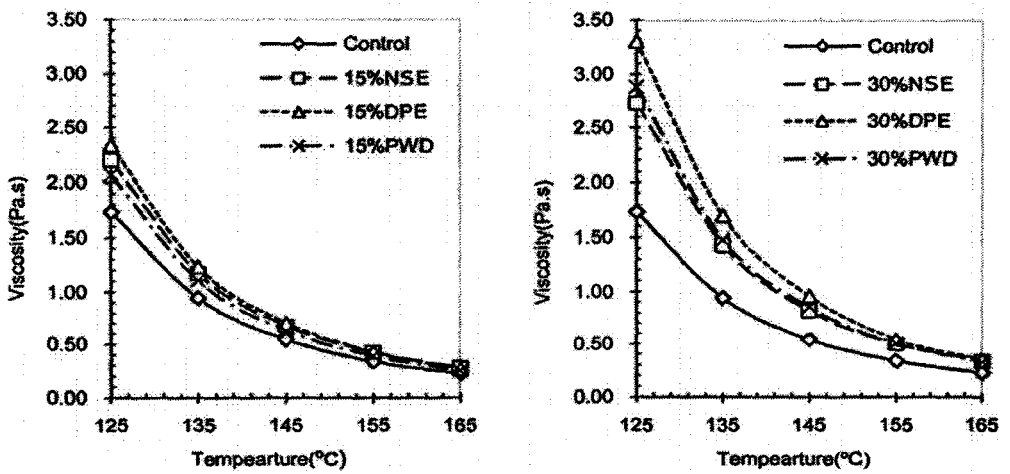
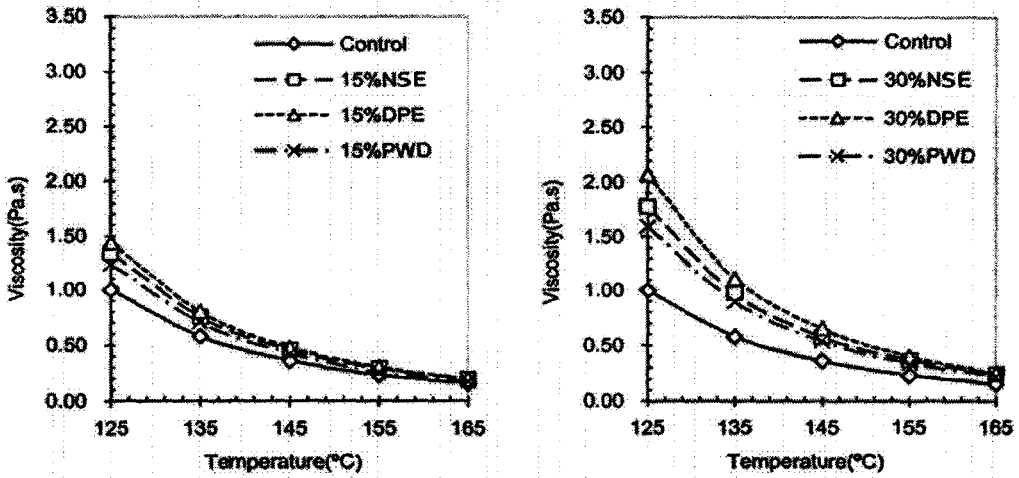
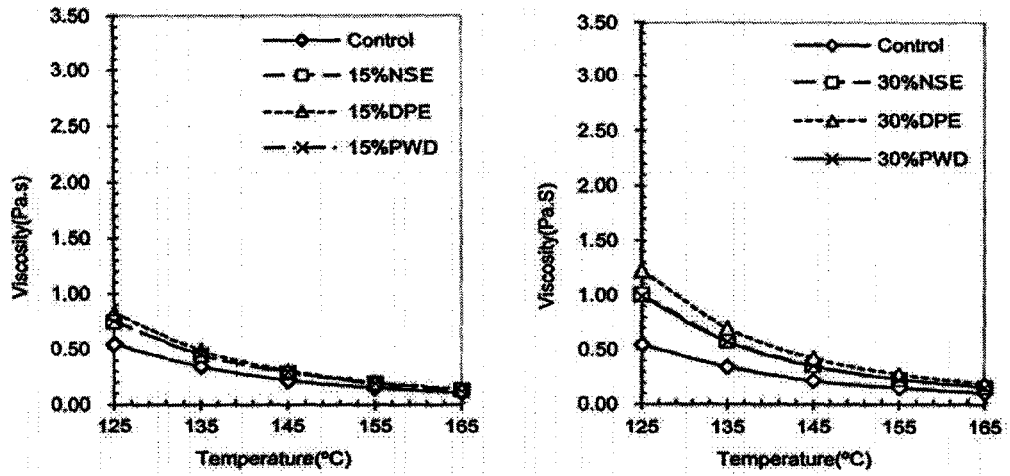


Figure 5.21: Viscosity-Temperature Dependency of Virgin and RAP Modified Binder

5.8.1.1 Effects of Sasobit® Content on Viscosity

Viscosity is a fundamental characteristic that describes the resistance of fluids to flow. In practice, it is necessary to ensure that asphalt binder has adequate viscosity to ease pumping and able to coat each aggregate particle during mixing. The relationships between viscosity and Sasobit[®] content of PG64 and PG70 binders subjected to different temperatures and aging conditions are shown in Figure 5.22.

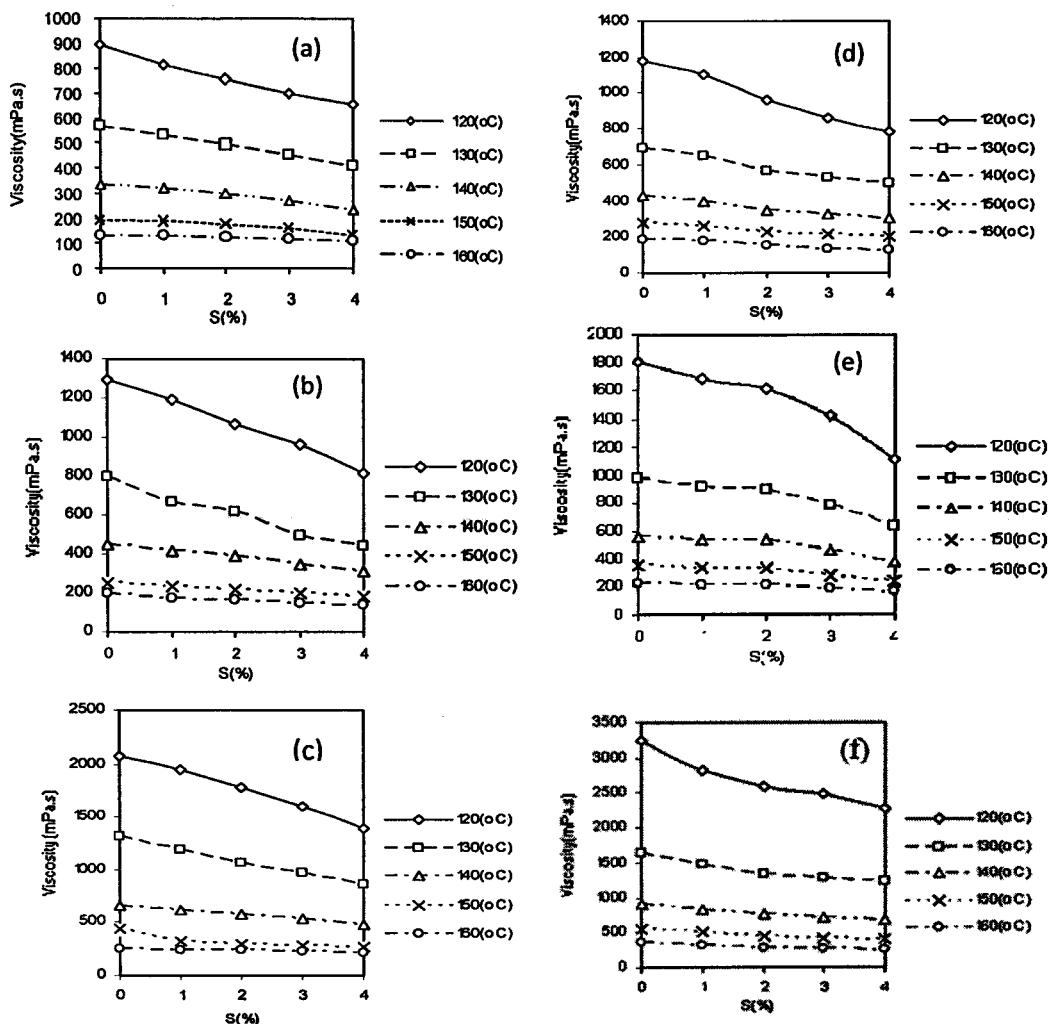


Figure 5.22: Viscosity–Sasobit[®] Content Dependency for (a) Unaged PG64, (b) Short Term Aged PG64, (c) Long Term Aged PG64, (d) Unaged PG70, (e) Short Term Aged PG70, (f) Long Term Aged PG70

Figure 5.22 shows that the addition of Sasobit[®] linearly decreases the binder viscosity of the asphalt binders tested and similar pattern can be observed for binders that are subjected to short term and long term aging. This decrease in viscosity is more pronounced when the binders are blended with 3% and 4% Sasobit[®] and tested at 120°C and 140°C for both binder types regardless of aging conditions.

5.8.2 Effects of RAP Binder on Construction Temperatures

In asphalt mix production, the binder should be fluidic enough to completely coat the aggregate particles and bind them together after compaction has ceased. In this regards, the Asphalt Institute recommends that the mixing and compaction temperatures should, respectively, correspond to viscosity ranges 170 ± 20 mPa s and 280 ± 30 mPa s (Asphalt

Institute, 2003). Using this guide, Table 6 shows the corresponding mixing and compaction temperatures of virgin and RAP modified binders.

From Table 5.15, the construction temperatures of RAP modified binder from NSE (N15 and N30) and PWD (P15 and P30) are identical. It can also be observed that D30 requires the highest mixing and compaction temperatures. Higher construction temperature can cause delay in opening pavement to traffic because the compacted mixes require more time to cool down. The P15 and N15 binders require the lowest construction temperature compared to the others.

Table 5.15: Construction Temperatures for Virgin and RAP Modified Binders

Parameter	Virgin	RAP modified binder					
		N15	N30	D15	D30	P15	P30
Mixing, °C	155	161	165	163	168	161	165
Compaction, °C	145	151	155	153	158	151	155

5.8.3 Selection of RAP Source and RAP Content

To choose a preliminary optimum RAP content and source, three critical parameters are selected to evaluate binder performance namely construction temperatures, Superpave™ fatigue, and aging factors. These parameters can be very advantageous because the chosen construction temperatures enable energy and environmental policy makers to assess increase in energy or fuel requirement and GHG emissions from different RAP sources since energy saving and reduction in GHG emission has been major current challenge in the world (Klemes et al., 2010; Jeong and Mo, 2009; Burandt and Barth, 2010) (Tables 13 and 14). If engineers and asphalt researchers need to evaluate binder performance and aging potentials of asphalt binder samples at the pavement in-service temperatures, then the Superpave™ fatigue, rutting and aging factors, respectively are useful (Fig. 3, Tables 7 and 10). Under these circumstances, the following viable scenarios can be suggested to select the preliminary optimum RAP binder content and source using the results of Superpave™ asphalt binder tests.

5.8.3.1 Scenario 1

If the in-service temperature of the asphalt pavement is high and the pavement is subjected to heavy traffic volume, then asphalt mix designated as D30M is recommended because incorporating such binder can upgrade the binder performance grade to PG76, which in turn increases its rutting resistance (Tables 7 and 9). However, it should be noted that the fuel requirement and the GHG emissions from asphalt mix D30M is the highest when compared to other mixes as shown in Tables 13 and 14.

5.8.3.2 Scenario 2

If the minimization of energy requirements and GHG emissions are of paramount importance due to the necessity to preserve the environment, then the most environmental friendly option is to adopt N15M because of the aging factor, the corresponding fuel requirement, and the GHG emissions are the least as shown in Tables 10, 13, and 14, respectively.

5.8.3.3 Scenario 3

If the in-service temperature is as low as 22 °C, then, resistance to fatigue must be considered. In this case, the highest permissible RAP content and the best source to satisfy the fatigue criteria are about 10% and sourced from PWD (P10M), respectively, as shown in Fig. 3. The above suggestions on RAP source and content selections are based on the binder test results. It is recommended to carry out mix performance tests for a more comprehensive mix evaluation.

5.9 Effects of Aged Binder Content on CO₂ Emission

Figures 5.23 and 5.24 illustrate the effects of various aged binder contents on CO₂ emission for different scenarios and fuel types used in an asphalt plant. It can be seen from the figures that natural gas contributes to the highest reduction of CO₂ emission especially when the aged binder incorporates Sasobit®.

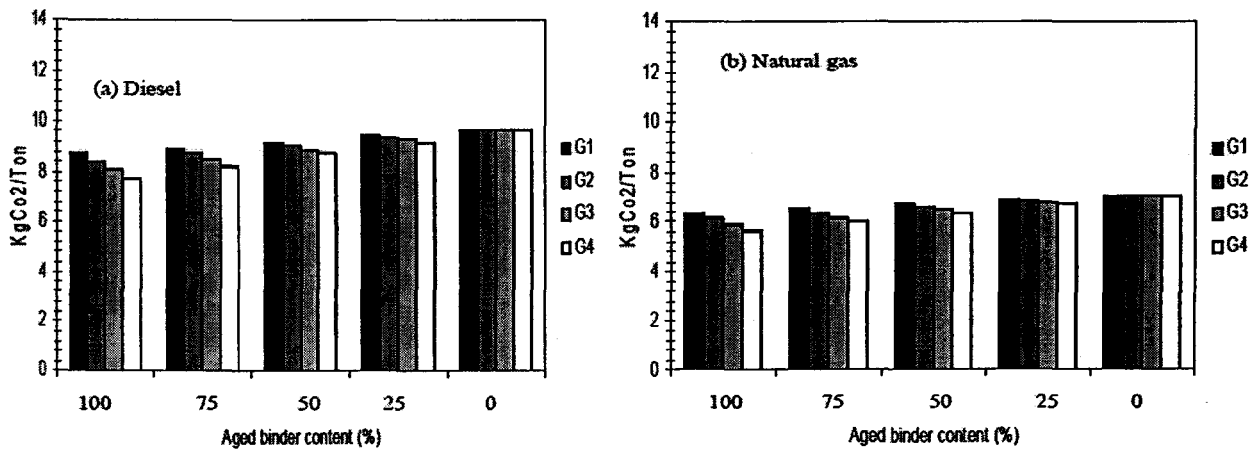


Figure 5.23: Effects of Aged Binder Content on CO₂ Emission for Scenario 1

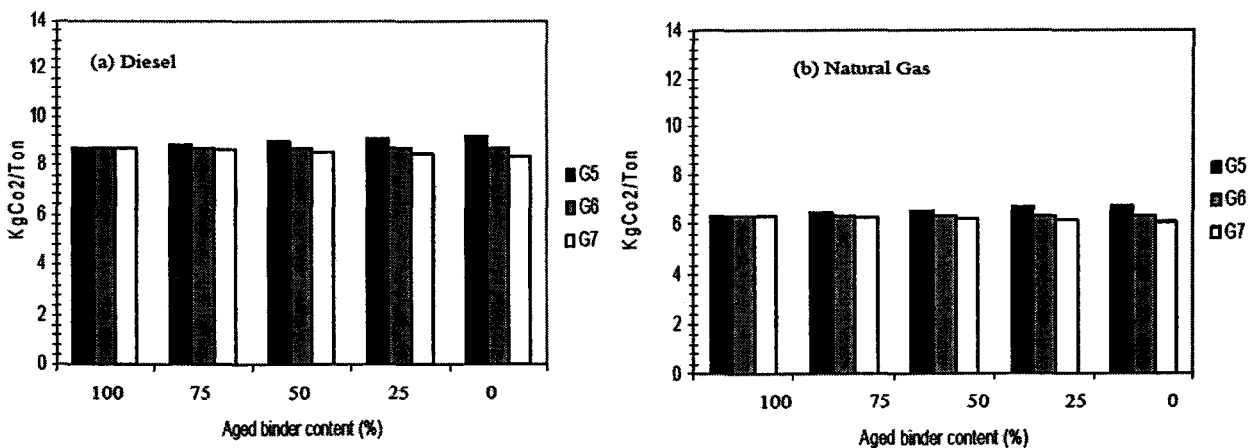


Figure 5.24: Effects of aged binder content on CO₂ emission for scenario 2

Analysis of the results from these two scenarios has shown that Sasobit® can reduce the required heat energy irrespective of aged binder content. In addition to that, use of Sasobit® helps to conserve the environment and contributes to cleaner technologies.

Although aged binders modified by Sasobit® exhibit lower heat energy to raise from ambient to mixing temperatures, it should be noted that these modified binders can be brittle and stiff at low and intermediate temperatures due to synergistic effects of long-term aging and the presence of Sasobit®. To offset the increase of binder stiffness caused by WMA additives and aged binders, Lee et al. (2009) recommended the use of lower performance grade virgin binder.

CHAPTER SIX

RAP MIXTURE PERFORMANCE

6.1 Introduction

RAP milled from ProjekLebuh Raya Utara-Selatan (PLUS) highway was studied at the USM. A mix design of RAP mixes with four different RAP contents (10%, 20%, 30% and 40%) was carried out to make the gradation for each RAP mix as close as possible to the control mix. The total asphalt binder content determined in the design of the virgin material mixes was used in the mixes containing RAP. The amount of virgin asphalt added to the RAP mixes was reduced to account for the asphalt binder contributed by the RAP material.

6.2 Indirect Tensile Strength Test

The potential of thermal cracking of RAP mixes was determined by evaluating the mix fracture strength characteristic. From Figure 6.1, it can be seen that there is a trend of increasing in tensile strength as higher percentages of RAP are incorporated in the mixes. This result is expected as higher percentages of RAP significantly increase mix stiffness. The tensile strength for mixes containing 10% RAP is comparable with control sample for all RAP sources. Mixes incorporating 40% RAP exhibit the highest strength for all RAP sources where the tensile strength increase range from 27% to 30% compared to control mixes.

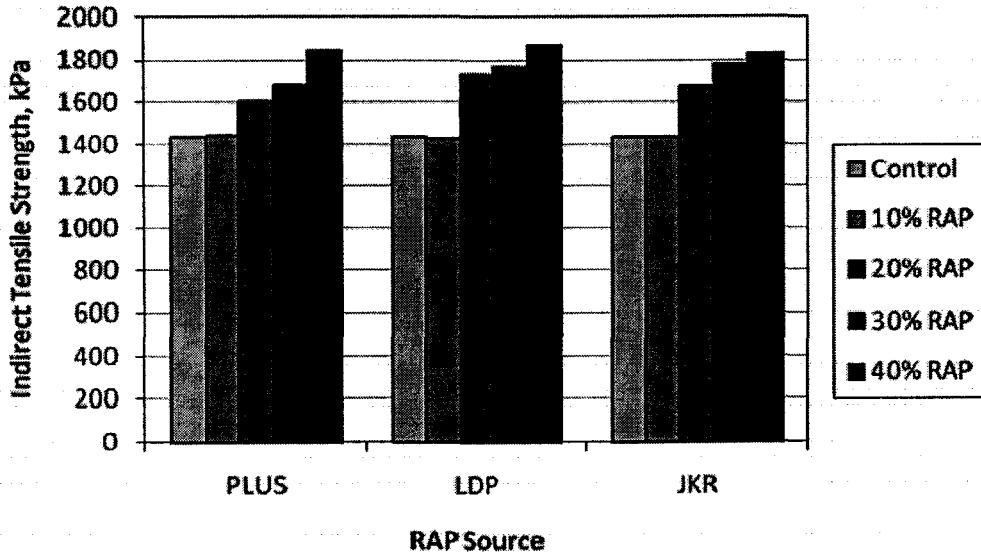


Figure 6.1: Indirect Tensile Strength of RAP Mixtures

A t-Test statistical analysis on each RAP source do not indicate significant differences between the control sample and mixes containing RAP up to 30% as shown in Table 6.1. In other words, adding RAP up to 30% do not affect the strength of mixes. However, mixes with 40% RAP demonstrates significant difference in strength for all RAP sources.

Table 6.1: Paired t-Test Comparisons of Strengths of Mixtures with different RAP Contents

RAP Source	% RAP	p-value	Conclusion
PLUS	10	0.833129	NSD
	20	0.165541	NSD
	30	0.171739	NSD
	40	0.043409	SD
LDP	10	0.923969	NSD
	20	0.245950	NSD
	30	0.065820	NSD
	40	0.041602	SD
JKR	10	0.988426	NSD
	20	0.211271	NSD
	30	0.149638	NSD
	40	0.033305	SD

NSD= Non Significant Difference SD= Significant Difference

6.3 Moisture Sensitivity Test

Specimens incorporating various percentages of RAP from PLUS highway were fabricated and compacted to $7\pm 1\%$ air voids to evaluate its moisture sensitivity using the freeze/thaw cycle procedure. Figure 6.2 shows that the addition of RAP in the mix increases the ITS of both dry and wet specimens compared to control specimen. The percentage increase in ITS is up to 39% and 31% for dry and wet specimens respectively. However, the ITS of dry specimens is always higher than the ITS of wet specimens. The difference in ITS values between dry and wet specimens increases as the percentage of RAP in the mix increases, the highest being equal to 16% at 40% RAP content. Generally, the Tensile Strength Ratios (TSR) of all mixes are greater than 0.80 even though the ratio slightly decreases as the RAP content increases. The TSR obtained indicates that the recycled asphalt specimens are resistant to moisture induced damage. Approximate saving of 19% in virgin binder can be made if 40% dry RAP is incorporated in the recycled asphalt mix. In general, the recycled asphalt mixes perform better than the control mix. Therefore, reclaimed asphalt pavement can be a potential material to partially replace virgin materials in producing asphaltic concrete.

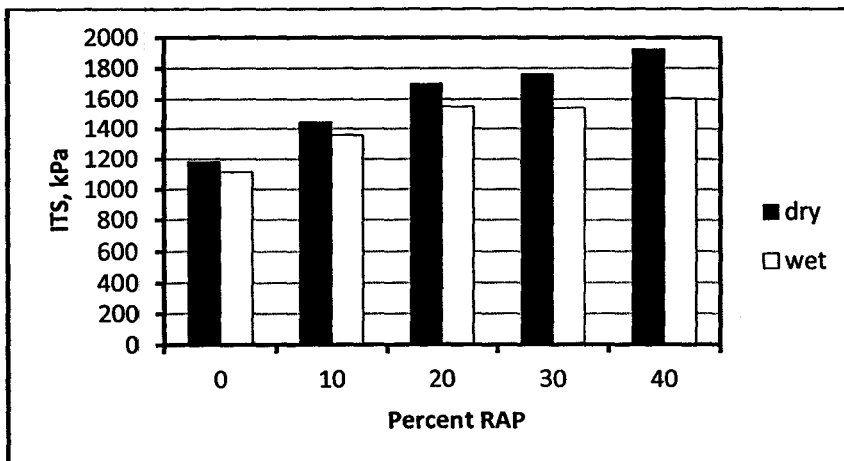


Figure 6.2: Moisture Sensitivity Test Results

6.4 Resilient Modulus

6.4.1 Resilient Modulus at Varying Binder Contents

The resilient modulus is simply the modulus of elasticity when the asphalt sample is loaded within its elastic range where the deformation is fully recoverable. It is defined as the ratio of the applied stress to the recoverable strain when a dynamic load is applied. The graphical illustration of the resilient modulus for 60P and SBS mixes versus binder content relationship of porous asphalt (PA) at 10°C and 25°C are presented in Figures 6.3 and 6.4. Both mixes show similar trend when their respective resilient modulus is related to the bitumen content.

The resilient modulus of PA increases until a maximum at 4.2% bitumen content, then decreases as the bitumen content increases. It is also observed that the resilient modulus of SBS mix is higher than those of 60P mixes, with the maximum resilient modulus of SBS mixes 37.60% (10°C) and 20.80% (25°C) higher than the maximum resilient modulus of 60P. The higher resilient modulus indicate less flexibility under loading. Based on the Figure, the resilient modulus for all mixes specimens reduces by approximately 58.65% to 67.40% when the test temperature increases from 10°C to 25°C.

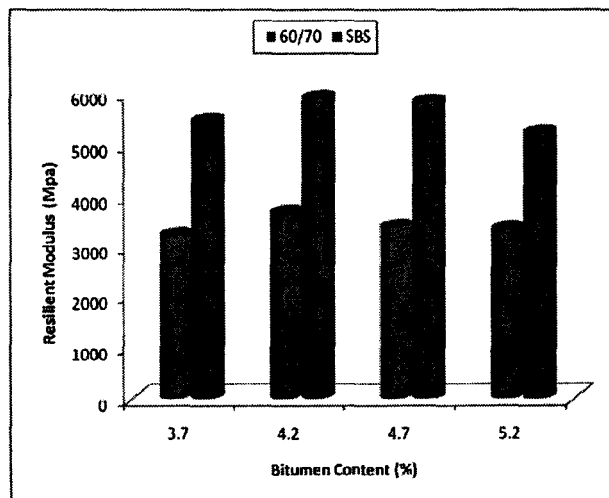


Figure 6.3: Resilient Modulus at 10°C versus Bitumen Content (Un-aged)

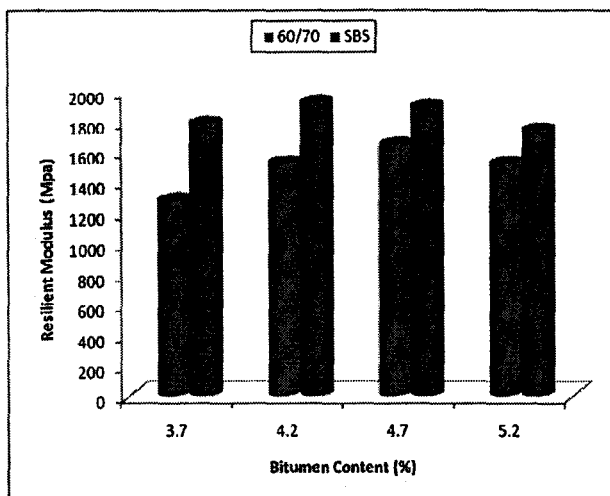


Figure 6.4: Resilient Modulus at 25°C versus Bitumen Content (Un-aged)

6.4.2 Effects of Short-term Ageing on Resilient Modulus of Porous Mixtures

The curves representing the relationship between resilient modulus and bitumen content of un-aged and aged specimens are illustrated in Figure 6.5 and summarized in Table 1. The points plotted are the average of two readings. In general, the resilient modulus of the all mix types increases after every ageing. For instance, 60P mix, at 4.2% bitumen content and 10°C test temperature, the resilient modulus of PA increases by almost 33.70% after short-term ageing. At 25°C, SBS mix, the resilient modulus of specimens with 4.2% bitumen content increase by 7.70% when subjected to STA. Ageing process causes oxidation and increases the hardening rate of the bitumen, thus resulting in the increasing resilient modulus.

As concluded that, the resilient modulus of PA increases after every ageing session. The effect of increased stiffness contributed towards longer service lifespan of pavements by increasing the rutting resistance. Based on the results shown in Table 6.2, the resilient modulus decreases drastically with the increase in temperature. When tested at 10°C, the resilient modulus of 60P mix equal 3242 Mpa, at 25°C test temperature, the corresponding value is 1276 Mpa which represent a 60.64% decrease.

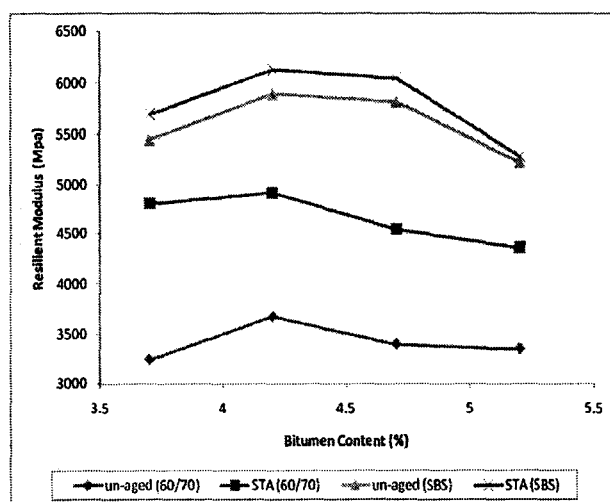


Figure 6.5: Resilient Modulus at 25°C versus Bitumen Content (Un-aged)

Table 6.2: Resilient Modulus Test Results Subjected to STA

Temperatures	Bitumen Content (%)	Type of Binder			
		60/70		SBS	
		Un-aged	STA	Un-aged	STA
10°C	3.7	3242	4802	5442	5687
	4.2	3676	4915	5887	6125
	4.7	3398	4543	5808	6043
	5.2	3353	4359	5222	5282
25°C	3.7	1276	1553	1788	1969
	4.2	1520	1652	1919	2067
	4.7	1647	1696	1896	2062
	5.2	1516	1601	1742	1797

6.4.3 Effects of Long-term Ageing on Resilient Modulus of Porous Mixtures

The results of the resilient modulus test for long-term ageing at varying bitumen content and temperatures are tabulated in Table 6.3. Regardless of bitumen type or test temperatures, all LTA mixes exhibit increased resilient modulus values compared to un-aged mixes. The general trend showing the resilient modulus decreases with the increase in temperature and the resilient modulus of LTA specimens are higher than un-aged specimens; are similar to STA specimens tested under the two temperature regimes. Thus, the effect of using SBS modified binder is to cause an increase in resilient modulus. Given the same test temperature, the SBS mixtures generally exhibit a higher increase in resilient modulus when tested at a particular temperature.

Table 6.3: Resilient Modulus Test Results Subjected to LTA

Temperatures	Bitumen Content (%)	Type of Binder			
		60/70		SBS	
		Un-aged	LTA	Un-aged	LTA
10°C	3.7	3242	4839	5442	6028
	4.2	3676	5735	5887	6447
	4.7	3398	5306	5808	6284
	5.2	3353	4539	5222	5380
25°C	3.7	1276	1705	1788	2067
	4.2	1520	1833	1919	2317
	4.7	1647	1881	1896	2245
	5.2	1516	1594	1742	1996

6.5 Characterization at Intermediate Temperatures

6.5.1 Rutting Parameter

According to Superpave™, rutting is controlled by limiting the $G^*/\sin \delta$ to a value greater than 1 kPa and 2.20 kPa for unaged and short term aged binders, respectively (Asphalt Institute, 2003). Table 6.4 shows the effects of RAP binder sources and contents on the rutting parameter of virgin and RAP modified binders at various temperatures. Table 6.5 presents the analysis of variance (ANOVA) for $G^*/\sin \delta$. The results indicate that RAP source and RAP content are significant factors affecting $G^*/\sin \delta$ at each aging state.

Table 6.4: $G^*/\sin \delta$ for Unaged and Short Term Aged Virgin and RAP Modified Binders

State	Temperature (°C)	Virgin	$G^*/\sin \delta$ (kPa)					
			RAP modified binder					
			N15	N30	D15	D30	P15	P30
Unaged	52	5.80	14.30	22.09	12.10	23.10	12.00	19
	58	2.44	5.46	8.47	4.55	8.69	4.58	7.44
	64	1.14	2.28	3.53	1.96	3.81	1.96	3.12
	70	0.57	1.09	1.59	1.01	1.71	0.94	1.43
	76	0.29	0.52	0.78	0.45	0.84	0.45	0.67
	82	0.18	0.26	0.39	0.22	0.41	0.23	0.34
STA ^a	52	13.09	28.31	37.34	37.34	76.84	28.81	47.09
	58	5.33	10.61	16.88	14.02	36.11	11.43	18.27
	64	2.68	4.31	7.35	5.71	15.48	4.51	7.37
	76	0.38	0.84	1.41	1.10	2.80	0.88	1.38
	82	0.29	0.41	0.67	0.53	1.24	0.42	0.65

^a Short-term aging

Table 6.5: Results of Analysis of Variance (ANOVA) for $G^*/\sin \delta$

Source	Sum of Squares	df	Mean Square	F	p-Value	Significant
Intercept	15594673255.967	1	15594673255.967	31217.653	< 0.001	Yes
Source	591842545.813	2	295921272.906	592.380	< 0.001	Yes
Temperature	23184211903.445	5	4636842380.689	9282.101	< 0.001	Yes
Aging	2994949568.535	1	2994949568.535	5995.335	< 0.001	Yes
RAP Content	1235878467.200	1	1235878467.200	2474.000	< 0.001	Yes
Source*Temperature	767727330.761	10	76772733.076	153.685	< 0.001	Yes
Source*Aging	547793190.597	2	273896595.298	548.290	< 0.001	Yes
Temperature*Aging	4327345560.076	5	865469112.015	1732.509	< 0.001	Yes
Source*Temperature*Aging	735868058.092	10	73586805.809	147.307	< 0.001	Yes
Source*Content	297041857.068	2	148520928.534	297.311	< 0.001	Yes
Temperature*Content	1567694820.293	5	313538964.059	627.647	< 0.001	Yes
Source*Temperature*Content	355020747.229	10	35502074.723	71.069	< 0.001	Yes
Aging*Content	303338196.540	1	303338196.540	607.227	< 0.001	Yes
Source*Aging*Content	189137239.567	2	94568619.783	189.309	< 0.001	Yes
Temperature*Aging*Content	320823466.882	5	64164693.376	128.446	< 0.001	Yes
Source*Temperature*Aging*Content	226387040.328	10	22638704.033	45.319	< 0.001	Yes
Error	71934713.607	144	499546.622			
Total	53311667962.000	216				
Corrected Total	37716994706.033	215				

The $G^*/\sin \delta$ of unaged and short term aged RAP modified binders increases significantly irrespective of their RAP sources at each test temperature. This is due to the effect of aged binder which increased binder samples stiffness and contribute to upgrading the performance grade of RAP modified binders as shown in Table 9.

Table 6.6 shows that the binder upgrading depends not only on the amount of RAP binder but also on the RAP binder source. For example, N15 is not upgraded to higher binder performance grade, while the performance grade of D15 increases to PG70. Meanwhile, D30 is able to promote binder grading to PG76, while the corresponding value of RAP modified binders from PWD and NSE only upgrade the binder grading to PG70.

Table 6.6: Upgrading of PG64 Binder due to Incorporating RAP Binder

Parameter	RAP Modified Binder					
	N15	N30	D15	D30	P15	P30
A	PG66	PG73	PG70	PG77	PG70	PG73
S	PG64	PG70	PG70	PG76	PG70	PG70

6.5.2 Effects of RAP Binder on Aging Factor

Aging changes the binder properties over time during construction and service life which makes the binder less adhesive, and becomes harder and brittle. To evaluate aging, the Aging Factor (AF) which is defined as the ratio between aged and unaged Superpave™ rutting parameter (Wasiuddin et al., 2007) is computed. Samples with lower AF values are the least susceptible to aging and are more desirable. The AF values for all RAP modified binders at different temperatures are presented in Table 6.7. From Table 6.7, two distinct trends can be observed. Firstly, AF increases from 52 °C and peaked at 64 °C for the virgin and RAP modified binder samples (N30). The same trend is observed for D30, P30, and P15 but at 58 °C. Beyond the peak, the AF decreases at the sweep temperatures. Secondly, AF decreases over the test temperatures (D15 and N15). The remaining RAP modified binder samples follow the second trend. Samples containing extracted RAP binder sourced from DPE (D15 and D30) exhibit the maximum AF value at each individual test temperature. It denotes that the characteristics of DPE RAP modified binder in terms of the AF based on $G^*/\sin \delta$ has changed significantly as a consequence of aging. Meanwhile, the minimum AF value takes place for NSE RAP modified binder (N15 and N30) in over the test temperatures. The AF values at this temperatures range are even less than the corresponding value of the virgin samples from 52 °C to 64 °C.

Table 6.7: AF Values for Virgin and RAP Modified Binders

Temperature (°C)	Virgin	Aging Factor					
		RAP Modified Binder					
		N15	N30	D15	D30	P15	P30
52	2.26	1.98	1.69	3.10	3.32	2.40	2.47
58	2.18	1.94	1.99	3.08	4.15	2.49	2.45
64	2.35	1.89	2.08	2.91	4.06	2.30	2.36
70	1.95	1.69	1.99	2.63	3.82	2.06	2.18
76	1.31	1.62	1.80	2.44	3.33	1.95	2.05

82	1.61	1.57	1.71	2.41	3.02	1.82	1.91
----	------	------	------	------	------	------	------

6.5.3 Fatigue Parameter

Incorporating RAP binder increases its $G^*/\sin \delta$, making it stiffer and subsequently subjecting the asphalt pavement to fatigue failure especially at low temperature. It is also necessary to establish a balance between the amount of RAP and its performance at intermediate temperatures. In this respect, the asphalt binder fatigue factor ($G^* \sin \delta$) obtained from the DSR test results is used to determine the RAP modified binder performance at intermediate temperatures. According to Superpave™ specifications (Asphalt Institute, 2003), the value of $G^* \sin \delta$ should be less than 5 MPa or the area located below the dashed horizontal line shown in Figure 6.6.

A lower value is more desirable from the viewpoint of resistance to fatigue failure. As anticipated, $G^* \sin \delta$ increases as the RAP binder content increases. However, the $G^* \sin \delta$ values differ according to RAP binder sources. For example, the highest percentage of extracted RAP binder which can satisfy the Superpave™ fatigue specifications at 22 °C is 5% sourced from NSE and DPE (Figure 6.6(a) and (b)), while the corresponding value is 10% for extracted binder from RAP sourced from PWD at 22 °C (Fig. 3(c)). It can also be seen that P30 can fully satisfy Superpave™ fatigue requirements at 28 °C, while N30 can only satisfy this demand at 31°C. However, D30 cannot even fulfill the Superpave™ requirements at 31 °C.

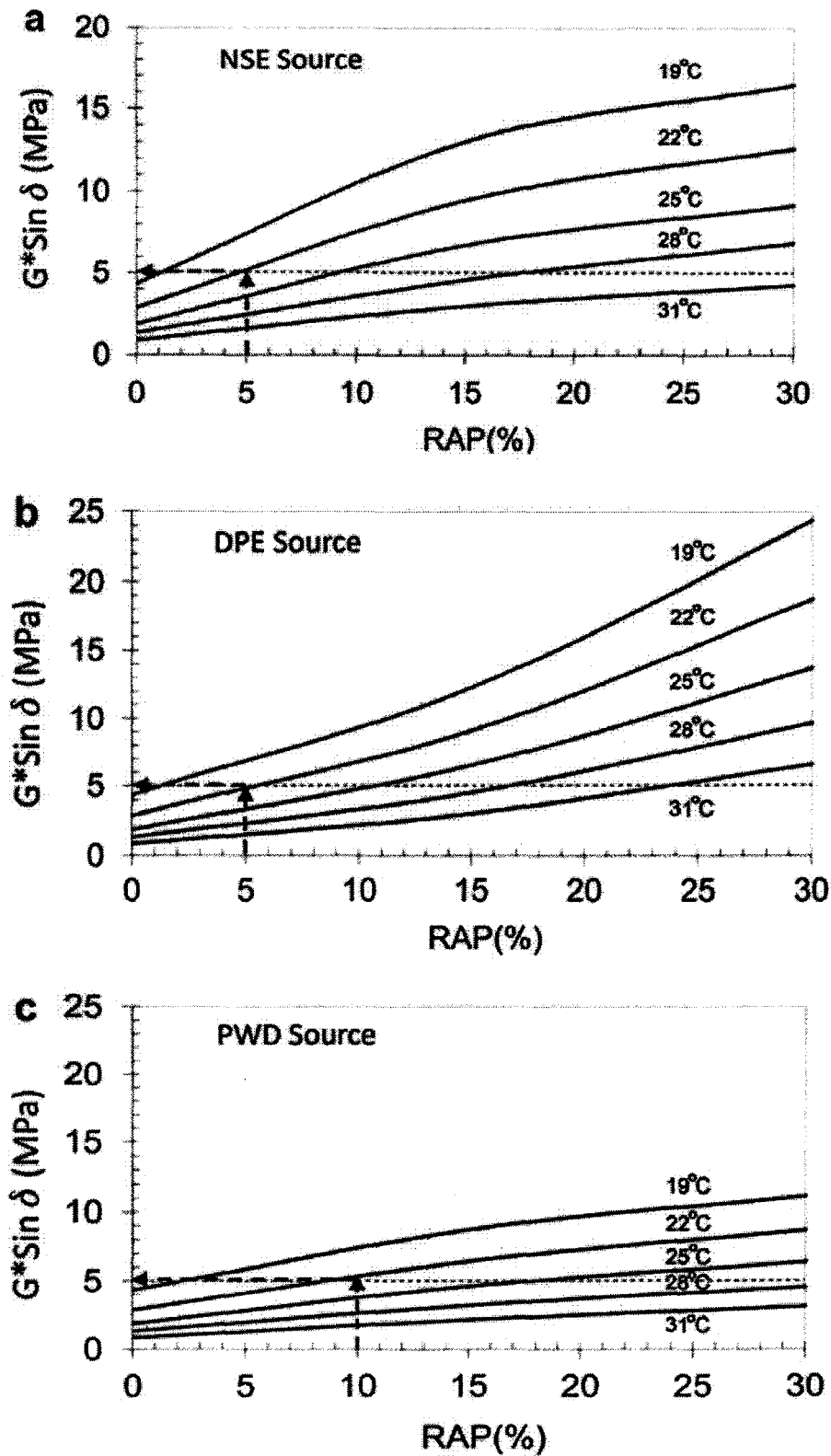


Figure 6.6: Relationship between $G^* \sin \delta$, Temperature, RAP Binder Source and Content

Therefore, RAP binder source can significantly affect the rheological property of the RAP modified binder in terms of the $G^* \sin \delta$ parameter. As RAP materials are used from various sources without considering their rheological properties, it is possible that asphalt

mixes become inhomogeneous and the asphalt pavement cannot react uniformly under traffic and environmental loadings during its service life. It is also possible to develop patterns of the pavement failures that do not follow the predictions by pavement management system sectors. Under these circumstances, short term and long term pavement maintenance and rehabilitation policies to select cost-effective strategy, can become inefficient.

6.5.4 Analysis of Fuel Requirement and GHG Emissions

It is very desirable for environmental policy makers and engineers to be able to measure the environmental loads of each RAP source to ensure cleaner asphalt production and field construction since asphalt binder and aggregate from different sources may exhibit different characteristics (Hamzah et al., 2010). Project managers and engineers should also quantify the fuel requirements, hence total cost of fuel consumption. The selected option should consider binder rheological properties, fuel requirements and the GHG emissions so that asphalt production by the mixing plant can be made more environmental friendly. In this regards, the required amount of fuel to heat up aggregate and binder from 25 °C (the assumed ambient temperature at the quarry) up to the mixing temperatures as specified in Table 6 are calculated using Equation (6.1).

$$(6.1) \quad Q = \sum_{i=n}^{j=n+1} mc\Delta\theta \quad \text{Equation}$$

Where

- Q = sum of required heat energy (J)
- m = mass of materials (kg)
- c = specific heat capacity coefficient (J/(kg°C))
- Δθ = difference between the ambient and mixing temperatures (°C)
- i, j = different material types

The specific heat capacity changes with temperature. The specific heat capacity values at the range of temperature, from ambient temperature to mixing points, were calculated using equations developed by Hamzah et al. (2010) and Waples and Waples (2004). The mix density and the other volumetric properties are based on the values for the control samples (Table 4) and the total materials required, including asphalt binder and aggregate, to pave a 10-km dual carriageway road with 3 lanes per direction and a 5 cm thick wearing course. Assume that coal, natural gas and diesel are the industrial fuels used in the asphalt plant. The required heat energy is converted to the required fuel types and GHG emissions (CO₂, N₂O, and CH₄) using conversion factors given in Table 6.8 (DTI, 2006) and Table 6.9 (DEFRA, 2010), respectively. Tables 6.8 and 6.9 show the required fuel types and the GHG emissions based on RAP source and RAP contents, respectively.

Table 6.8: Conversion Factors for Different Fuel Types (DTI, 2006)

Fuel Type	Unit	Coefficient
Coal	ton/MJ	0.00004263
Natural Gas	m ³ /MJ	0.02610824
Diesel	ton/MJ	0.00002181

Table 6.9: Conversion Factors for GHG (DEFRA, 2010)

Fuel Type	CO ₂ (kg CO ₂ /Unit)	CH ₄ (kg CO ₂ e/Unit)	N ₂ O (kg CO ₂ e/Unit)
Coal	2295.3	1.8	39.4
Natural Gas	2.023	0.003	0.0012
Diesel	3164.3	1.8	35

From Tables 6.10 and 6.11, the highest fuel requirements and the GHG emissions hence the most hazardous, are for asphalt mix impregnated with D30M corresponding to the highest construction temperatures (Table 6.11). Higher construction temperature can lead to emissions of more fumes in the asphalt mix plant and paving site. The fumes contain polycyclic aromatic hydrocarbons (PAHs), some of which are carcinogenic and hence their emission can make paving site hazardous for asphalt paving crews (Tsai et al., 2004; Karkaya et al., 1999; Kuo et al., 2008). The most environmental friendly options are asphalt mixes incorporating N15M and P15M. It can also be seen that the increase in fuel requirement and GHG emissions are different based on RAP source and RAP content irrespective of fuel type. In the asphalt mixing plant, the actual amount of GHG emissions and fuel requirement is enormous since both are calculated for large-scale asphalt production for huge road construction projects. Tables 6.10 and 6.11 can be used as guidelines for a preliminary evaluation in the choice of RAP sources and contents. The fuel requirement and the GHG emissions can be different based on the efficiency of an asphalt plant.

Table 6.10: Fuel Requirements based on RAP Source and RAP Content

Mixes	Q _{agg} (TJ)	Q _b (TJ)	Q _T (TJ)	Fuel type			Increase in fuel (%)
				Coal (ton)	Natural gas (m ³)	Diesel (ton)	
Virgin	2.95	0.161	3.11	133	81,197	68	
N15M	3.10	0.169	3.27	139	85,374	71	4.7
N30M	3.20	0.174	3.37	144	87,985	74	8.5
D15M	3.15	0.171	3.32	142	86,679	72	6.5
D30M	3.27	0.178	3.45	147	90,073	75	10.6
P15M	3.10	0.169	3.27	139	85,374	71	4.7
P30M	3.20	0.174	3.37	144	87,985	74	8.5

TJ: tera joule; Q_{agg}: Required energy to heat up aggregate; Q_b: required energy to heat up asphalt binder; and Q_T: required energy to heat up aggregate and asphalt binder.

Table 6.11: GHG Emissions^a based on RAP Source and RAP Content

Mixes	Coal			Increase in GHG emission (%)	Diesel			Increase in GHG emission (%)	Natural gas			Increase in GHG emission (%)
	CO ₂ (kgCO ₂ /t)	N ₂ O (kgCO ₂ e/t)	CH ₄ (kgCO ₂ e/t)		CO ₂ (kgCO ₂ /t)	N ₂ O (kgCO ₂ e/t)	CH ₄ (kgCO ₂ e/t)		CO ₂ (kgCO ₂ /m ³)	N ₂ O (kgCO ₂ e/m ³)	CH ₄ (kgCO ₂ e/m ³)	
Virgin	305274.9	5240.2	239.4		215,172	2380	122		164,262	98	244	
N15M	319046.7	5476.6	250.2	4.51	224,665	2485	127	4.41	172,712	103	256	5
N30M	330523.2	5673.6	259.2	8.27	234,158	2590	133	8.82	177,994	106	264	8.5
D15M	325932.6	5594.8	255.6	6.76	227,829	2520	129	5.88	175,352	104	260	6.8
D30M	337409.1	5791.8	264.6	10.52	237,322	2625	135	10.29	182,218	108	270	11
P15M	319046.7	5476.6	250.2	4.51	224,665	2485	127	4.41	172,712	103	256	5
P30M	330523.2	5673.6	259.2	8.27	234,158	2590	133	8.82	177,994	106	264	8.5

6.6 Dynamic Modulus

Figure 6.7 shows the effects of RAP content, temperature and loading frequency on the dynamic modulus of asphalt mixtures. At 20°C, the dynamic modulus consistently increases as the RAP content increases. The average percentage increase is from 1% to 6% when up to 20% RAP is added. The dynamic modulus increases from 13% to 17% when incorporated with 30% to 40% RAP. When the temperature doubles to 40°C, the dynamic modulus dramatically reduces to 80% and 78% for asphalt mixes incorporating 10% and 40% RAP, respectively. As the temperature increases from 40°C to 50°C, the dynamic modulus is significantly reduced to 70% and 64% for asphalt mixes with 10% and 40% RAP, respectively. Similar decreasing trend in dynamic modulus between 71% to 87% and 61% to 68% is observed when loading frequency decreases as temperature increases from 20°C to 40°C and 40°C to 50°C, respectively.

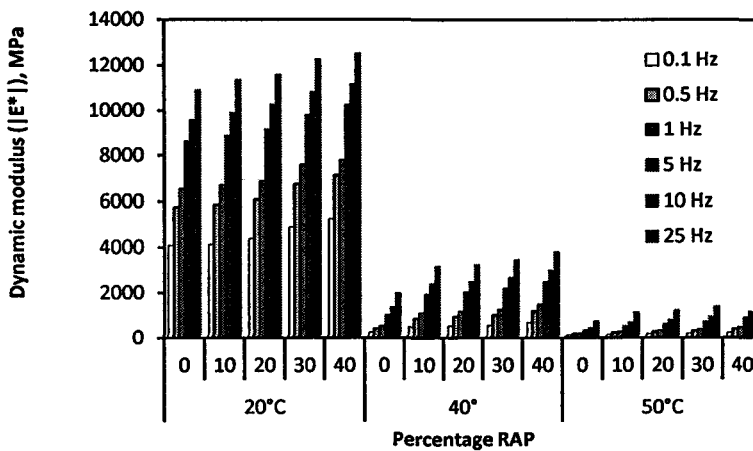


Figure 6.7: Dynamic Modulus at different RAP Content, Temperature and Frequency

For a given RAP content, the reduction in the dynamic modulus at 40°C is more evident compared to samples tested at 20°C. However, for samples tested at 40°C, the dynamic modulus increases from 47% to 50% and 53% to 59% when 20% and 40% RAP are added, respectively compared to control mixtures. This takes place because RAP materials contain aged asphalt binder where resins turn into asphaltenes which in turn affects the elastic solid behavior of the aged asphalt binder¹²⁻¹⁴. However, the higher amount of RAP incorporated in virgin mixtures implicates an increased amount of fuel requirement and green house gas emission during asphalt production in the mixing plants¹⁴⁻¹⁵.

The dynamic modulus increases from 42% to 56% as the loading frequency increases from 0.1 Hz to 25 Hz. As the test temperature further increases to 50°C, the dynamic modulus reduces significantly to 94% and 92% for asphalt mixes incorporating 10% and 40% RAP, respectively. For specimens tested at 50°C, in comparison with control mixes, the dynamic modulus increases from 32% to 40% and 47% to 57% when blended with 20% and 40% RAP, respectively. The increase of the dynamic modulus at that respective RAP content is less than 10% compared to those samples tested at 40°C. However, the dynamic modulus increases from 90% to 96% as the loading frequency increases from 0.1 Hz to 25 Hz. This increase in mixture stiffness is attributed to the visco-elastic property of the aged binder

from the RAP. Higher RAP content incorporated in the asphalt mixes results in increased mix stiffness that enable the mix to withstand the detrimental effects of high temperature and low loading frequency.

An analysis of variance (ANOVA) was performed to determine the effect of RAP content, temperature, frequency and interaction of the main effects on measured dynamic modulus. Table 6.12 shows the results of ANOVA which indicate that all main effects as well as their interactions have significantly influenced the measured dynamic modulus at 5% significance level. It can be noticed that main effect of temperature has the highest F-ratio value which indicates that an increase in temperature would dramatically affects the dynamic modulus of the asphalt mixes.

Table 6.12: ANOVA Results on Main and Interaction Effects on Dynamic Modulus

Source	Sum of Squares	df	Mean Square	F	p-value	Significant
Intercept	2194763907.200	1	2194763907.200	1159029.442	<0.001	Yes
RAP	22284799.244	4	5571199.811	2942.086	<0.001	Yes
Temperature	2059022431.433	2	1029511215.717	543672.969	<0.001	Yes
Frequency	278791124.267	5	55758224.853	29445.274	<0.001	Yes
RAP * Temperature	6156365.289	8	769545.661	406.388	<0.001	Yes
RAP * Frequency	2159036.622	20	107951.831	57.008	<0.001	Yes
Temperature * Frequency	145407902.300	10	14540790.230	7678.823	<0.001	Yes
RAP * Temperature * Frequency	501909.644	40	12547.741	6.626	<0.001	Yes
Error	170426.000	90	1893.622			
Total	4709257902.000	180				
Corrected Total	2514493994.800	179				

Figure 6.8 shows the interaction plot of temperature and RAP against dynamic modulus at 10 Hz. The plot displays increasing trend of estimated marginal means of the dynamic modulus as RAP content increases. At 40°C, a sharp increase in estimated marginal mean of the dynamic modulus is observed for asphalt mixes with 10% RAP. The effect of high temperature drastically reduces the stiffness of the asphalt mixes regardless of RAP contents. However, addition of RAP in asphalt mixes at a particular temperature has improved mix stiffness compared to control mixes.

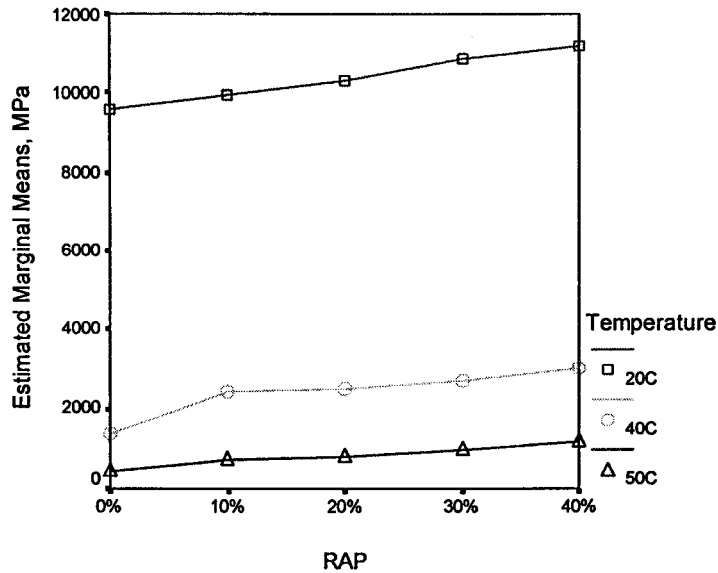


Figure 6.8: Interaction Plot of Temperature and RAP against Dynamic Modulus at 10 Hz

6.6.1 Phase Angle

Figure 6.9 shows the effects of RAP content, temperature and loading frequency on the phase angle of the asphalt mixes tested. Generally, at 20°C the phase angle decreases as RAP content increases with average percentage decreases of 0.5% when up to 20% RAP is added and further decreases between 8% to 14% when incorporating 20% to 40% RAP, compared to control mixes. When the temperature doubles to 40°C, the phase angle for asphalt mixture incorporating up to 20% RAP, increases sharply between 12% to 52%, while for asphalt mixes incorporating 30% to 40% RAP, the phase angle increases between 23% to 54%. In addition, as the loading frequency increases, the phase angle consistently increases from 12% to 54%. When the test temperature increases from 40°C to 50°C, the phase angle initially reduces from 14% and 8% when incorporating 10% and 40% RAP, respectively. However, as the frequency progressively increases, the phase angle also increases up to 19% at 40% RAP. For specimens tested at 40°C, the phase angle slightly increases at 0.1 Hz for all RAP percentages but decreases up to 25% for the rest of the loading frequencies compared to control samples. At 50°C, in comparison with control mixes, the phase angle increases up to loading frequency equivalent to 10 Hz. However, at 25Hz frequency, the phase angles slightly decreases up to 9%. This decrease in phase angle can be explained in terms of aggregate interlocking effects.

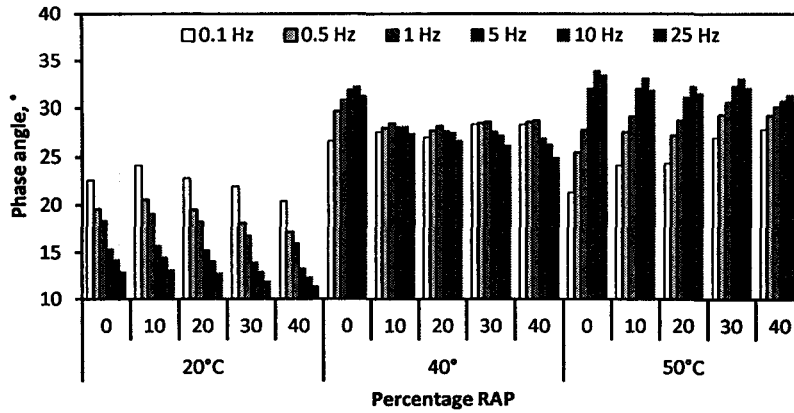


Figure 6.9: Phase Angle at Different RAP Content, Temperature and Frequency

An analysis of variance (ANOVA) is carried out to determine the effects of RAP content, test temperature, frequency and interaction of the main effects on the measured phase angle. Table 6.13 shows the ANOVA results which indicate that all the main effects as well as their interactions have significantly influence the measured phase angle at 5% significance level. Similar to dynamic modulus, temperature is a dominant main effect since temperature exhibits the highest F-ratio which indicates that temperature increase will significantly affects the phase angle of the asphalt mixes.

Table 6.13: ANOVA Results on Main and Interaction Effects on Phase Angle

Source	Sum of Squares	df	Mean Square	F	p-value	Significant
Intercept	111122.244	1	111122.244	2214865.125	<0.001	Yes
RAP	40.843	4	10.211	203.517	<0.001	Yes
Temperature	6129.408	2	3064.704	61085.032	<0.001	Yes
Frequency	37.189	5	7.438	148.250	<0.001	Yes
RAP * Temperature	119.215	8	14.902	297.020	<0.001	Yes
RAP * Frequency	87.996	20	4.400	87.696	<0.001	Yes
Temperature * Frequency	1126.096	10	112.610	2244.511	<0.001	Yes
RAP * Temperature * Frequency	57.246	40	1.431	28.525	<0.001	Yes
Error	4.515	90	.050			
Total	118724.752	180				
Corrected Total	7602.508	179				

Figure 6.10 shows the interaction plot of temperature and RAP against phase angle at 10 Hz. The plot clearly indicates that generally the estimated marginal means of the phase angle decreases as RAP content increases. Improvement in elasticity property of asphalt mix incorporating RAP compared to control mixes is particularly evident at 40°C. The

contribution of aged bitumen from reclaimed asphalt pavement has effectively enhanced the mix visco-elastic characteristics which results in improved stiffness of the asphalt mixes at high temperature.

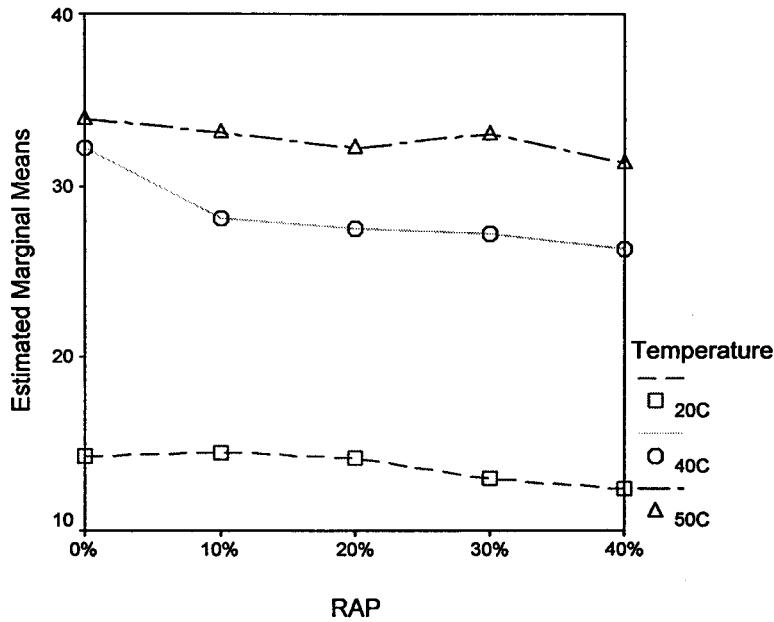


Figure 6.10: Interaction Plot of Temperature and RAP against Phase Angle at 10 Hz

Figures 6.11 illustrates the Cole–Cole curve of the relationship between the elastic or storage modulus (E') and the viscous or loss modulus (E'') of the asphalt mixtures based on results obtained from the AMPT. The Cole–Cole curve is suggested to validate the test data for a master curve at any frequency or temperature¹¹. The acceptable data are independent of temperature and frequency and form a single curve. As illustrated in Figure 5, the relationship between E' and E'' are linear and form a single curve with R^2 equal to or greater than 90%, for all test temperatures. This implies that the data from the master curves illustrated in Figures 3, and 1 are valid.

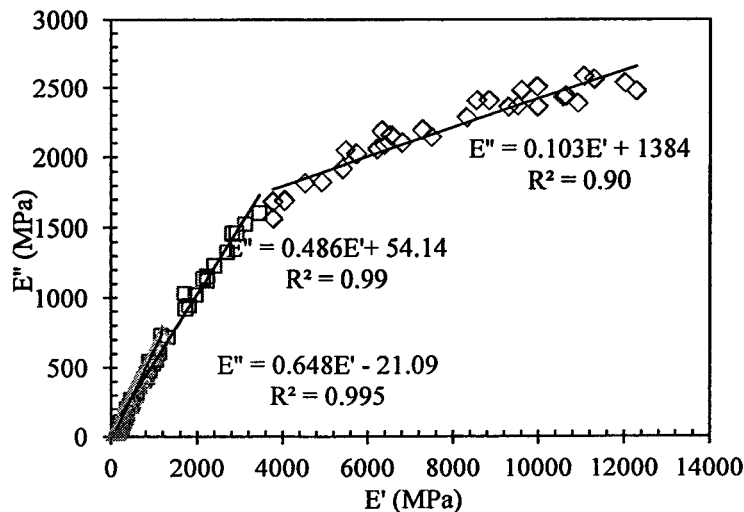


Figure 6.11: Cole–Cole Curve of the Relationship between E' and E''

6.6.2 Effect size of the main and interaction effects

The effect size of the main and interaction effects on measured dynamic modulus and phase angle are categorized into 3 Groups as shown in Table 6.14. It can be seen that effect size of temperature is distinctly large for both dynamic modulus and phase angle when temperature becomes one of the main effects as in Groups 1 and 2. In Group 3, frequency has the largest effect size compared to main effect of RAP on dynamic modulus. However, with the same main effects (frequency and RAP), the effect sizes are comparable in the measured phase angle. Even though RAP has significantly contributed to asphalt mixture stiffness at high temperature, the effect size is fairly low compared to temperature and frequency except for measured phase angle where its effect size is 0.24. Similarly, the effect size for the interaction effects is considerably low compared to the main effects with exception when measuring the phase angle. The interaction effect between frequency and RAP in phase angle has effect size of 0.51, is the highest among the interaction effects (temperature x frequency and temperature x RAP) in the tests. Even though the effect size of the interaction effect analysis is limited to two main effects only, it can be expected that the effect size of the interaction effect of three main effects (RAP x temperature x frequency) is much less than the interaction effect of two main effects based on the lowest F-ratio of the interaction effect of RAP x temperature x frequency compared to other interaction effects.

Table 6.14: Effect Size (ω^2) of the Main and Interaction Effects

Group	Measured parameter	Main effect		Interaction effect
		Temperature	Frequency	Temperature x Frequency
1	Dynamic Modulus	0.83	0.11	0.05
	Phase Angle	0.84	0.005	0.15
		Temperature	RAP	Temperature x RAP
2	Dynamic Modulus	0.99	0.01	0.003
	Phase Angle	0.97	0.006	0.02
		Frequency	RAP	Frequency x RAP
3	Dynamic Modulus	0.92	0.07	0.007
	Phase Angle	0.22	0.24	0.51

6.7 Asphalt mixtures stiffness

Figure 6.12 displays the dynamic modulus master curve for mixes with 5 RAP contents, tested at three test temperatures (20°C, 40°C and 50°C) and six loading frequencies (25, 10, 5, 1, 0.5 and 0.1 Hz). The master curve was developed taking 25°C as the reference test temperature. Generally, the mix stiffness increases as the RAP content increases. These increases in RAP content have significantly increase the dynamic modulus which directly translates into improved load spreading ability of the asphalt mixtures incorporating RAP. Figure 6.13 shows that the measured dynamic modulus $|E^*|$ match reasonably well with the predicted dynamic modulus $|E^*|$ calculated based on Witczak model without any significant bias with regression coefficient equal to 0.983.

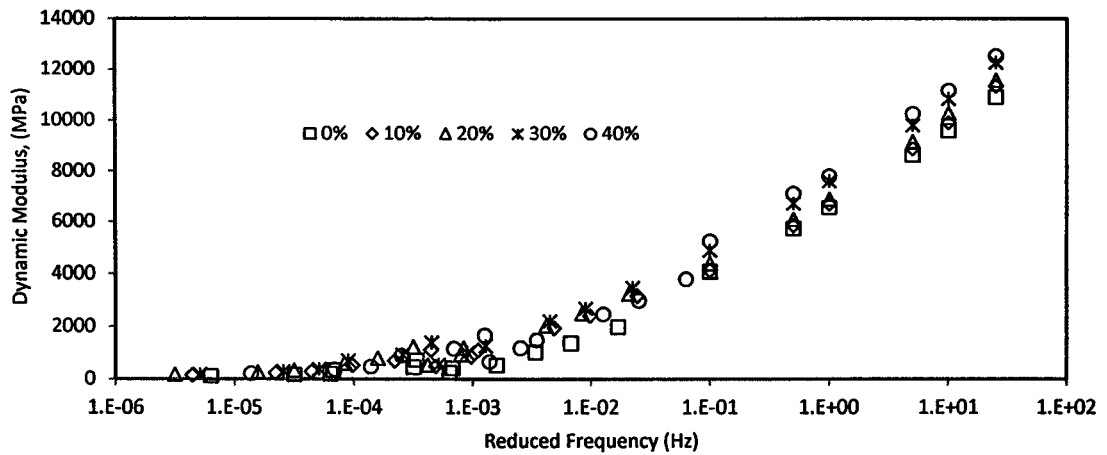


Figure 6.12: Master Curves at Different RAP Percentages

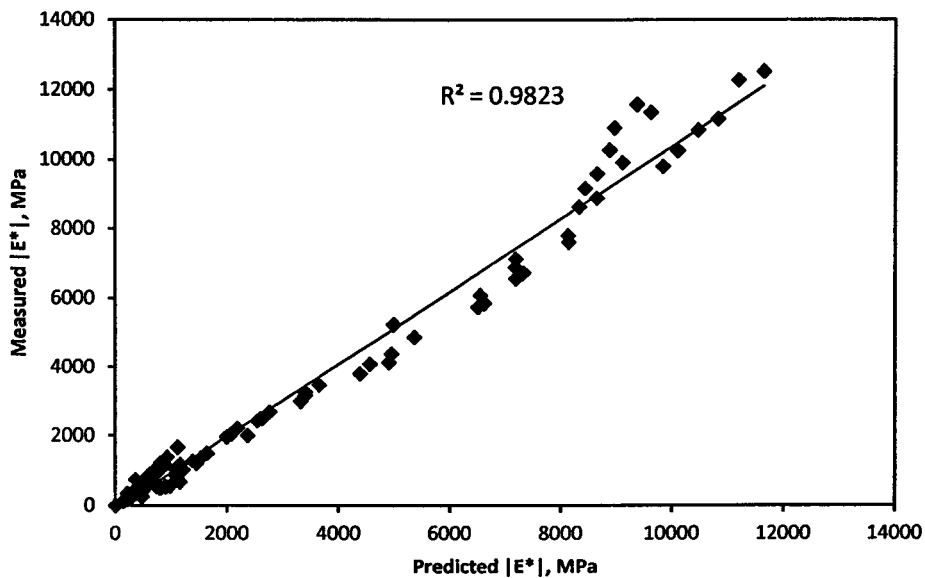


Figure 6.13: Relationship between Measured $|E^*|$ Laboratory and $|E^*|$ Predicted

An improved resistance to rutting and fatigue in mixtures incorporating RAP is further illustrated in Figures 6.14 and 6.15, respectively. For instance, rutting factor, $|E^*|/\sin \delta$ at 50°C and 10Hz has significantly increased by 37 % and 64%, respectively for mixtures incorporating 10% and 40% RAP. Interestingly, the fatigue parameter, $|E^*| \cdot \sin \delta$ at 20°C and 10 Hz slightly increased up to 5% at 20% RAP and 1% for mixture incorporating 40% RAP, and which is comparable to the fatigue parameter of control mixtures.

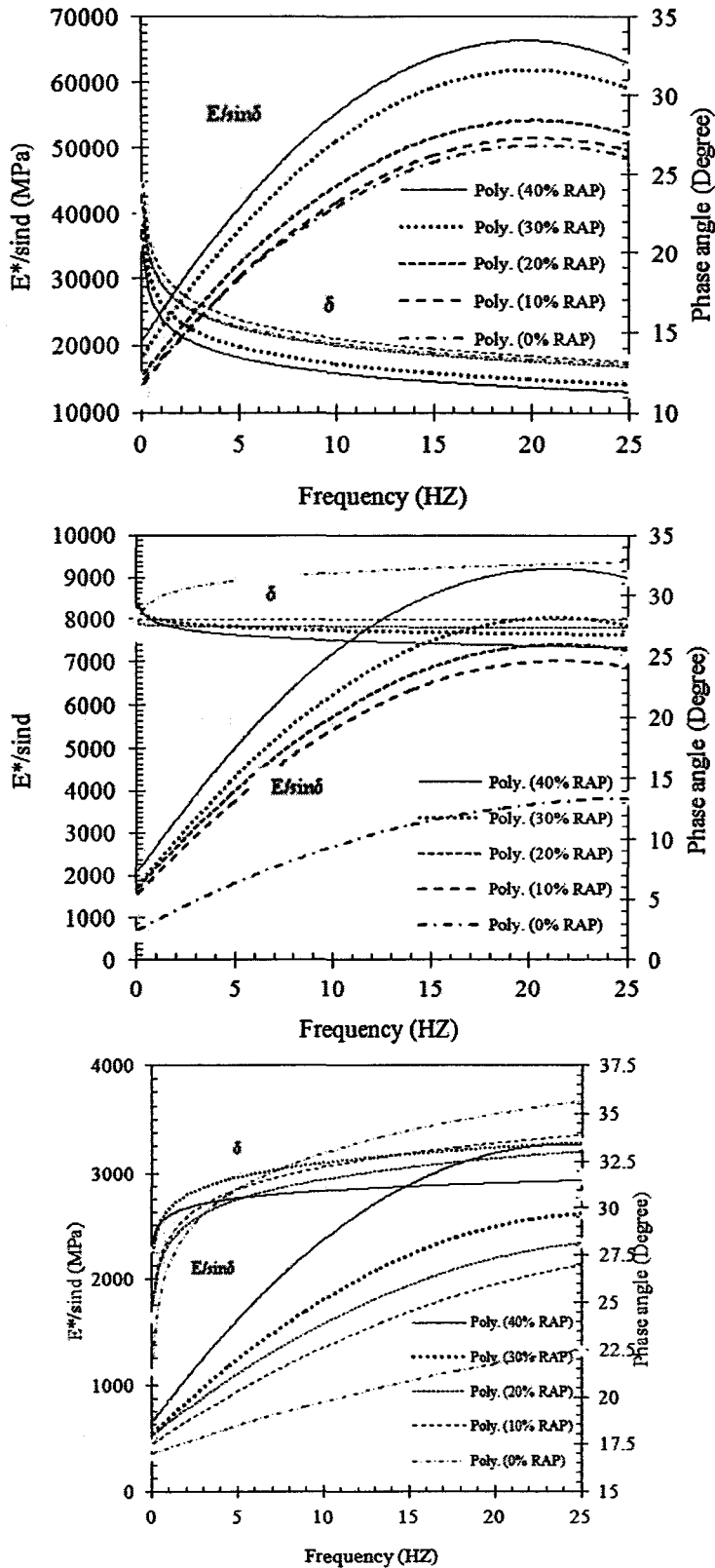


Figure 6.14: Master Curve of Rutting Factor versus Frequency Sweep at Designated Temperatures

From Figures 6.14, it can be seen that the maximum rutting factor takes place at approximately 20 Hz at each test temperature, while the maximum fatigue factor is from 15 Hz to 20 Hz as shown in Figures 6.15. Therefore, it is recommended that the frequency of

total traffic loading to achieve maximum rutting and fatigue performance should be in the range 15 to 20 Hz for the asphalt mixtures tested using RAP from DPE. Since aged binder in RAP materials supplied from various sources may have different rheological properties, it is expected to affect the engineering properties of asphalt mixtures containing RAP from different sources (Jamshidi et. al., 2012). Therefore, the recommended range of frequency to obtain maximum rutting and fatigue factors can vary for asphalt mixtures constructed using RAP from other sources.

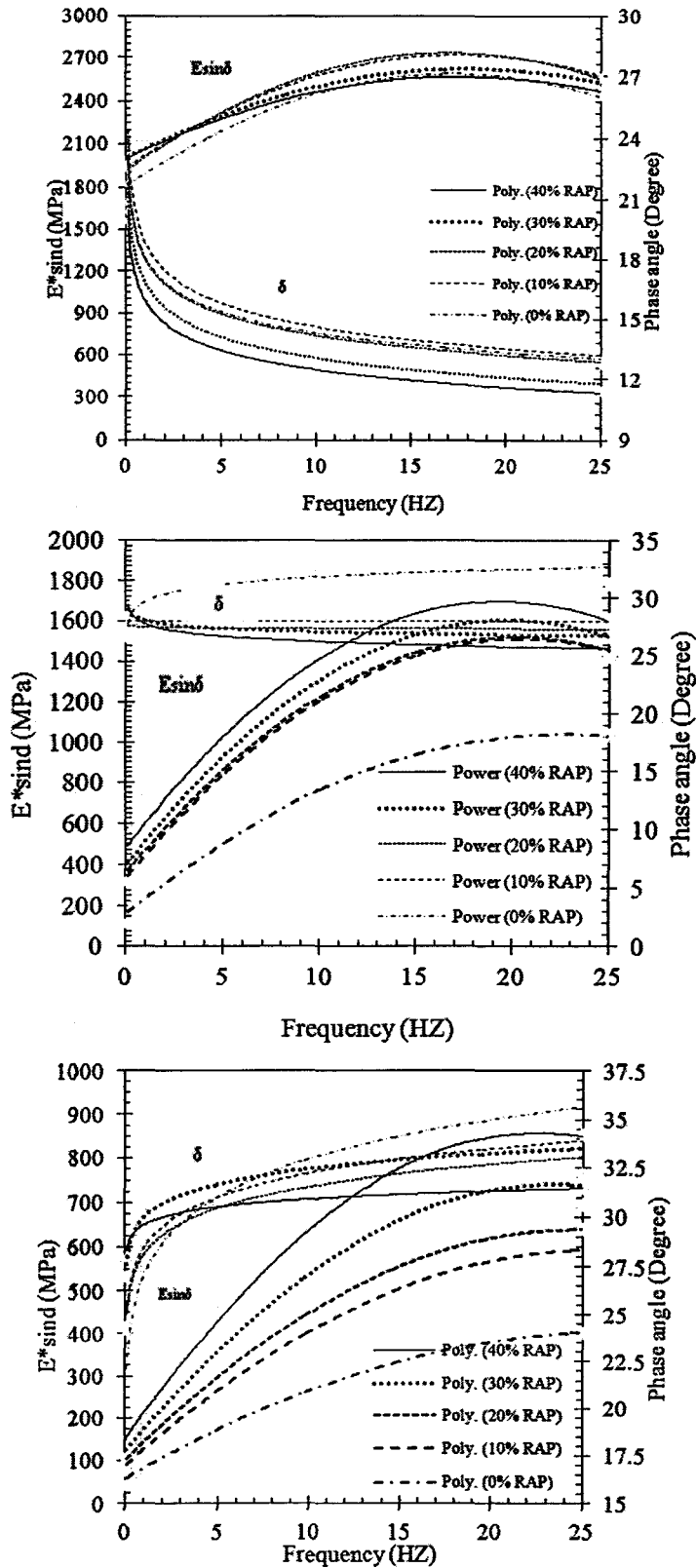
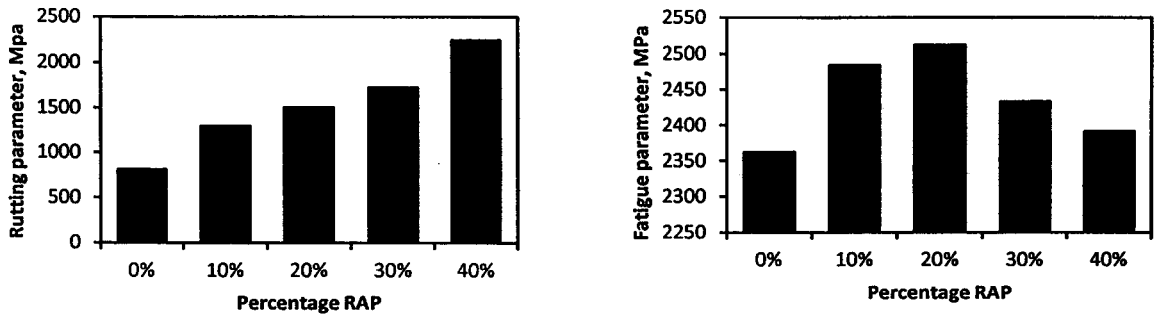


Figure 6.15: Master Curve of Fatigue Factor versus Frequency Sweep at Designated Temperatures

Improved resistance to rutting in mixes incorporating RAP is further illustrated in Figure 6.16. From Figure 6.16, rutting factor, $|E^*|/\sin \delta$ at 50°C and 10Hz has significantly increased by 37 %

and 64%, respectively for mixes incorporating 10% and 40% RAP. Interestingly, the fatigue parameter $|E^*| \cdot \sin \delta$ at 20°C and 10 Hz slightly increased up to 5% at 20% RAP and 1% for mix incorporating 40% RAP, and which is comparable to the fatigue parameter of control mixes.



(a) Rutting factor ($|E^*|/\sin \delta$) at 50°C and 10 Hz

(b) Fatigue parameter at 20°C and 10 Hz

Figure 6.16: Rutting Factor and Fatigue Parameter

6.8 Effects of RAP source and Content on energy activations of asphalt binders

When a fluid flows, the layers of the fluid molecules slide over each other, while intermolecular forces resist the motion and cause resistance to flow (Haider et al., 2011). Therefore, in order to flow in the fluids, energy is required that should be higher than the intermolecular forces, called activation energy (AE). The higher AE indicates higher energy is required to flow. The Equation (6.2), called Arrhenius equation, was used to model the viscosity-temperature dependency of asphalt binders in this study.

$$\nu = A e^{\frac{E_f}{RT}} \quad (6.2)$$

Where ν is viscosity (Pa.s), A is regression constant, E_f activation energy for flow(kJ/mol), T is temperature(°K) and R is universal gas constant(8.34 J/mol/°K).

6.8.1. AE based on viscosity

Tables 6.15 and 6.16 present the energy activation computed using viscosity for the unaged and short-term-aged asphalt blends, respectively.

Table 6.15: AE for the asphalt blends based on viscosity

Unaged			Short-term-aged		
Asphalt binder	Energy(kj/mol)	Change (%)	Asphalt binder	Energy (kj/mol)	Change (%)
Control	60.76	-	Control	66.63	-
N15U	63.36	4.26	N15S	69.24	3.93

N30U	66.63	9.64	N30S	72.15	8.29
D15U	64.66	6.41	D15S	71.54	7.37
P15U	63.75	4.91	P15S	70.15	5.29
P30U	66.34	9.18	P30S	70.10	5.20

U: Unaged; S: Short-term-aging

From Tables 6.15, it can be seen that the asphalt blends show higher energy activation in comparison with control binder for each aging state. It takes place because the recovered binder is aged binder, containing a lot of Asphaltene, making the stiffer asphalt binder. Consequently, higher energy activation is required to capture intermolecular forces for the asphalt binder blends. For example, the energy activation for N15U is 63.36 kJ/mol, while it is 66.63 for N30U, as indicated in Table 6.15.

Although incorporating recovered asphalt binder in the asphalt binder increase the energy activation, amount of increase in the energy activation depends on the recovered binder source. For instance, Table 6.16 presents that percent of change in the energy activation for D15U is 6.41%, while it is 4.91 % for P15U. Table 6.15 also shows that the maximum energy activation as well as maximum change percent in energy activation is for D30U and D30S samples. The N15U and N15S asphalt blends show the minimum energy activation.

Aging is another factor influence on the energy activation, as shown in Table 6.15, the energy activation of short-term-aged asphalt blends increases compared to unaged asphalt blends. Amount of changing in the energy activation is show in Table 6.16.

Table 6.16: Difference in AE values and change percentage due to short-term-aging

Asphalt binder	Difference in Energy(kj/mol)	Change (%)
Control	5.86	+9.64
N15	5.88	+9.29
N30	5.52	+8.29
D15	6.87	+10.63
D30	8.62	+12.76
P15	6.40	+10.04
P30	3.74	+5.65

Interaction available Asphaltene in the recovered binder and new produced Asphaltene after short term aging increases intermolecular resistance forces to flow. That is why the energy activations of all the short-term-aged asphalt blends are higher than the unaged blends. However amount increase in the energy activation depends on recovered binder source, as presented in Table 6.16.

6.8.2. AE based on $G^*/\sin \delta$

Table 6.17 shows the AE values based on $G^*/\sin \delta$. It can be seen that AE increases as recovered binder is added to the asphalt binder. However, amount of increase in AE depends on recovered binder source and content.

Table 6.17: AE for the asphalt blends based on $G^*/\sin \delta$

Unaged			Short-term-aged		
Asphalt binder	Energy(kj/mol)	Change (%)	Asphalt binder	Energy (kj/mol)	Change (%)
Control	111873	-	Control	127353	-
N15U	127279	13.77	N15S	135476	6.37
N30U	128692	15.03	N30S	129681	1.82
D15U	126372	12.96	D15S	136183	6.93
D30U	127902	14.32	D30S	133148	4.55
P15U	125641	12.30	P15S	135676	6.53
P30U	128584	14.9%	P30S	137231	7.56

U: Unaged; S: Short-term-aging

Table 6.17 also presents that the maximum AE values for each aging state is P30U and P30S, as highlighted by grey color, while Table 6.15 shows the maximum AE value is for D30U and D30S. It implies that the maximum amount of AE values depends on rheological parameter selected to study AE. Furthermore, the temperature sweep of DSR to find $G^*/\sin \delta$ is different from that of RV test.

As similar as AE values based on RV results, amount of AE increases after aging because of higher stiffness in the short-term-aged asphalt blends as indicated in Table 18. From the AE values in Table 6.18, it can be seen that amount of increase in AE values also depend on RAP source. Table 6.18 also shows that the minimum change in AE is for N30 that is less than 1%. It means that N30 asphalt binder is not susceptible to short term aging in terms of AE.

Table 6.18: Difference in AE values and change percentage due to short-term-aging

Asphalt binder	Difference in Energy(kj/mol)	Change (%)
Control	5.86	+13.83
N15	5.88	+6.44
N30	5.52	+0.76
D15	6.87	+7.76
D30	8.62	+4.10
P15	6.40	+7.98
P30	3.74	+6.72

6.8.3. AE based on $G^*.\sin \delta$

Table 6.19 shows AE values based on $G^*.\sin \delta$, the AE values based $G^*.\sin \delta$ decrease. It can be seen that the AE values decrease by adding the recovered binder, while AE values of the asphalt blends computed using viscosity and $G^*/\sin \delta$ increase. The reason behind such decreasing trend is that AE in Table 6.19 are computed based on $G^*.\sin \delta$.

Therefore, the lower AE values can mean that less energy activation is required to happen flow in terms of fatigue cracking as recovered binder is added in asphalt binder.

Table 6.19: AE for the asphalt blends based on $G^* \cdot \sin \delta$

Asphalt binder	AE (kJ/mol)	Difference in AE (kJ/mol)	Change (%)
Control	98903.34	-	-
N15L	90556.09	-8347.26	-8.43981
N30L	81377.43	-17525.9	-17.7202
D15L	86340.89	-12562.5	-12.7017
D30L	80770.51	-18132.8	-18.3339
P15L	86058.21	-12845.1	-12.9876
P30L	78251.37	-20652	-20.881

L: Long-term-aging

From Table 6.15, the N15L has the maximum AE values based on $G^* \cdot \sin \delta$, while D30U and P30U showed the maximum AE values in terms of viscosity and $G^*/\sin \delta$, respectively. This can be attributed to the difference in DSR and RV test nature. It means that RV is designed to measure asphalt binder shear resistance to flow, while the DSR measure the visco-elastic properties. Furthermore, the asphalt binder conditions for RV and sweep temperature to evaluate $G^*/\sin \delta$ are unaged and short-term-aged, while the condition to evaluate $G^* \cdot \sin \delta$ is long-term aging. In addition, the temperatures tested of $G^* \cdot \sin \delta$ are lower than those of $G^*/\sin \delta$ and viscosity.

CHAPTER SEVEN

CONCLUSIONS

7.1 Conclusion

In this final chapter, the main conclusions of this research are summarized. From the analysis carried out, the following conclusions can be made:

1. Blended asphalt binder properties are directly influenced by the chemical composition of saturates, aromatics, resin and asphaltenes upon aging. Improper use of virgin asphalt grade could result early structural failure of pavement due to stiffness contributed by aged binder from the RAP material in the hot asphalt mix especially in fatigue. Generally, recycled mixture with certain percentage of RAP has significantly improved the strength and durability of mixture in tensile strength, resilient modulus, rutting, fatigue, moisture damage and dynamic modulus compared to virgin mixtures.
2. The original coarse aggregate fraction of RAP aggregates has become finer than virgin aggregate primarily due to disintegration during the milling process and also previous handling and placement of the materials. The amount of RAP binder content in RAP particles passing 5 mm sieve is higher compared to those retained on 5 mm sieve since finer particles have larger surface area by volume. The amount of virgin asphalt requires in the recycled asphalt mixture decreases as percentage of RAP increases. An average saving of 38% in virgin binder when 40% dry RAP is incorporated in the recycled asphalt mixture.
3. The recovered RAP binders were further tested for rheological property for unblended and blended of unaged recovered RAP binders. The average value of $G^*/\sin \delta$ for unblended RAP binders at high temperature test decreased as the temperature is increased. The binder extracted from JKR RAP has the highest stiffness at all temperatures. This is in parallel with this RAP binder having the lowest penetration and highest softening values. Both recovered binder from PLUS and LDP RAP exhibit similar stiffness. From this result, the high temperature performance grade can be estimated at a PG88 for all recovered RAP binders.
4. The results of DSR testing on the unaged blended binders show that doubling the RAP binder concentration from 15% to 30% resulted in increasing the stiffness from 46 to 91 percent. PLUS RAP blend has the highest stiffness effect after doubling the concentration. The temperature – stiffness curves depicts LDP and JKR blends are identical while LDP and PLUS blends curves almost overlap with each other which suggests that both RAP blends exhibit similar stiffness property. For all RAP binder types, the addition of 15% of RAP binder increases the stiffness of the binder blend one grade higher to PG70 than that of the base virgin binder (PG64). As the RAP binder concentration doubles to 30%, the stiffness of the blend increase by two grades to become PG76 compared to base virgin binder.

5. For all aging conditions and RAP type the viscosity increased with increasing addition of RAP binders. It can be noted that LDP RAP has the highest percent increased in viscosity and it follows by PLUS RAP and JKR RAP for all aging conditions. However, at temperature 155°C and 165°C, blended binder with 30% JKR RAP binder has greater percent increased in viscosity compared to 30% PLUS RAP binder at unaged and short-term aging conditions. Subsequently, at long-term aging condition, blended binder with 30% PLUS RAP binder has lower increased in viscosity compare to JKR RAP binder at all temperatures. Percent of increased in viscosity is dropping as blended binders undergoes aging process from unaged to short-term and long-term aged.
6. The penetration and softening point consistently decrease and increase, respectively after severe aging conditions for all RAP modified binders. The penetration index and viscosity aging index significantly increase as the RAP modified binders are further aged. The RAP modified binders for all RAP binder sources and proportions exhibit distinct change in binder chemical evolution after subjected to short and long term aging. The carbonyl and sulfoxide groups namely C=O and S=O consistently show significant increase in the area ratio at each level of oxidation. The DPE and PWD RAP modified binders incorporating 15% and 30% RAP binders respectively are the most aged binders after long term aging.
7. The virgin-RAP binder blend shows that the stiffness of the binder blend increase with RAP content. The addition of RAP samples in virgin mixes produces stiffer and high strength mixes. The effect of RAP in mixes is more when pronounced when more than 20% RAP was added. All three RAP sources (PLUS, LDP, and JKR) exhibit almost similar physical and rheological properties. The results also showed that recycled mixes when added to virgin mixes exhibit equivalent if not higher indirect tensile strength compared to virgin mixes but depends on the percentages addition of RAP.
8. At constant test temperature, the dynamic modulus increases as the loading frequency and RAP content increase. The phase angle decreases as the loading frequency and RAP content increases at 20°C. However, at 40°C and 50°C, the phase angle increases up to loading frequencies 1Hz and 10Hz, respectively beyond which it reduces. At constant frequency, the dynamic modulus decreases as temperature increases, while the phase angle increases as temperature increases. Temperature and frequency have significant effects with high effect size on the measured dynamic modulus and phase angle. The interaction effect of frequency and RAP has the highest effect size among the interaction effects on the dynamic modulus test particularly on the phase angle. Rutting parameter increases as RAP content increases and fatigue parameter is well below the maximum limit and in fact the fatigue parameter further decreases with addition of more than 20% RAP. From the rutting and fatigue versus frequency master curves, the recommended cumulative traffic loading frequency for the asphalt mixtures tested ranges from 15 to 20 Hz.
9. The resilient modulus of porous asphalt increases until a maximum at 4.2% bitumen content, then decreases as the bitumen content increases. There is a general trend for the resilient modulus to decrease when the test temperature

increases. Polymer modified bitumen, which has been used for short and long term aging shows encouraging results, high resilient modulus values at higher temperatures as compared to the conventional mix.

10. Activation energy was also studied for all the asphalt blends. The results indicated that the amount of AE can vary based on recovered binder source and content. The evaluation of AE values also showed that adding the recovered binder changed the activation energy for each recovered binder source and content. The change can be positive or negative, depending on the asphalt binder rheological property selected to compute AE. As viscosity and $G^*/\sin \delta$ were chosen to find AE, the amount of AE and percentage change were positive with the addition of the recovered binder. However, if $G^* \cdot \sin \delta$ is chosen, the AE of the asphalt blends would be negative.

REFERENCES

- AASHTO, (2002a). AASHTO T84. Specific Gravity and Absorption of Fine Aggregate. Standard Specifications for Transportation Materials and Method of Sampling and Testing, Washington D.C.
- AASHTO, (2002b). AASHTO T85. Specific Gravity and Absorption of Coarse Aggregate. Standard Specifications for Transportation Materials and Method of Sampling and Testing, Washington D.C.
- AASHTO, (2002c). AASHTO T315-02. Determining the Rheological Properties of Asphalt Binder Using Dynamic Shear Rheometer. Standard Specification for Transportation Materials and Methods of Sampling and Testing. T315-02 Part 2B. American Association of State Highway and Transportation Officials.
- AASHTO, (2002d). AASHTO T240. Standard Test Method of Test for Heat on Air on a Moving Film of Asphalt (Rolling Thin Film Oven Test). American Association of State Highway and Transportation Officials, Washington D.C.
- AASHTO, (2002e). AASHTO T27. Standard Test Method for Sieve Analysis of Fine and Coarse Aggregates. American Association of State Highway and Transportation Officials. Washington D.C.
- Ahma, J., Rahman M.Y.A. and Din K., (2004). Degradation and Abrasion of Reclaimed Asphalt Pavement Aggregates. International Journal of Engineering and Technology, Vol. 1, No. 2, pp. 139-145.
- Al-Qadi I.L., Elseifi M. and Carpenter S.H., (2007). Reclaimed Asphalt Pavement - A Literature Review. FHWA-ICT-07-001. Illinois Center for Transportation, USA.
- Aravind K. and Das A., (2007). "Pavement Design with Central Plant Hot Mixed Recycled Asphalt Mixes". Construction and Building Materials, pp 928–936.
- Aravind K. and Das A., (2007). Pavement Design with Central Plant Hot Mix Recycled Asphalt Mixes. Construction and Building Materials, Vol. 21, pp. 928–936.
- Asphalt Institute, (1997). Mix Design Methods for Asphalt Concrete and Other Hot-Mix Types. Asphalt Institute Manual Series No. 2 (MS-2), 6th Ed, Lexington, K. Y.
- ASTM, (2003). ASTM Standard Test Designation D2041. Standard Test Method for Theoretical Maximum Specific Gravity and Density of Bituminous Paving Mixtures. 1998 Annual Book of ASTM Standards, Vol. 04.03, American Society for Testing and Materials, Philadelphia, USA.
- ASTM, (2006a). ASTM Standard Test Designation D5-97. Standard Test Method for Penetration of Bituminous Materials. 1998 Annual Book of ASTM Standards, Vol. 04.03, American Society for Testing and Materials, Philadelphia, USA.

ASTM, (2006b). ASTM Standard Test Designation D36. Test Method for Softening Point of Bituminous Material, Vol. 04.03, Annual Book of ASTM Standards, American Society for Testing and Material, Philadelphia, USA.

ASTM, (2006c). ASTM Standard D4402. Standard Test Method for Viscosity Determination of Asphalt at Elevated Temperatures Using a Rotational Viscometer. ASTM International, West Conshohocken, PA, DOI: 10.1520/D4402-06, www.astm.org.

Bahr B.V. and Steen B., (2004). Reducing Epistemological uncertainty in Life Cycle Inventory. Cleaner Production, Vol. 17, No. 2, 369-388.

Bukowski J.R., (1997). Guidelines for the Design of Superpave Mixture Containing Reclaimed Asphalt Pavement (RAP). Memorandum, ETG Meeting, FHWA Superpave Mixtures Expert Task Group, San Antonio, Texas.

Chiu C.T., Hsu T.H. and Yang W.F., (2008). Life Cycle Assessment on using Recycled Materials for Rehabilitating Asphalt Pavements. Res. Conserv. Recycling, Vol. 52, No. 3, pp. 545-556.

Dovi V.G., Friedler F., Huisingsh D. and Klemes J.J., (2009). Cleaner Energy for Sustainable Future. Cleaner Production, Vol. 17, No. 10, pp. 889-895.

FHWA, (1997). U.S. Department of Transportation, Pavement Recycling Guidelines for State and Local Government, Participant's Reference Book, FHWA-SA-98-042, Dec.

Gabel K., Forsberg P. and Tillman A.M., (2004). The Design and Building of a Life Cycle-Based Process Model for Simulating Environmental Performance, Product Performance and Cost in Cement Manufacturing. Cleaner Production, Vol. 12, No. 1, pp. 77- 93.

Giavarini C. and Pochetti F., (1972). Characterization of Petroleum Products by DSC Analysis. Journal of Thermal Analysis, Vol. 5, pp. 83-94.

Gui-Ping H. and Wing-Gun W., (2008). Effects of Moisture on Strength and Permanent Deformation of Foamed Asphalt Mix Incorporating RAP Materials. Construction and Building Materials, Vol. 22, pp. 30-40.

Haider, S. W., Mirze, M. W., Thottempudi, A. K., Bari, J. and Baladi, G. Y.(2011).Characterizing Temperature Susceptibility of Asphalt Binders Using Activation Energy Flow,Transportation and Development Institute Congress 2011: Integrated Transportation and Development for a Better Tomorrow,Chicago, Illinois, USA.

Hamzah M.O. Jamshidi A., Shahadan Z., (2010). Evaluation of the Potential of Sasobit® to Reduce Required Heat Energy and CO₂Emission in the Asphalt Industry. Journal of Cleaner Production, Vol. 18, No.18, pp.1859-1865.

Hekkert M.P., Joosten, L.A.J. and Worrell E., (2000). Reduction of CO₂ Emissions by Improved anagement of Material and Product Use: the Case of Transport Packaging. Res. Conserv. Recycl, Vol. 30, No. 1, pp. 1-27.

Holtz H. and Eighmy T.T. "Scanning European Advances in the Use of Recycled Materials in Highway Construction". *Public Roads*, Vol. 64, No. 1, <http://www.tfhr.gov/pubrds/julaug00/recycscan.htm>. Accessed January 17, 2009.

Holtz K. and Eighmy T.T., (2000). Scanning European Advances in the Use of Recycled Materials in Highway Construction. *Public Roads*, Vol. 64, No. 1.

Holtz K., Eighmy T.T., (2000). Scanning European Advances in the Use of Recycled Materials in Highway Construction. *Public Roads*, Vol. 64, No. 1, July/August.

Horvath A., (2003). Life Cycle and Economic Assessment of Using Recycled Materials for Asphalt Pavement. Technical Report, University of California, Berkeley, September.

Huang B., Li G., Vukosavljevic D., Shu X. and Egan B.K., (2005). Laboratory Investigation of Mixing Hot-Mix with Reclaimed Asphalt Pavement. *Journal of the Transportation Research Board*, No. 1929, pp. 37-45.

Huang Y., Bird R. and Heidrich O., (2009). Development of a Life Cycle Assessment Tool for Construction and Maintenance of Asphalt Pavements. *Cleaner Production*, Vol. 17, No. 2, pp. 283-296.

Huang Y., Bird R.N. and Heidrich O., (2007). A Review of the use of Recycled Solid Waste Materials in Asphalt Pavements. *Res. Conserv. Recycl*, Vol. 52, No. 1, pp. 58-73 .

Jahromi S.G. and Khodaii A., (2009). Effect of Nanoclay on Rheology Properties of Bitumen Binder. *Construction and Building Materials*, Vol. 23, pp. 2894-2904.

JKR, (2008). Standard Specification for Road Works (SPJ 2008-Section4: Flexible Pavement). *CawanganJalan, JabatanKerja Raya Malaysia*, Kuala Lumpur.

Kandhal P.S. and Mallick R., (1997). "Pavement Recycling Guidelines for State and Local Governments", FHWA, U.S. Department of Transportation.

Kandhal P.S., Rao S.S., Watson D.E. and Yound B., (1995). Performance of Recycled Hot Mix Asphalt Mixtures. National Center for Asphalt Technology, Report No. 95-1.

Kennedy T.W., Tam W.O. and Solaimanian M., (1998). Effect of Reclaimed Asphalt Pavement on Binder Properties Using the Superpave System. Center for Transportation Research, Bureau of Engineering Research, the University of Texas at Austin, Research Report 1250-1, September.

Khoo H.H., Tan R.B.H. and Chng K.W.L., (2010). Environmental Impacts of Conventional Plastic and Bio-Based Carrier Bags Part 1: Life Cycle Production. *Life Cycle Assessment*, Vol. 15, No. 3, pp. 284-293.

Lamontagne J., Dumas P., Mouillet V. and Kister J., (2001). Comparison by Fourier Transform Infrared (FTIR) Spectroscopy of Different Ageing Techniques: Application to Road Bitumen. *Fuel*, Vol. 80, pp. 483-488.

- Le Guern M., Chailleux E., Farcas F., Dreessen S. and Mabile I., (2010). Physico-Chemical Analysis of Five Hard Bitumens: Identification of Chemical Species and Molecular Organization before and after Artificial Aging Fuel, Vol. 89, pp. 3330-3339.
- Lee J.C., Edil B.E., Tinjum J.M. and Benson C.H., (2010). Quantitive Assessment of Environmental and Economy Benefits of Recycled Materials in Highway Construction. Transportation Research Record 2158, pp. 138-142.
- Lee K.W., Soupharath N., ShuklaArun., Franco C.A. and Manning F.J., (1999). Rheological and Mechanical Properties of Blended Asphalt containing Recycled Asphalt Pavement Binders. Journal of the Association of Asphalt Paving Technologist, Vol. 68, pp. 89-125.
- Lesueur D., (2009). The Colloidal Structure of Bitumen: Consequences on the Rheology and on the Mechanisms of Bitumen Modification. Advances in Colloid and Interface Science, Vol. 145, pp. 42-82
- Lesueur D., (2009). The Colloidal Structure of Bitumen: Consequences on the Rheology and on the Mechanisms of Bitumen Modification. Advances in Colloid and Interface Science, Vol. 145, pp. 42-82.
- Lewis A.J.N., (2004). "Developments in Road Pavement Recycling in the Far East". Proceedings of the 8th Conference on Asphalt Pavements for Southern Africa.
- Li X., Marasteanu M.O., Aliiliams R.C. and Clyne T.R., (2008). Effect of Reclaimed Asphalt Pavement (Proposition and Type) and Binder Grade on Asphalt Mixture. Journal of the Transportation Research Board, Transportation Research Board of the National Academies, Washington D.C., No. 2051, pp. 90-97.
- Lu X. and Isacson U., (2002). Effect of Ageing on Bitumen Chemistry and Rheology. Construction and Building Materials, Vol. 16, pp. 15-22.
- Lu X. and Isacson U., (2002). Effect of Ageing on Bitumen Chemistry and Rheology. Construction and Building Materials, Vol. 16, pp. 15-22.
- Manfredi S., Tonini D. and Christensen T.H., (2011). Environmental Assessment of Different Management Options for Individual Waste Fractions by Means of Life-Cycle Assessment Modeling. Res. Conserve. Recycle, Vol. 55, No. 11, pp. 995-1004.
- McDaniel R. and Anderson R.M., (2001). NCHRP Report 452: Recommended Use of Reclaimed Asphalt Pavement in the Superpave Mix Design Method: Technician's Manual. Transportation Research Board, National Research Council, Washington, D.C.
- McDaniel R. and Anderson R.M., (2001). NCHRP Report 452: Recommended Use of Reclaimed Asphalt Pavement in the Superpave Mix Design Method: Technician's Manual. Transportation Research Board, National Research Council, Washington, D.C.
- Memon G.M. and Chollar B.H., (1997). Glass Transition Measurements of Asphalts by DSC. Journal of Thermal Analysis, Vol. 49, pp. 601-607.

Millet D., Bistagnino L., Lanzavecchia C., Camous R. and Poldma T., (2010). Does the Potential of the use of LCA Match the Design Team Needs? *Cleaner Production*, Vol. 15, No. 4, pp. 335-346.

Nassar K. and Nassar W., (2006). Reclaimed Asphalt Pavement Detection and Quantity Determination. *Practice Periodical on Structural Design and Construction*, Vo. 1, No. 3, pp. 171-176.

National Asphalt Pavement Association (NAPA), (2009). *Black and Green: Sustainable Asphalt, Now and Tomorrow*. Special Report 200, NAPA, Maryland, USA.

National Cooperative Highway Research Program (NCHRP), (2004). *Guide for Mechanistic Empirical Design of New and Rehabilitated Pavement Structures*. Project 1-37A.

Oliver J.W.H., (2001). The Influence of the Binder in RAP on Recycled Asphalt Properties. *International Journal of Road Materials and Pavement Design*, Vol.2, No.3, pp. 311-325.

Optis M. and Wild P., (2010). Inadequate Documentation in Published Life Cycle Energy Reports on Buildings. *Life Cycle Assess*, Vol. 12, No. 4, pp. 644-651.

Puttagunta R., Oloo S.Y. and Bergan A.T., (1997). A Comparison of the Predicted Performance of Virgin and Recycled Mixes. *Canadian Journal of Civil Engineering*, Vol. 24, pp. 115 -121.

Read J. and Whiteoak D., (2003). *The Shell Bitumen Handbook*, 5th Ed. London: Thomas Telford Publishing.

Siddiqui M.N. Ali M.F. and Shirokoff J., (2002). Use of X-ray Diffraction in Assessing the Aging Pattern of Asphalt Fraction. *Fuel*, Vol. 81, pp. 51-58.

Siddiqui M.N. and Ali M.F., (1999). Studies on the Aging Behaviour of the Arabian Asphalts. *Fuel*, Vol. 78, pp. 1005-1015.

Siddiqui M.N. and Ali M.F., (1999). Studies on the Aging Behaviour of the Arabian Asphalts. *Fuel*, Vol. 78, pp. 1005-1015.

Su K., Hachiya Y. and Maekawa R., (2009). Study on Recycled Asphalt Concrete for use in Surface Course in Airport Pavement. *Resources, Conservation and Recycling*, Vol. 54, pp. 37-44.

Su K., Hachiya Y. and Maekawa R., (2009). Study on Recycled Asphalt Concrete for use in Surface Course in Airport Pavement. *Resources, Conservation and Recycling*, Vol. 54, pp. 37-44.

Sufian Z., Hussain M.Z., Abd Aziz N., Matori M.Y., (2007). Research Characteristics of Stabilised Full Depth (FDR) Pavement Layer. *Seventh Malaysia Road Conference*, 17 – 19 July.

Toteva V., Georgiev A. and Topalova L., (2009). Oxidative Desulphurization of Light Cycle Oil Monitoring by FTIR Spectroscopy. *Fuel Processing Technology*, Vol. 90, pp. 965-970.

USDOT, (1994). Background of SUPERPAVE Asphalt Binder Test Methods. U.S. Department of Transportation, FHWA-SA-94-069.

Valcke E., Rorif F. and Smets S., (2009). Ageing of EUROBITUM Bituminised Radioactive Waste: an ATR-FTIR Spectroscopy Study. *Journal of Nuclear Materials*, Vol. 39, pp. 175-185.

Widyatmoko I., (2008). Mechanistic-Empirical Mixture Design for Hot Mix Asphalt Pavement Recycling. *Construction and Building Materials*, Vol. 22, pp. 77-87.

Widyatmoko I., (2008). Mechanistic-Empirical Mixture Design for Hot Mix Asphalt Pavement Recycling. *Construction and Building Materials*, Vol. 22, pp. 77-87.

Witczak M.W., Kaloush K., Pellinen T., El-Basyouny M. and Von Quintus H., (2002). Simple Performance Test for Superpave Mix Design. Report No. 465, Transportation Research Board, National Research Council, Washington, D.C.

Xiao F., Amir Khanian S. and Juang C.H., (2007). Rutting Resistance of Rubberised Asphalt Concrete Pavement Containing Reclaimed Asphalt Pavement Mixture. *Journal of Materials in Civil Engineering*, Vol. 1, No. 6, pp. 475-483.

Xiao F., Amir Khanian S. and Juang H., (2007). Rutting Resistance of Rubberized Asphalt Concrete Pavements Containing Reclaimed Asphalt Pavement Mixture. *Materials in Civil Engineering*, Vol. 19, No. 6, pp. 475-483.

Yufeng Y., Shuyuan L., Fuchen D. and Hang Y., (2009). Change of Asphaltene and Resin Properties after Catalytic Aquathermolysis. *Petroleum Science*, pp. 194-200.

Zhang F., Yu J. and Han J., (2011). Effect of Thermal Oxidative Ageing on Dynamic Viscosity, TG/DTG, DTA and FTIR of SBS and SBS/Sulphur-Modified Asphalt. *Construction and Building Materials*, Vol. 25, pp. 129-137.